**UNIVERSIDAD DE ANTIOQUIA**

# REMOVAL OF PHARMACEUTICALS IN URINE USING ACTIVATED CARBON FROM RICE HUSKS (*Oryza Sativa*)

**Jhonnaifer José Romero Hernández**

**Research work to apply for the title of: Master's in Environmental Engineering**

**Advisor:**

**Ricardo Antonio Torres Palma, PhD.**

**Co advisor:**

**Javier Silva Agredo, PhD.**

**University of Antioquia**

**Faculty of Engineering**

**Postgraduate in Environmental Engineering**

**Medellín, Antioquia, Colombia**

**2022**

| Cita | (Romero Hernández, 2022) |
|---|---|
| **Referencia** <br> **Estilo APA 7 (2020)** | Romero Hernández, J. J. (2022). *Removal of pharmaceuticals in urine using activated carbon from rice husks (Oryza Sativa)* [Tesis de maestría]. Universidad de Antioquia, Medellín, Colombia |

Maestría en Ingeniería Ambiental

Grupo de Investigación en Remediación Ambiental y Biocatálisis (GIRAB)

Ciudadela Universitaria

UNIVERSIDAD DE ANTIOQUIA
Vicerrectoría de Docencia

Sistema de Bibliotecas

**Biblioteca Carlos Gaviria Diaz**

**Repositorio Institucional:** http://bibliotecadigital.udea.edu.co

Universidad de Antioquia – www.udea.edu.co

**Rector:** John Jairo Arboleda Céspedes

**Decano/Director:** Jesús Francisco Vargas Bonilla.

**Jefe departamento:** Diana Catalina Rodríguez Loaiza.

# SUMMARY

Water is a scarce natural resource, indispensable for human life and for the environmental sustainability, which with the passage of time, has suffered an alarming deterioration as a result of the rapid human and economic development. For years, quantities of pharmaceutical compounds, such as acetaminophen (ACE), ciprofloxacin (CIP), diclofenac (DIC) and sulfamethoxazole (SUL), have been present in municipal, hospital and industrial wastewater, and due to the inefficiency of the conventional water treatment methods, these compounds have been detected, in both natural and drinking waters, producing adverse effects on the living beings of the aquatic and terrestrial ecosystems. Therefore, the study of the behavior of these compounds in the environment, and their possible elimination in wastewaters, is a subject of growing interest for researchers around the world.

Alternatives such as membrane filtration, advanced oxidation processes and adsorption by using activated carbon are among the most promising options to deal with pharmaceutics in wastewaters. The use of activated carbons is of particular interest thanks to their high efficiency and easy application. In addition, activated carbons can be obtained from organic wastes, such as coconut husks, bamboo, fruit seeds and peels, sawdust, coffee pulp and rice husks (RH).

Among them, RH are of special interest, because in many developing countries, including Colombia, it is considered an environmental problem. In fact, large volumes of this waste are produced annually, and a significant part of them are not used or inadequately disposed, generating environmental pollution. Therefore, the use of this waste for the production of activated carbon for water treatment allows the simultaneous treatment of two environmental concerns: the elimination of waste generated by the RH and the elimination of contaminants, such as pharmaceuticals, from waters.

Considering the aforementioned, this work focused on the preparation of activated carbons from RH to be used in the elimination of various pharmaceuticals in aqueous solution. Activated carbons prepared from RH wastes were activated with NaOH, $ZnCl_2$ and $FeCl_3$ at 800°C. Initially, these materials were applied in the elimination of a mix of ACE, CIP, SUL, and DIC in distilled water. The results showed that NaOH activated RH carbon is the most effective in removing all of four contaminants. Then, several NaOH activated RH carbons with different ash content, RH-NaOH-800°C (activated carbon from RH activated with NaOH at 800°C), RH-NaOH-800°C pretreated and RH-NaOH-800°C post-washed, were tested on its ability to remove the organic pollutants. The results confirmed that a decrease in the percentage of ash increases the BET surface area, and consequently the adsorption capacity of activated carbon. The best activated carbon, RH-NaOH-800°C post-washed, was then tested on adsorption of the pharmaceuticals in both distilled water and synthetic urine, to determine the effect of the chemical structure of the contaminant and the complexity of the matrix on the adsorption capacity. CIP, due to its zwitterion structure, was the pharmaceutical that presented the highest affinity with the adsorbent surface, while ACE was the one with the lowest affinity. Both, ACE and CIP, were then selected to better understand the process by investigating isotherms (Langmuir, Freundlich and Redlich-Peterson models), kinetics (pseudo first-order, pseudo-second order and intraparticle diffusion models), and thermodynamics involved during the adsorption. The best fit, of both pharmaceuticals, for the Langmuir isotherm, which was confirmed by the Redlich-Peterson model, suggested a monolayer-type adsorption, presenting maximum adsorption capacities of 555.56 and 210.55 mg $g^{-1}$ for CIP and ACE, respectively, in RH-NaOH-800°C post-washed. Concerning the kinetic models, the best fit, of ACE and CIP, to the pseudo second order model suggests that the adsorption capacity is proportional to the number of active centers of the adsorbent. Furthermore, the intraparticle diffusion model indicated that ACE and CIP adsorption occur both on the surface and within the pores of the

activated carbon. Thermodynamic studies such as activation energy ($E_a$), enthalpy change ($\Delta H°$) and Gibbs free energy change ($\Delta G°$) suggest that the physisorption of both pollutants takes place in a spontaneous process. However, the thermodynamic data showed that ACE physisorption is an exothermic process, while the CIP physisorption process is endothermic, suggesting that the material developed temperature-dependent functional groups.

These results presented in this work show the possible application of RH residues as an promissory option for the elimination of pharmaceutical pollutants from water and urine. The best activated carbon prepared from RH and activated with NaOH can be effectively used for adsorption, in a complex matrix like urine, of various types of pharmaceutical contaminants with different chemical structures, such as ACE, CIP, SUL, and DIC, presenting adsorption percentages of 71.97, 98.36, 94.23 and 97.87%, respectively, in 5 minutes of treatment.

# TABLE OF CONTENTS

# LIST OF FIGURES

## LIST OF TABLES

**CHAPTER 1**

**1.1. Introduction**

Pollution with contaminants of emerging concern (CECs) is nowadays one of the most important environmental problems, due to their continuous introduction into the environment. In fact, even at low concentrations, CECs causes adverse effects on the available resources. Water, is one of the most affected natural resources, which are of particular interest due to the variety of CECs that are not removed by conventional water treatment systems. A wide variety of CECs, such as human and veterinary pharmaceuticals, has been widely reported in freshwater environments [1], [2], which can elicit effects at very low environmental concentrations in both plants and animals [3]–[5]. Pharmaceutical products are of great concern given that, although these compounds are at trace levels (from ng $L^{-1}$ to µg $L^{-1}$) in the environment, they produce accumulative effects due to their high persistence [6], [7]. Furthermore, the combined effects of pharmaceuticals increases the risk due to negative synergistic effects [8].

To deal with this, it is necessary to implement effective treatments for pharmaceuticals at the source, thus minimizing the pollutant charges of conventional treatment plants. Otherwise, advanced tertiary treatment can be used as a complement of conventional treatment systems. Thus, the treatment of waters and wastewaters containing pharmaceuticals have been tested using solar photo-Fenton [9], [10], photolysis [11], heterogeneous photocatalysis [12], electrochemical oxidation [13], activated sludges [14], filtration [15] and adsorption [16], [17]. However, these methodologies have shortcomings, such as high costs, high generation of sludge [18] or dangerous by-products generation [9], [10]. Therefore, the search for more effective, economic and safe wastewater treatment methods is a need.

Adsorption-based systems present some advantages for the treatment of effluents contaminated with pharmaceuticals, such as low-cost implementation and easy operation. In this sense, low-

cost biomass can be pyrolyzed in absence of oxygen to produce biochar. This carbon material can be utilized raw, or activated with chemicals to improve its adsorbent properties [19]. Among the vegetable residues used in the production of activated carbons, rice husk (RH) is of special interest, because in many developing countries it is considered an environmental problem. In fact, in 2011 it was reported that 400 thousand tons of RH are produced annually in Colombia [20].

Considering the abundance of this waste in Colombia, and the fact that several studies confirm the use of this material as an good adsorbent of different pollutants [21], to implement a strategy that minimizes the presence of RH in the environment and at the same time contributes to the removal of pharmaceuticals from water is of particular interest.

## 1.2. Problem Statement

The presence of pharmaceutically active compounds in the environment has drawn attention over years [22], due to their toxicity [23], ubiquity, persistence, and biological activity [24]–[26]. Furthermore, in Colombia, the legal requirements for their discharge into surface water bodies have not yet been established. In general, the freshwater environment is thought to be an important sink for different types of pharmaceuticals [27]. These compounds are continuously discharged into the environment, as the initial product or as human metabolites, and during their passage through urban wastewater systems they can be subjected to several transformation reactions, giving rise to by-products, which may have greater toxicity than the precursor compounds [28]–[31].

Acetaminophen (ACE), ciprofloxacin (CIP), diclofenac (DIC) and sulfamethoxazole (SUL) are pharmaceutical compounds that have been detected in both influents and effluents of WWTP [32].

ACE is a pharmaceutical widely used as anti-inflammatory and analgesic [33]. DIC is a non-steroidal analgesic, anti-inflammatory, antirheumatic and antiarthritic compound, which has been classified as toxic, and one of the most widely used pharmaceuticals [34].

SUL is a sulfonamide-type antibiotic, which is used in the prevention and treatment of infections. CIP, is a synthetic antibiotic used to treat a wide variety of bacterial infections, such as respiratory tract infections, urinary tract, skin, bone, gastrointestinal tract and ear canal, among others [35].

The continued presence of antibiotics in the water, even at low concentrations, can have detrimental effects on the ecosystem. For example, presence of SUL and CIP in natural waters can lead to the development of antibiotic resistance in microorganisms, which cause suppression of the therapeutic efficacy of antibiotics against pathogens [36], [37]. Furthermore, the photosynthesis mechanism of some plants, such as algae, can be inhibited by the presence of antibiotics in the water [38].

ACE, used to treat pain and fever, is widely consumed in Colombia; in fact this is sold without medical prescription [39]. ACE is metabolized (up to 90%) in the body by hepatic biotransformation into glucuronic acids and sulfonate conjugates, which are renally eliminated [40]. Only 3-5% of ACE is excreted unmetabolized by the kidneys [41]. Despite its high metabolism, it has been estimated that the worldwide amount of this chemical that reaches the WWTP is 292-585 Ton/year [40]. Thus, this contaminant has often been found in municipal wastewater effluents in concentrations up to 65 $\mu$g L$^{-1}$ [42]. In Colombia 29.66, 0.16 and 15 $\mu$g L$^{-1}$ of ACE has been detected in effluents of municipal WWTP from Bogotá, Medellín and the Amazonian region, respectively [32]. Although the concentration of ACE detected in natural waters in generally below the range of $\mu$g L$^{-1}$ [33], its presence can affect aquatic organisms [43], due to the capacity of this chemical to bioaccumulate [44]–[47].

On the other hand, agro-industrial processing and production has always resulted in some type of waste in the form of a solid, liquid or gas. The waste generated has high values of biological oxygen demand and can cause problems in different aspects, including the cost of collection, disposal, treatment, and the consequent loss of valuable raw materials [48]. For example, the annual global production of RH is approximately 148 million metric tons [49], where more than 96% of RH is produced in developing countries [50]. Of all the RH production around the world, only 17% is reused in several applications [51]. Thus, large volumes of RH are burned in open spaces or end up in the environment causing negative impacts on the living organisms.

Therefore, in order to contribute in two environmental issues: the contamination by pharmaceuticals in wastewaters and the pollution occasioned by RH wastes, the adsorption capacity of activated carbons prepared from RH was evaluated in the removal of four pharmaceuticals models (ACE, DIC, SUL and CIP) from waters. The elimination of the selected contaminants in urine, which is a primary source of water contamination by pharmaceuticals was particularly considered. Special attention is paid in the effect of different activating agents ($ZnCl_2$, NaOH and $FeCl_3$) on the adsorption capacity of the contaminants.

### 1.3. Hypothesis

- RH waste present in Colombia (from the Huila department) or activated carbons obtained from this residue can be effectively applied to the removal of pharmaceuticals such as ACE, CIP, SUL and DIC, even in urine.

- Activated carbons obtained from the RH waste are better adsorbents of pharmaceuticals than their corresponding natural raw material.

**1.4. Objectives**

General objective

- To evaluate the behavior of activated carbons prepared from rice husks (*Oryza Sativa*) in the removal of pharmaceuticals present in urine.

Specific objectives

- To develop activated carbons from rice husks (*Oryza Sativa*) for use as adsorbent.

- To characterize physiochemically the activated carbons obtained from rice husk (*Oryza Sativa*).

- To evaluate the effect of both the activating agent and the chemical structure of the contaminant on the process of adsorption.

- To establish the adsorption capacity of the activated carbon of rice husk with better behavior compared to a commercial activated carbon during the removal of the tested pharmaceuticals.

- To determine the adsorption mechanism of pharmaceuticals for the most efficient activated carbon obtained.

**1.5. Theoretical framework and background**

Pharmaceutical products are a group of bioactive chemical compounds used in veterinary, animal farms, and humans medicine [52]. Various investigations have shown that pharmaceuticals are present in surface waters, seawater and even in groundwater [3], [53], [54], [55]. Much of the pharmaceuticals are not metabolized and are released into sewage systems [56]. Therefore, a high concentration of pharmaceuticals can be found in raw wastewater [57]–[59]. According to studies the range of pharmaceutical concentrations in raw wastewater is $10^{-3}$ to $10^2 \, \mu g \, L^{-1}$ [60]. Additionally, common wastewater treatment plants (WWTPs) cannot efficiently remove these substances from liquid and sludge effluents [32]. When found in

wastewater, these compounds become dangerous pollutants to both aquatic environment and humans due to their adverse effects on aquatic life [55].
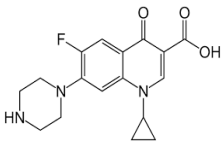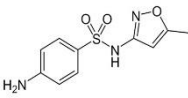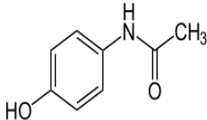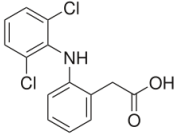
The appearance of pharmaceuticals in the environment depends on many variables, the most obvious route is through urine and feces, but other anthropogenic mechanisms must be considered [61], [62], such as:

- Direct disposal from home by consumers (by expiration).

- Direct contamination of these residues to soil, through the biosolids from treatment plants (activated sludge).

- Veterinary products released into the urine and animal excreta, later used as fertilizer, and which due to runoff causes water contamination.

- Pharmaceutical products and their metabolites from aquaculture; which are dumped directly into surface waters.

- Effluents from pharmaceutical production plants.

Pharmaceutical compounds are subdivided into a diverse group of organic compounds such as antibiotics, hormones, anti-inflammatories, antiepileptics, blood lipid regulators, beta-blockers, contrast media and cytostatic drugs, antimicrobial agents, synthetic musk, insect repellents, preservatives and UV protection filters [63]. Within this great variety, different studies published since the beginning of the new century have shown that ACE, DIC, SUL and CIP are among the most frequently detected pharmaceutical residues in water bodies water [64], [65]. ACE is a pharmaceutical with analgesic and antipyretic properties used mainly to treat fever and mild and moderate pain. DIC is a pharmaceutical that is a member of the non-steroidal anti-inflammatory family, which is indicated to both reduce inflammation and as an analgesic. SUL is a sulfonamide-type bacteriostatic antibiotic that is frequently used for the treatment of urinary infections. CIP is an antibiotic from the group of fluoroquinolones that contain fused aromatic

rings and a carboxyl group attached; the mode of action of this antibiotic is by interfering the replication and transcription of bacterial DNA, and is active against Gram-positive and Gram-negative bacteria. Table 1, describes some physicochemical properties of the studied pharmaceutical and Figure 1, shows their chemical structures, in accordance with their pKa values.

**Table 1.** Physicochemical properties of studied pharmaceuticals.

| | CIP | SUL | ACE | DIC |
|---|---|---|---|---|
| **Chemical structure** |  |  |  |  |
| **Chemical formula** | $C_{17}H_{18}N_3FO_3$ | $C_{10}H_{11}N_3O_3S$ | $C_8H_9NO_2$ | $C_{14}H_{11}NCl_2O_2$ |
| **Use** | Antibiotic | Antibiotic | Analgesic, anti-inflammatory | Anti-inflammatory |
| **Molecular weight** | 331.346 g/mol | 253.279 g/mol | 151.17 g/mol | 296.148 g/mol |
| **Water solubility** | 30000 mg/L (20°C) | 610 mg/L (37 °C) | 12.78 mg/mL (20°C) | 2.37 mg/L (25°C) |
| **pKa** | pKa$_1$: 6.3 pKa$_2$: 8.6 | pKa$_1$: 2.0 pKa$_2$: 6.2 | pKa$_1$: 9.38 | pKa$_1$: 4.5 |
| **Average life** | 4 hours | 10 hours | 1 – 4 hours | 1.5 – 2 hours |
| **Excretion** | Renal: 60% bile: 15% | Urine: 20% unchanged | Renal: 85-90% | DIC unchanged: bile, 1% in urine; metabolites: 35% bile, 65% urine. |
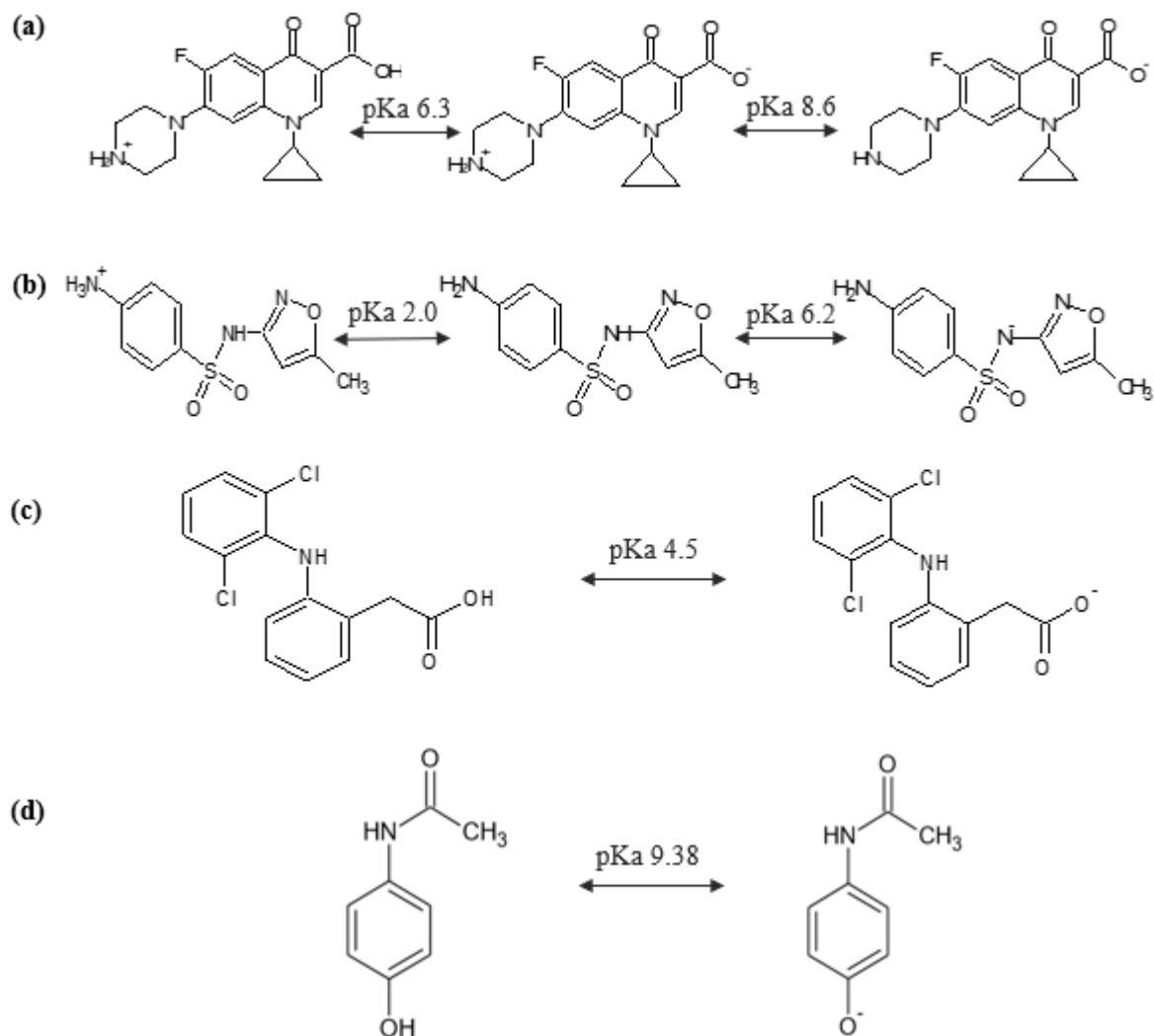
**Figure 1.** Chemical structure of pharmaceuticals according to pKa. (a) CIP; (b) SUL; (c) DIC; (d) ACE.

Pharmaceutical contaminants in raw wastewater from hospitals, homes, veterinary clinics, and health care units eventually end up in WWTPs. Unfortunately, WWTPs employing conventional methods do not efficiently remove these compounds, and they can remain in effluent wastewater (EWW) at concentrations similar, or even higher, than in influent wastewater (IWW) [66]–[69], even after applying tertiary treatment [70]. Consequently, the pharmaceutical products still present in the treated wastewater are introduced into the aquatic environment, bringing serious damage to the ecosystem, thus becoming a danger to human health [66], [71]. For this reason, it is important to identify and evaluate the efficiency of

technologies for water treatment, in order to propose alternatives that allow minimizing the presence of pharmaceutical compounds at a low economic, energy and environmental cost.

Some promising alternatives for the elimination of pharmaceutical in water are ozone [72], electrochemical oxidation [73], [74], homogeneous photodegradation [75], [76], membrane separation [77], [78], osmosis [79], electrocoagulation [80], ion exchange processes [77], [78] and adsorption [81]. The last one is among the most attractive options, due to its easy operation, efficiency, and relative low cost in the elimination of antibiotics [81].

On the other hand, the manufacture and transformation of agro-industrial products results in large amounts of solid organic waste, with the consequent cost of its collection, treatment, and disposal [48]. Therefore, it is necessary to look for alternatives of using such wastes in order to reduce their negative impact on the environment. In the last decade, the scientific community has investigated the use of activated carbon with materials obtained from biomass as an interesting option for the treatment of water contaminated with pharmaceuticals. Figure 2 provides an overview on adsorption studies (published in January-March 2021) according to the type of pharmaceutical, adsorbent precursor and type of activation to prepare the adsorbent.



**PHARMACOLOGICAL GROUP**

Synthetic hormones 3%
Antihypertensive 6%
Anticonvulsants 3%
NSAIDs 19%
Antibiotics 44%
Analgesics 25%

**(a)**
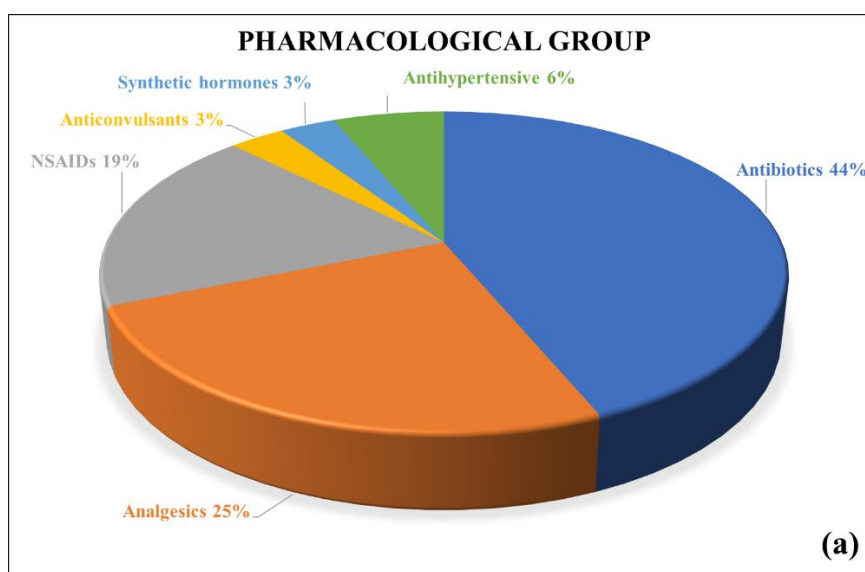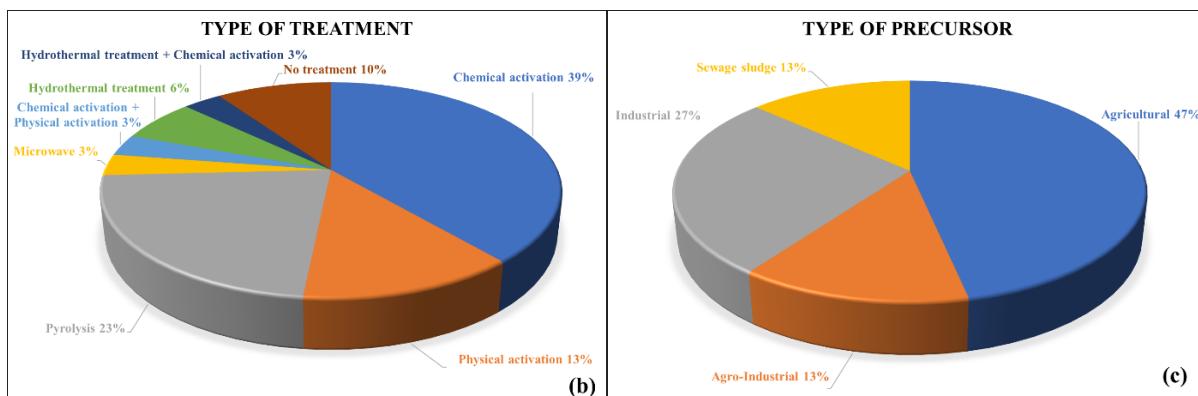
**Figure 2.** Percentage of published studies on the elimination of pharmaceutical products by alternative adsorbents classified according to the specific pharmaceutical product (a), type of treatment during the production of activated carbon (b), and type of precursor of the adsorbent (c).

As seen in Fig. 2, practically a half of the precursors used as adsorbent are coming from agriculture activities. The most promising agro-industrial waste products used in obtaining activated carbons for the treatment of contaminants include coconut husk and palm seeds [82], potato husk [83], pods of corn [84], peanut stick wood [85], cotton stalk [86], rubberwood sawdust [87], coffee husk [88], RH [89], among others [90]. Furthermore, high internal surface areas, well-developed internal pore structures and the presence of a wide spectrum of surface functional groups have been reported in these materials [88], [91]. In recent years, RH has received a special interest due to its high availability, slow degradation and the consequent environmental problems it generates. In fact, activated carbons obtained from RH have been tested and applied in the adsorption of dyes as methylene blue [92], heavy metals as $Pb^{2+}$ [93] and $Cr^{6+}$ [94], pharmaceutical contaminants as ACE [89], pesticides as carbofuran [95], and other organic contaminants such as phenol [96]. Therefore, the conversion of this agricultural waste into activated carbon would decrease the accumulation of its waste and make it a value-added material with potential applications in water treatment.

The production of activated carbon from RH can mainly be carried out through two methods: physical or chemical activation [88], [97]. Physical activation consists of carbonization of the raw material in an inert atmosphere at a temperature between 600°C – 900°C, followed by activation at elevated temperature (between 600°C – 1000°C) in presence of a gas oxidant such as water vapor, air, or carbon dioxide [98]. On the other hand, chemical activation can be carried out by means of one stage or two stages. Two-stage activation consists of precarbonization of the precursor, in an inert atmosphere, followed by addition of the activating agent and pyrolysis at 400°C – 900°C; while one stage activation consists of a single step, in which carbonization and activation occurs simultaneously in an inert atmosphere.

Chemical activation has advantages over physical activation, such as the use of lower temperatures and the availability of numerous activating agents ($ZnCl_2$, KOH, NaOH, $FeCl_3$, $H_2SO_4$, $H_3PO_4$ and $K_2CO_3$), which inhibit the production of volatile substances during the process [99]. The use of $FeCl_3$ as an activating agent is interesting given that the amount of residual iron that remains in the activated carbon could allow its use as a catalyst in advanced oxidation processes. In the same way, the use of $ZnCl_2$ and NaOH as activating agents produces activated carbons with well-defined porous structures and high surface areas [100], [101], which favors adsorption since there would be greater availability of active sites on the surface of the adsorbent to be occupied by the adsorbate molecules, decreasing the concentration of the contaminant in the solution.

The relationship between the adsorbed amount of the pollutant and its concentration in known as isotherms or adsorption curves. The most common isotherms to describe the adsorption characteristics of activated carbon used in water treatment are the Freundlich, Langmuir and Redlich-Peterson isotherms. The basic assumptions of the Langmuir isotherm are: (i) the surface of the solid is homogeneous, so that the adsorption energy is similar in all centers, (ii) the adsorption on the surface occurs only on the active centers and (iii) each active center can

accumulate only one molecule of adsorbate. The Langmuir isotherm can be calculated using the following equation [154]:

$$q_e = q_m \frac{K_L C_e}{1 + K_L C_e} \quad Eq.(1)$$

The Eq. 1 can be rearranged into a linear form:

$$\frac{C_e}{q_e} = \frac{C_e}{q_m} + \frac{1}{K_L q_m} \quad Eq.(2)$$

Where $C_e$ (mg L$^{-1}$) and $q_e$ (mg g$^{-1}$) are equilibrium concentration and the amount of adsorbate adsorbed per unit mass of adsorbent, respectively; $q_m$ (mg g$^{-1}$) is the amount of pharmaceutical adsorbed per unit mass of adsorbent equivalent to formation of a complete monolayer. The affinity constant, $K_L$ (L mg$^{-1}$), is the equilibrium constant of the adsorption process. Thus, a plot of $C_e/q_e$ vs $C_e$, $q_m$ can be done, and from the slope $K_L$ from the intercept. The essential characteristics of Langmuir isotherm can be expressed by a dimensionless equilibrium parameter, also known as separation factor, which is defined as follow [154]:

$$R_L = \frac{1}{1 + K_L C_0} \quad Eq.(3)$$

Where $R_L$ values indicate the type of adsorption: irreversible ($R_L = 0$), favorable ($0 < R_L < 1$), linear ($R_L = 1$) or unfavorable ($R_L > 1$); and $C_0$ (mg L$^{-1}$) is the initial concentration of the pollutant.

In it turn, the Freundlich isotherm is used in systems where the adsorption surface is energetically heterogeneous. The Freundlich isotherm can be studied using the following equation [155]:

$$q_e = K_F C_e^{1/n} \quad Eq.(4)$$

Where $K_F$ and $n$ are indicators of the adsorption capacity and the adsorption intensity, respectively. The $n$ value indicates the intensity of adsorption as follows: If the value of $n = 1$, the adsorption is linear; if $n < 1$, the adsorption is a chemical process; while if $n > 1$, the adsorption is a favorable physical process [156]. Rearranging *Eq. 4* we get,

$$Ln\ q_e = Ln\ K_F + \frac{1}{n}Ln\ C_e \quad Eq.\,(5)$$

Furthermore, the Redlich-Peterson isotherm is a much more versatile model than previous models since it can be used not only in homogeneous systems, but also in heterogeneous ones [102]. The Redlich-Peterson model can be represented as follows:

$$q_e = \frac{K_{RP}C_e}{1 + a_R C_e{}^{\beta}} \quad Eq.\,(6)$$

Where $K_{RP}$ $(L\ g^{-1})$ and $a_R$ $(L\ mg^{-1})^{\beta}$ are the Redlich-Peterson isotherm constants and $\beta$ is an exponent that lies between 0 and 1. *Eq. 6* can be linearized by taking logarithms of both sides, to produce *Eq.7*:

$$ln\left(K_{RP}\frac{C_e}{q_e} - 1\right) = ln\ a_R + \beta\ ln\ C_e \quad Eq.\,(7)$$

On the other hand, the kinetics describes the adsorption rate of the adsorbate on the adsorbent and determines the time at which equilibrium is reached. Owing to their interesting results, pseudo first order, pseudo second order and intraparticle diffusion are the most employed [106]. The pseudo first order Lagergren equation is the oldest and most typical adsorption rate model. This describes a reversible equilibrium of the adsorbate and adsorbent [165]. The pseudo first order kinetic model assumes that the rate of occupation of adsorption sites is proportional to the number of unoccupied sites [166]. Using this model, the rate of adsorption can be determined by the following equation [167]:

$$ln\ (q_e - q_t) = ln\ q_e - k_1 t \quad Eq.\,(8)$$

Where $q_t$ is the amount of the pharmaceutical adsorbed (mg g$^{-1}$) at the time $t$ (min), $q_e$ is the amount of pharmaceutical adsorbed at the equilibrium (mg g$^{-1}$), and $k_1$ is the equilibrium rate constant of pseudo first order adsorption (min$^{-1}$). The pseudo-second order model assumes that the rate of occupation of adsorption sites is proportional to the square of the number of unoccupied sites [168]. Hence, the pseuso second order kinetic rate law can be written as [169]:

$$\frac{t}{q_t} = \frac{1}{k_2 q_e{}^2} + \frac{t}{q_e} \qquad Eq.\,(9)$$

Where $k_2$ is the pseudo-second order rate constant of adsorption (mg g$^{-1}$ min$^{-1}$).

Since the previous kinetic models do not allow to identify the diffusion mechanism, it is important to apply the intraparticle diffusion model, which allows to predict the rate-limiting step in the adsorption process. This model can be determined using the equation proposed by Weber and Morris [172]:

$$q_t = k_{id} t^{1/2} + C \qquad Eq.\,(10)$$

Where $q_t$ (mg g$^{-1}$) is the amount of pollutant adsorbed at time $t$, $k_{id}$ is the intraparticle rate constant (mg g$^{-1}$ min$^{-1/2}$), while $C$ is a constant that indicates the thickness of the boundary layer. Then, a larger intercept means a greater effect of the boundary layer [156]. The plot $q_t$ versus $t^{1/2}$ allows us to obtain a straight line with slope $k_{id}$ and intercept $C$.

On the other hand, to further investigate the adsorption mechanism, the feasibility and spontaneous nature of the processes, it is necessary to evaluate the behavior of adsorption processes when subjected to thermal changes. In the adsorption process, $E$a (kJ mol$^{-1}$) is defined as the minimum energy that the adsorbate molecules must overcome. It can be estimated from the Arrhenius equation as follows [167]:

$$\ln k_2 = \ln A_0 - \frac{E_a}{RT} \qquad Eq.\,(11)$$

Where $A_0$ is the Arrhenius constant, $R$ is the universal gas constant (8.314 J mol$^{-1}$ K$^{-1}$), and $T$ is the temperature ($K$). The $E_a$ for the contaminants can be calculated from the slope of the plot $ln\ k_2$ vs $1/T$. The thermodynamic parameters: $\Delta S°$, $\Delta H°$ and $\Delta G°$ are determined using the following equations [174]:

$$Ln\ K_c = \frac{\Delta S°}{R} - \frac{\Delta H°}{RT} \quad Eq.\,(12)$$

$$\Delta G° = \Delta H° - T\Delta S° \quad Eq.\,(13)$$

$R$ is the ideal gas constant and $T$ the temperature (in Kelvin). $K_c$ is the apparent equilibrium constant of the adsorption process defined as $K_c = MW*55.5*1,000*K_L$, where $MW$ is the molecular weight of the adsorbate, factor 55.5 is the number of moles of pure water per liter, $K_L$ is the affinity constant of Langmuir and the term $K_c$ is dimensionless. The $Ln\ K_c$ versus $1/T$ plots are used to calculated the slope and the intercept, which determined the parameters $\Delta H°$ and $\Delta S°$, respectively.

Finally, with this work it can be inferred that the use of RH as a precursor material to obtain activated carbon could address two serious environmental problems: the elimination of residues from rice processing and the elimination of pharmaceuticals from water.

**CHAPTER 2**

## 2.1. Methodology

### 2.1.1. Reagents

ACE ($C_8H_9NO_2$), CIP ($C_{17}H_{18}N_3FO_3$), SUL ($C_{10}H_{11}N_3O_3S$) and DIC ($C_{14}H_{11}NCl_2O_2$) were supplied by Allianz Group International Ltda. Sodium chloride (NaCl), acetonitrile ($C_2H_3N$), sulfuric acid ($H_2SO_4$), urea ($CH_4N_2O$), methanol ($CH_3OH$), hydrochloric acid (HCl), ammonium chloride ($NH_4Cl$), sodium dihydrogen phosphate ($NaH_2PO_4$), sodium sulfate ($Na_2SO_4$), sodium hydroxide (NaOH), calcium chloride ($CaCl_2$), potassium chloride (KCl), magnesium chloride ($MgCl_2$), zinc chloride ($ZnCl_2$) and ferric chloride ($FeCl_3$) were obtained from Merck. Commercial activated carbon (extraction cartridge) was supplied by Y-Carbon, Inc. All solutions were prepared with distilled water, except for those solutions used for chromatographic analysis, which were made with purified water from a Millipore Milli-Q® system.

### 2.1.2. Adsorbents preparation

#### 2.1.2.1. Natural adsorbent

RH was collected from agroindustry of the Huila department in Colombia. The material was washed repeatedly with distilled water to remove dust and soluble impurities, and then dried in an oven at 60°C for 48 h. The RH was ground to power and sieved to obtain uniform size between 75 – 150 µm. The material was then stored in plastic bottles before use.

#### 2.1.2.2. Activated carbons

The preparation process consisted of two steps: carbonization and activation. RH was centered in a furnace (KSY-6D-16B, Electric Furnace Factory) and purged with $N_2$ gas (purity of 99.995%) at a flow rate of 60 mL min$^{-1}$. The temperature was increased by 5°C min$^{-1}$ until the desired temperature was reached (500°C, temperature determined by thermogravimetric

analysis (TGA)). This temperature was then maintained for 2 h to complete the carbonization process.

Subsequently $ZnCl_2$, $FeCl_3$ and NaOH were selected as activating agents, and used at mass ratios agent/carbonized of 3:1 in order to develop high surface area [103]. In addition, since activated carbons prepared from RH are characterized by developing greater surface areas at activation temperatures of 800°C [89], this temperature was chosen as the activation temperature. Therefore, the mixtures were heated at 5°C min$^{-1}$ up to the activation temperature of 800°C for 1 h.

After activation, all samples were immersed in HCl 0.1 M to remove the excess of NaOH, $FeCl_3$ and $ZnCl_2$ and other impurities. Later, the activated carbons were washed with distilled water until the pH of the rinse became neutral (pH 6.8-7.0), followed by drying at 105°C for 24 h. Finally, the materials were stored in plastic bottles for use.

### 2.1.3. Characterization of natural adsorbent and activated carbons

The natural adsorbent and activated carbons obtained were characterized using different techniques. Elemental analysis was carried out using CHSN/O elemental analyzer (Leco Truspec micro) according to standard procedure ASTM D-5373-08 method. TGA was carried out using a Q500 TA Instruments equipment, the temperature was increased from 40°C up to 120°C with an isotherm of 12 min, then it was increased up to 800°C at 40°C/min with an isotherm of 10 min, the two previous stages were carried out in a Nitrogen atmosphere. Then, the gas was changed to $O_2$, and the system was left at 800°C for 25 min.

The textural properties of natural adsorbent and activated carbons were determined by nitrogen adsorption at 77.15 K using Micrometrics ASAP 2020 surface area and porosity analyzer. Specific surface areas ($S_{BET}$) were determined by applying the Brunauer-Emmett-Teller (BET) equation to the isotherm. Additionally, the total pore volume ($V_{TP}$), which corresponds to the

liquid nitrogen volume adsorbed at a relative pressure (P/Po) of 0.98 was determined. The volume of the micropores ($V_{\mu P}$) and external surface area ($S_{EXT}$) were determined using the t-Plot method. The external volume ($V_{EXT}$) was calculated using the difference between $V_{TP}$ and $V_{\mu P}$. The average pore diameter ($D_{AP}$) was calculated using the $4V_{TP}/S_{BET}$ ratio.

Surface functional groups were investigated with Fourier transformed infrared spectroscopy (FTIR) on a Spectrum Two (PerkinElmer, Waltham, Massachusetts, USA), using attenuated total reflectance (ATR). The point of zero charge ($pH_{PZC}$) for all adsorbents were calculated using the addition solid method [104]. Additionally, surface morphology of RH was examined by using a scanning electron microscopy (SEM), using a JEOL JSM-6490LV model. Besides, an energy dispersive spectrometer (EDS) was coupled to the SEM to identify the relative content of elements.

### 2.1.4. Adsorption experiments

### 2.1.4.1. Preparation of synthetic urine

The experimentation process was carried out using distilled water and synthetic urine prepared in the laboratory. The preparation of synthetic urine was carried out according to previous reports [73]. Table 2 details the chemical composition of the urine. The adsorption processes were carried out at room temperature and at 200 rpm using a magnetic stirrer

**Table 2.** Chemical composition of fresh urine [73].

| Fresh urine | |
|---|---|
| Concentration [mg $L^{-1}$] | |
| Urea | 16000 |
| $Na_2SO_4$ | 2300 |
| $NH_4Cl$ | 1800 |
| $NaH_2PO_4$ | 2900 |
| KCl | 4200 |
| $MgCl_2*6H_2O$ | 790 |
| $CaCl_2*2H_2O$ | 680 |

| NaOH | 120 |
|------|-----|

### 2.1.4.2. Operational strategy

For the adsorption tests, a dose of 0.2 g L$^{-1}$ of adsorbents obtained from RH was initially used to evaluate the simultaneous adsorption of AC, DIC, SUL and CIP pharmaceuticals (15 µM) in both distilled water and synthetic urine. The best adsorbent material was chosen based on the percentage of adsorption (%) (Eq. 1).

$$(\%) = \frac{(C_0 - C_e)}{C_0} * 100 \quad \text{Eq. (1)}$$

Where $C_0$ is the initial pollutant concentration (µM) and $C_e$ is the equilibrium pollutant concentration (µM).

The best performing activated carbon was compared against a commercial activated carbon (extraction cartridge) supplied by Y-Carbon, Inc.

### 2.1.5. Adsorption isotherms

### 2.1.5.1. Determination of the adsorption mechanism

To understand the adsorption mechanism of the best-performing activated carbon, concentrations between 5 and 120 mg L$^{-1}$ of ACE and CIP were used. The data were fitted to the Langmuir, Freundlich and Redlich-Peterson isotherms. In addition, kinetic models of pseudo first order, pseudo second order and intraparticle diffusion were evaluated. The comparisons of the applicability of each model of isotherms and kinetics were made on the basis of the linear correlation coefficient ($R^2$ values). To further validate the results, an average percentage error (*APE*) and a normalized standard deviation ($\Delta q$ (%)) were also calculated for the three models obtained, using the following equation:

$$APE\ (\%) = \frac{\sum_{i=1}^{N}\left|\left(\frac{q_{exp} - q_{cal}}{q_{exp}}\right)\right|}{N} * 100 \quad \text{Eq. (2)}$$

$$\Delta q \ (\%) = 100 \ \sqrt{\frac{\Sigma\left(\frac{q_{exp}-q_{cal}}{q_{exp}}\right)^2}{N-1}} \qquad \text{Eq. (3)}$$

Where $q_{exp}$ and $q_{cal}$ are, respectively, the experimental and calculated amounts of pharmaceuticals adsorbed at equilibrium; while *N*, represent the number of measurements. As can be seen, the *APE* and *Δq* indicates the fit between the experimental and predicted values of adsorbed amounts, while $R^2$ shows the fit between the experimental data and linearized forms of the isotherm and kinetic equations. The higher the values of $R^2$ and the lower values of *APE* and *Δq*, the better the goodness of fit.

Furthermore, the thermodynamic parameters of the adsorption of ACE and CIP, in synthetic urine, were determined at different temperatures (25-65°C), adding 0.01 g of adsorbent to 50 mL of ACE and CIP solutions at 40 mg $L^{-1}$. Finally, an adsorption mechanism of the pharmaceuticals evaluated in the proposed matrix was proposed.

Additionally, all the experimental tests were performed at least by duplicate considering a confidence level of 90%.

### 2.1.6. Pharmaceuticals Analysis

The concentration of the pharmaceutical contaminants was monitored using an Agilent 1200 chromatograph, equipped with a LiChrospher® RP-18 column (5 µm) and a UV detector (254, 267, 279 and 276 nm for ACE, SUL, CIP and DIC, respectively). The injection volume was 50 µL. The eluents were acetonitrile (A) and formic acid (10 mM) (B). The flow rate of the mobile phase was 0.5 mL $min^{-1}$. The following gradient was used: 0-3 min 10:90 (A:B v/v); 3-13 min 80:20 (A:B v/v); 13-20 min 100:0 (A:B v/v); 21-25 min 10:90 (A:B v/v).

## CHAPTER 3

## Preparation and characterization of activated carbons from RH and their evaluation in the removal of pharmaceuticals

### 3.1. Introduction

A lot of organic wastes, such as RH, had shown to be efficient in removing different types of pollutants such as pharmaceuticals [105]. However, this adsorptive property can be improved by transforming them in char or activated carbons. Therefore, this chapter evaluate the use of RH as a natural adsorbent and the preparation of char at temperatures of 500°C and 800°C; as well as activated carbons with NaOH, $ZnCl_2$ and $FeCl_3$ as activating agents at 800°C. These materials were characterized by techniques such as TGA, nitrogen adsorption, elemental analysis, FTIR, SEM and EDS. Subsequently, the materials were tested in the elimination of a mixture of ACE, CIP, SUL and DIC in distilled water. Once the materials were evaluated, the best adsorbent was identified, and several washing procedures were applied, decreasing the silica content, to further improve its adsorption capacity. Additionally, the best activated carbon, obtained from the RH, was compared with a commercial activated carbon. Then, the effect of the chemical and mixing structure of the pharmaceuticals and the adsorption on a complex matrix (simulated urine) was evaluated. To better understand the adsorption process in the urine matrix of the two pharmaceuticals with the highest and lowest adsorption percentages, the data were adjusted to the Langmuir, Freundlich and Redlich-Peterson isotherms and the kinetic models of pseudo first order, pseudo second order and intraparticle diffusion were evaluated. On the other hand, thermodynamic parameters such as activation energy (Ea), enthalpy change ($\Delta H°$), entropy change ($\Delta S°$) and Gibbs free energy change ($\Delta G°$) were obtained. Finally, through the FTIR analysis it was possible to propose an adsorption mechanism for the two pharmaceuticals that presented the highest and lowest adsorption percentage.

## 3.2. Results and Discussion

### 3.2.1. Characterization of the activated carbons and starting material

The material adsorption capacity depends on several highly interrelated factors, such as the physicochemical properties of the adsorbent, the chemical characteristics of the adsorbates and the prevailing experimental conditions [106]. Initially, the physicochemical properties of RH, were studied to know some characteristics of the raw material and predict its behavior in the adsorption of pharmaceuticals. However, the surface area BET of RH is low ($0.902 \pm 0.101$ m$^2$ g$^{-1}$), which suggests a poor adsorption ability [89]. Thus, it seems necessary to prepare activated carbons to increase the surface area of the materials and consequently improve the capacity as adsorbents of pharmaceuticals. $ZnCl_2$, NaOH and $FeCl_3$ are among the most widely used activating agents, which are characterized by producing activated carbons with a variety of functional groups, high surface areas and high porous structures [107]. To achieve these good characteristics in the material, this must be activated at high temperatures (between 500°C and 800°C) [89]. Therefore, RH was used as raw material for the preparation of a carbonized at 500°C, and then it was activated with $ZnCl_2$, NaOH and $FeCl_3$ at a temperature of 800°C. The materials obtained were denoted with the initials of the precursor, followed by the activating agent and finally the temperature at which they were activated. Therefore, the carbons were denoted as follow: RH-NaOH-800°C, RH-$ZnCl_2$-800°C, RH-$FeCl_3$-800°C, as well the controls of the carbonized at 500 and 800°C (RH-500°C and RH-800°C, respectively) were prepared. In this way, to know the elemental composition and the stability of the materials, a TGA analysis was carried out for RH, RH-500°C, RH-800°C, RH-NaOH-800°C, RH-$ZnCl_2$-800°C and RH-$FeCl_3$-800°C (Fig. 3 (a), (b), (c), (d), (e) and (f), respectively).
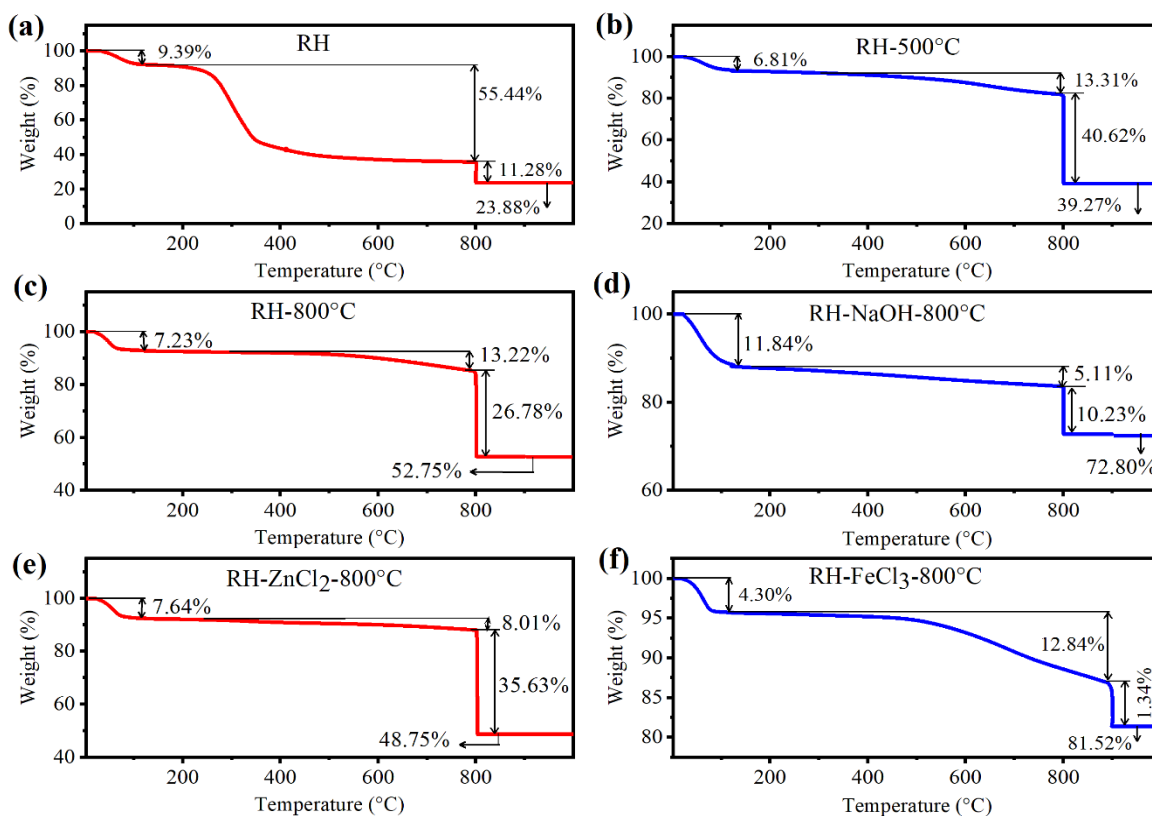
**Figure 3.** TGA profile of RH and activated carbons prepared from RH. (a) RH; (b) RH-500°C; (c) RH-800°C; (d) RH-NaOH-800°C; (e) RH-ZnCl2-800°C; (f) RH-FeCl3-800°C.

Fig. 3 (a) show three events for RH. The first event happens at a temperature lower than 150 °C, which corresponds to the released of moisture and adsorbed water from the surface. The subsequent stage at 150 – 400 °C shows a steep weight loss of approximately 55.44%, which can be associated to the de-volatilization of hemicellulose and cellulose [108]. Then, the third stage at reaction temperature of 500 – 800 °C with total weight loss of 11.28%, corresponds to the decomposition of lignin [109].

In the case of RH carbonized at 500 and 800°C (Fig. 3 (b), (c), respectively) and of the activated carbons RH-NaOH-800°C, RH-ZnCl$_2$-800°C and RH-FeCl$_3$-800°C (Fig. 3 (d), (e), (f), respectively) three stages in the TGA are also evident. The first stage (<150 ° C) showed a lower humidity loss than the starting material suggesting that these material have a more

hydrophobic character. However, RH-NaOH-800°C (Fig 3 (d)) presented a humidity higher than RH indicating a high hydrophilicity on the activated carbon surface [110]. Next, the second stage occurred between 150 and 800°C for all materials (Fig. 3 (b), (c), (d), (e), (f)), which showed with respect to RH (Fig. 3 (a)), a decrease of volatile compounds equal or higher to 37%. These results indicate the efficiency of high temperatures and activating agents to eliminate volatile compounds, which give rise to a carbon-rich structure. Consequently, the third stage for some materials occurred at 800°C or 900°C (Fig. 3 (b)-(f)). RH-500°C and RH-800°C (Fig. 3 (b), (c), respectively) showed a fixed carbon content higher than RH. This is consistent with the high temperatures used in their preparation, which breaks the least stable chemical bonds present in the material, remove heteroatoms in the form of simple gas or liquid compounds, and consequently order the carbonaceous structure [111]. Additionally, RH-$ZnCl_2$-800°C (Fig. 3 (e)), presented a higher percentage of fixed carbon than RH, due to the fact that $ZnCl_2$ acts as a dehydrating agent and at high temperatures it evaporates giving rise to the formation of a porous structure with high carbon content [112]. The opposite happened for RH-NaOH-800°C and RH-$FeCl_3$-800°C (Fig. 3 (d), (f), respectively), which decreased the percentage of fixed carbon with respect to the starting material. The phenomenon occurred with $FeCl_3$, is because this activating agent at high temperatures react strongly with the carbonaceous matrix causing in some cases the destruction of the carbon [113]. While that the result with NaOH is attributed to the reaction that this activation agent has with the C, where $CO_2$ is produced generating porosity [114]). Finally, at 800°C or 900°C, the atmosphere was changed from $N_2$ to $O_2$, where all the materials prepared showed, as expected, a higher percentage of ashes than those reported for RH. The percentage of volatile material, fixed carbon and ash in dry base of the raw material and activated carbons obtained from the TGA profiles are summarized in Table 3.

**Table 3.** Yield, elemental and proximate analysis of natural adsorbent, RH carbonized at different temperatures without activating agents and activated carbons prepared from RH.

| Adsorbent | Elemental Analysis | | | | | Proximate Analysis (dry base) | | |
|---|---|---|---|---|---|---|---|---|
| | Yield (wt. %) | C (wt. %) | H (wt. %) | N (wt. %) | O (wt. %) | Volatile Matter (wt. %) | Fixed Carbon (wt. %) | Ash (wt. %) |
| **RH** | - | 36.00 | 3.9 | 0.56 | 38.00 | 61.19 | 12.45 | 26.37 |
| **RH-500°C** | 40.00 | 54.6 | 0.7 | 0.0 | 5.2 | 14.27 | 43.56 | 42.17 |
| **RH-800°C** | 39.00 | 28.1 | 0.0 | 0.0 | 18.9 | 14.22 | 28.88 | 56.90 |
| **RH-NaOH-800°C** | 18.70 | 27.4 | 0.0 | 0.0 | 0.0 | 5.79 | 11.58 | 82.63 |
| **RH-ZnCl$_2$-800°C** | 17.76 | 36.8 | 0.0 | 0.7 | 13.5 | 8.66 | 38.57 | 52.77 |
| **RH-FeCl$_3$-800°C** | 43.88 | 27.3 | 0.0 | 0.8 | 0.0 | 13.42 | 1.40 | 85.18 |

Conventions: The first two letters refer to the starting material, NaOH, ZnCl$_2$ and FeCl$_3$ are the agents used to activate the carbons, and the number means the temperature at which the carbons were activated.

The information of Table 3 confirms that the carbonized and activation processes at high temperatures reduces in the materials the content of volatile material, and according to the activating agent, increase or decrease the fixed carbon content. In addition, the preparation process increased the ash content in the material. FTIR analysis of RH, as well as the carbonized at different temperatures without activating agents and activated carbons prepared from RH are shown in Fig. 4.
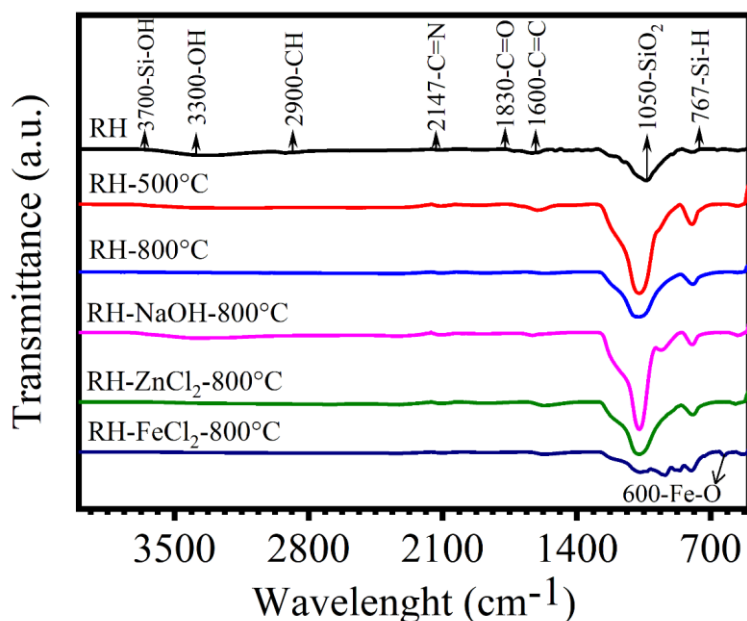
**Figure 4.** FTIR spectrum of natural adsorbent, RH carbonized at different temperatures without activating agents and activated carbons prepared from RH.

In Fig. 4, a band between 3200 cm$^{-1}$ and 3700 cm$^{-1}$ assigned to the -OH stretching of carboxyl groups (-COOH), alcohols (R-OH) and phenols (-Ph-OH) [115] is observed in RH. The peak between 3000 cm$^{-1}$ and 2800 cm$^{-1}$ could be attributed to the vibration of aliphatic groups (C-H) of cellulose and hemicellulose present in RH [112-113]. Also, cyanate groups can be observed through –N=C=O vibrations at wavelength 2147 cm$^{-1}$ [118]. Vibrations between 1700 cm$^{-1}$ and 1800 cm$^{-1}$, are attributed to the C=O stretching in the ketones or carboxyl groups [119], [120]. Others vibrations around 1440 cm$^{-1}$ and 1600 cm$^{-1}$, are associated with the aromatic skeleton C=C stretching [121]. The materials presented a band between 900 cm$^{-1}$ and 1200 cm$^{-1}$, which is characteristic of the $SiO_2$ functional groups [122], the band at 767 cm$^{-1}$ is attributed to the Si-H functional groups, while the band in the region at 3700 cm$^{-1}$ can be assigned to the Si-OH stretching [122].

Besides, after the carbonization and activation process, the Fig. 4 showed a decrease in the band between 3200 cm$^{-1}$ and 3700 cm$^{-1}$ of the OH stretching for RH-NaOH-800°C, while for the

other materials prepared, this band disappears. This is associated with the elimination of alcohols and phenols present in cellulose, hemicellulose and lignin, respectively. The result was confirmed by elemental analysis, which showed a decrease or elimination of O and H for all materials with respect to the starting material (Table 3).

On the other hand, Fig. 4 shows that compared to RH, in the prepared materials the band at 2900 cm$^{-1}$ disappeared due to the breaking of the chains of the aliphatic groups of cellulose, hemicellulose and lignin. Regarding the band around 2147 cm$^{-1}$ of the –N=C=O vibrations of the cyanate groups, it continues to be observed for all materials. However, the elemental analysis only reports the presence of N for RH-ZnCl$_2$-800°C and RH-FeCl$_3$-800°C (Table 3), possibly because the nitrogen content of the other materials is below of the detection limit of the technique. Furthermore, there was an increase in the C=C band around 1600 cm$^{-1}$ for RH-500°C (Fig. 4) and RH-ZnCl$_2$-800°C (Fig. 4) due to the formation of aromatic rings, which agrees with the higher C content reported in elemental analysis for these two materials (Table 3). The other materials prepared (RH-800°C, RH-NaOH-800°C and RH-FeCl$_3$-800°C (Fig. 4), showed a decrease in this band, associated with the effect of high temperature (800°C) and the use of NaOH and FeCl$_3$, which managed to destroy a large part of the carbonaceous structure. This was confirmed by the low percentage of C determined in the elemental analysis (Table 3).

Surprisingly, the band at 1050 cm$^{-1}$ increased its sharpness for carbonized and activated carbons with NaOH and ZnCl$_2$ (Fig. 4), evidencing an increase in SiO$_2$ functional groups in the structure of the materials. For the case of RH-FeCl$_3$-800°C (Fig. 4), the band was less sharp, due to the iron loading [123], in fact bands under 600 cm$^{-1}$ associated to the Fe-O vibrations are observed [124]. Additionally, the band at 767 cm$^{-1}$ increased for all materials (Fig. 4), indicating the increase of Si-H functional groups in the carbonaceous structure. Thus, the presence of SiO$_2$ and Si-H in charred and activated carbons can be related to the high ash content reported by the

TGA analysis (Table 3). The superior ash percentage for the iron activated carbon, can be explained with the iron incorporation to the material.

Despite the disappearance and elimination of some bands in the charred and activated carbons, it is important to highlight that RH-500°C and RH-800°C, presented interesting yields in the process (Table 3). This indicates the import of high temperatures in the preparation of the materials [125]. However, RH-FeCl$_3$-800°C was the one that presented the highest yield (Table 3), this can be due to the loaded iron species on the surface of the material [126], [127].

Additionally, the surface area of RH, carbonized materials and activated carbons was studied by nitrogen physisorption applying the BET methodology (Fig. 5 (a) and (b)) and their characteristic parameters of the porous structure are summarized in Table 4.
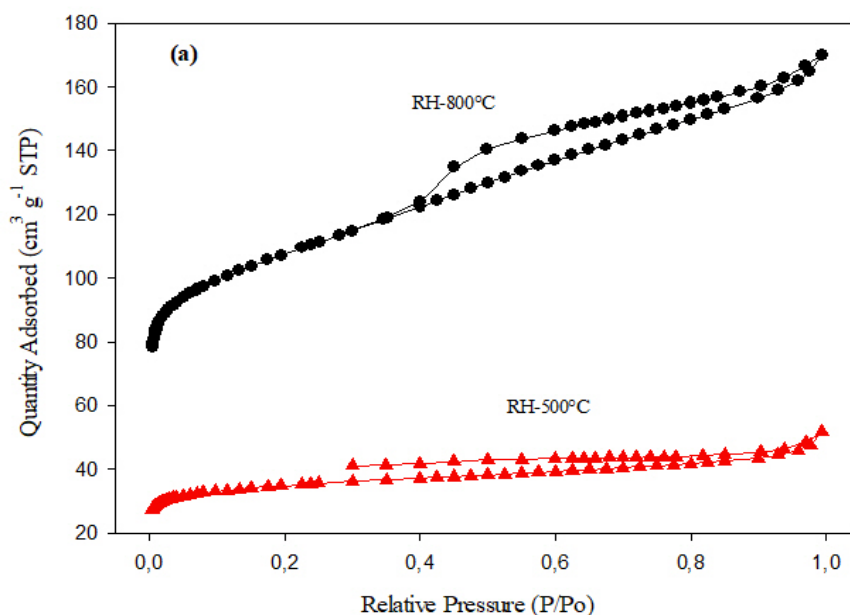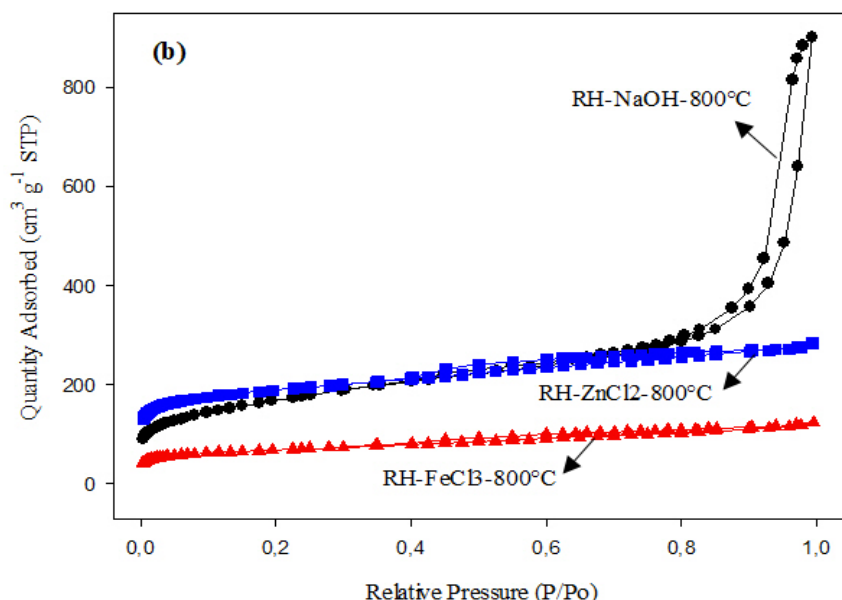
**Figure 5.** Nitrogen adsorption/desorption isotherms. (a) RH carbonized at different temperatures without activating agents; (b) Activated carbons prepared from RH.

**Table 4.** Characteristic parameters of the porous structure of natural adsorbent, RH carbonized at different temperatures without activating agents and activated carbons prepared from RH.

| Adsorbent | N₂ Physisorption | | | | | | |
|---|---|---|---|---|---|---|---|
| | $S_{BET}$ (m² g⁻¹) | $S_{UP}$ (m² g⁻¹) | $S_{EXT}$ (m² g⁻¹) | $V_{UP}$ (cm³ g⁻¹) | $V_{EXT}$ (cm³ g⁻¹) | $V_{TP}$ (cm³ g⁻¹) | $D_{AP}$ (nm) |
| **RH** | $0.902 \pm 0.101$ | - | - | - | - | - | - |
| **RH-500°C** | $106.09 \pm 2.862$ | 66.40 | 39.69 | 0.037 | 0.043 | 0.08 | 3.015 |
| **RH-800°C** | $341.55 \pm 6.550$ | 159.65 | 181.90 | 0.087 | 0.173 | 0.26 | 3.079 |
| **RH-NaOH-800°C** | $579.12 \pm 7.627$ | 45.24 | 533.88 | 0.027 | 1.363 | 1.39 | 9.629 |
| **RH-ZnCl₂-800°C** | $573.48 \pm 19.877$ | 293.37 | 302.36 | 0.160 | 0.280 | 0.44 | 2.959 |
| **RH-FeCl₃-800°C** | $223.49 \pm 4.123$ | 77.12 | 146.36 | 0.043 | 0.147 | 0.19 | 3.410 |

Conventions: The first two letters refer to the starting material, NaOH, ZnCl₂ and FeCl₃ are the agents used to activate the carbons, and the number means the temperature at which the carbons were activated. Specific surface areas ($S_{BET}$), micropores surface area ($S_{UP}$), external surface area ($S_{EXT}$), volume of the micropores ($V_{UP}$), external volume ($V_{EXT}$), the total pore volume ($V_{TP}$), average pore diameter ($D_{AP}$).

The nitrogen adsorption/desorption isotherms of Fig. 5 (b), showed that the amount of $N_2$ adsorbed with increasing relative pressure (P/P$_0$) was higher for RH-NaOH-800°C and decreased for RH-ZnCl$_2$-800°C, followed by RH-800°C (Fig. 5 (a)), RH-FeCl$_3$-800°C (Fig. 5 (b)) and RH-500°C (Fig. 5 (a)). Consequently, the V$_{TP}$ followed the order: RH-NaOH-800°C >RH-ZnCl$_2$-800°C> RH-800°C> RH-FeCl$_3$-800°C> RH-500°C (Table 4). Regarding the S$_{BET}$ for RH-NaOH-800°C and RH-ZnCl$_2$-800°C was higher than in the other materials (Table 4), obtaining values of 573.48 and 579.12 m$^2$ g$^{-1}$ for activated carbons with ZnCl$_2$ and NaOH, respectively (Table 4); for the latter, similar BET surface areas were reported in the literature [128]. The development of higher surface area obtained for activated carbon with NaOH is attributed to the high reactivity, which breaks the C-O-C and C-C bonds of the carbonized. Thus, NaOH is reduced to metallic sodium Na, hydrogen gas and sodium carbonate Na$_2$CO$_3$. In the presence of $N_2$ gas under elevated temperature, further activation occurs by the degradation of Na$_2$CO$_3$ into CO, CO$_2$ and Na. Then, Na ions are entrapped into the pores, which leads to the development of porosity [129]. Additionally, NaOH has a boiling point of 883°C, which is above of the activation temperature. This allowed a controlled reaction where the Na was diffused into the layer of carbon, causing the enhancement of porosity in the material which increasing the surface area [128], [130]. For the case of RH-ZnCl$_2$-800°C, the boiling point of ZnCl$_2$ is 732°C, therefore, at 800°C the smaller pores are prone to collapse, hence decreasing the surface area, showing S$_{BET}$ similar to RH-NaOH-800°C (Table 4) [131]. On the other hand, RH-FeCl$_3$-800°C presented a lower S$_{BET}$ (Table 4), because the high activation temperature resulted in a stronger interaction of the iron with the carbon matrix forming iron oxides [132]. These species of iron are not efficiently extracted during the washing step, which is consistent with the significant increase in the ash content (Table 3) [124]. Results for RH-500°C and RH-800°C (Table 4) suggest that for the development of materials with prominent surface areas the

use of high temperatures is preferred. In fact, 800°C is more efficient to break the chains of cellulose, hemicellulose and lignin, which benefices the formation of a porous structure [133]. However, if greater surface area development is required the addition of NaOH or $ZnCl_2$ should be considered.

Additionally, the isotherms of Fig. 5 (a) and (b) can be classified according to IUPAC [134]. RH-500°C, RH-800°C, RH-NaOH-800°C, RH-$ZnCl_2$-800°C and RH- $FeCl_3$-800°C (Fig. 5 (a) for carbonized materials without activating agents and (b) for activated carbons), show type IV isotherms of mesoporous adsorbents [134]. The analysis is consistent with that reported in Table 4, which indicates that these materials have higher $S_{EXT}$ and lower $S_{\mu P}$. Consequently, carbonized materials and activated carbons have a higher $V_{EXT}$ than $V_{\mu P}$ (Table 4). The higher development of $S_{EXT}$ in carbonized materials and activated carbons is associated with the high content of silica in RH. Silica was not completely eliminated at 800°C or using NaOH, $ZnCl_2$ and $FeCl_3$, which prevented the rupture of some lignin bonds and the penetration of activating agents into the internal structure of RH, generating carbonized and activated carbons with large pores [135]. Additionally, according to the IUPAC classification, the isotherms for RH-500°C, RH-800°C, RH-$ZnCl_2$-800°C and RH-$FeCl_3$-800°C (Fig. 5 (a) for carbonized materials without activating agents and (b) for activated carbons) showed hysteresis loops H4 associated with a narrow slit-like pore, while RH-NaOH-800°C (Fig. 5 (b)) had a hysteresis H3 loops indicating the formation of slit-shaped pores [134]. On the other hand, the pore size distribution (PSD$_S$) of carbon samples prepared from RH is shown in Fig. 6.
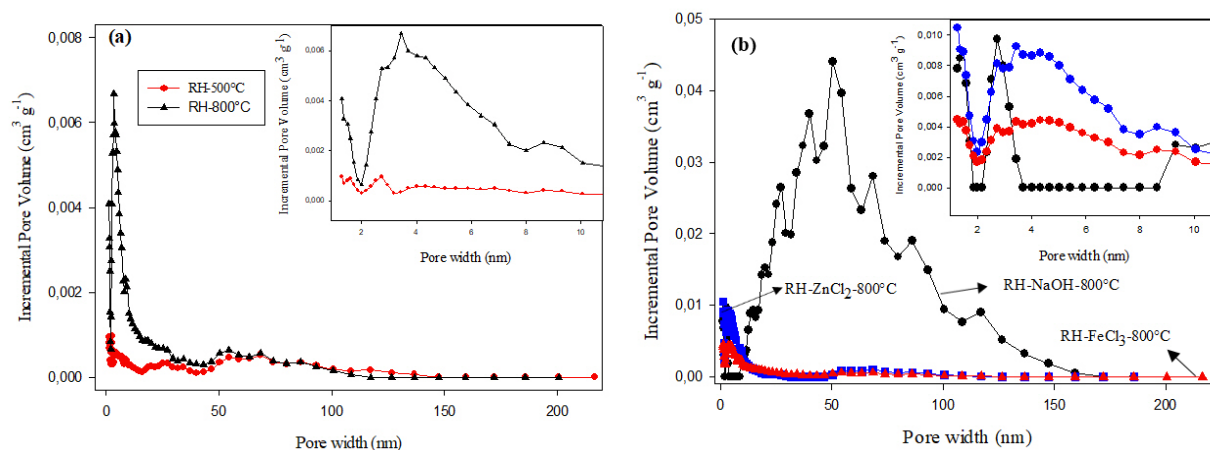
**Figure 6.** PSD$_S$ of carbons samples prepared from RH. (a) RH carbonized at different temperatures without activating agents; (b) Activated carbons prepared from RH to 800°C.

The PSD$_S$ shows that RH-500°C, RH-800°C, RH-ZnCl$_2$-800°C and RH-FeCl$_3$-800°C have the highest pore distribution in a region below 8.0 nm (Fig. 6 (a) and (b)). In fact, a D$_{AP}$ between 2.950 and 3.410 nm was reported for these materials (Table 4), confirming a higher development of mesoporosity. For the case of RH-NaOH-800°C, a wide distribution of pores is observed in the range between 8.0 nm and 160 nm (Fig. 6 (b)); having a D$_{AP}$ of 9.629 nm (Table 4). This is consistent with its superior development of mesopores.

The development of porosity can be observed in the SEM micrographs of the Fig. 7. As seen in Fig. 7 (a), RH present a rough surface. RH-NaOH-800°C shows a significant increase in the porosity (Fig. 7 (d)). A less porous surface was observed for RH-ZnCl$_2$-800°C, followed by RH-800°C, RH-FeCl$_3$-800°C, and RH-500°C (Fig. 7 (e), (c), (f) and (b), respectively). These results confirm the effect of high temperatures and activating agents in the preparation of porous materials.
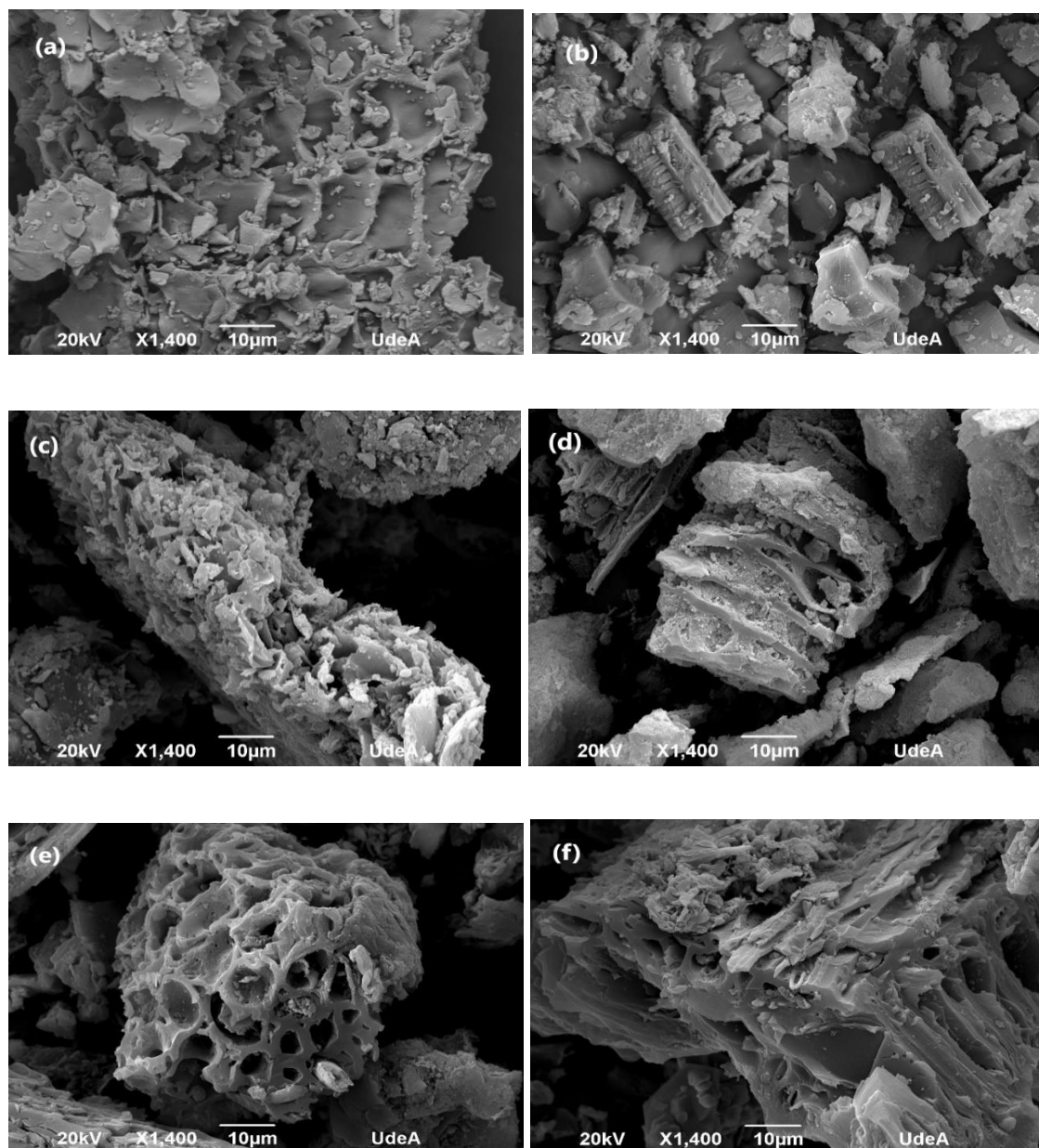
**Figure 7.** SEM micrographs carbonaceous materials prepared from RH. (a) RH; (b) RH-500°C; (c) RH-800°C; (d) RH-NaOH-800°C; (e) RH-ZnCl2-800°C; (f) RH-FeCl3-800°C.

The carbonized materials and activated carbons showed a series of physicochemical characteristics such as the presence of functional groups and the development of high surface with pores of different sizes which makes them interesting to be evaluated in the removal of pharmaceuticals from waters. Therefore, in the next section, the ability of materials prepared from RH, will be evaluated in the removal of ACE, CIP, SUL and DIC.

### 3.2.2. Preliminary evaluation of the adsorption of pharmaceutical in waters on the prepared material

The starting material (RH) (Fig. 8 (a)), carbonized materials at 500°C and 800°C (Fig. 8 (b) and (c), respectively) and activated carbons RH-NaOH-800°C, RH-ZnCl$_2$-800°C and RH-FeCl$_3$-800°C (Fig. 8 (d), (e) and (f), respectively) were used to remove the pharmaceuticals ACE, CIP, SUL, DIC present in a mix in distilled water.
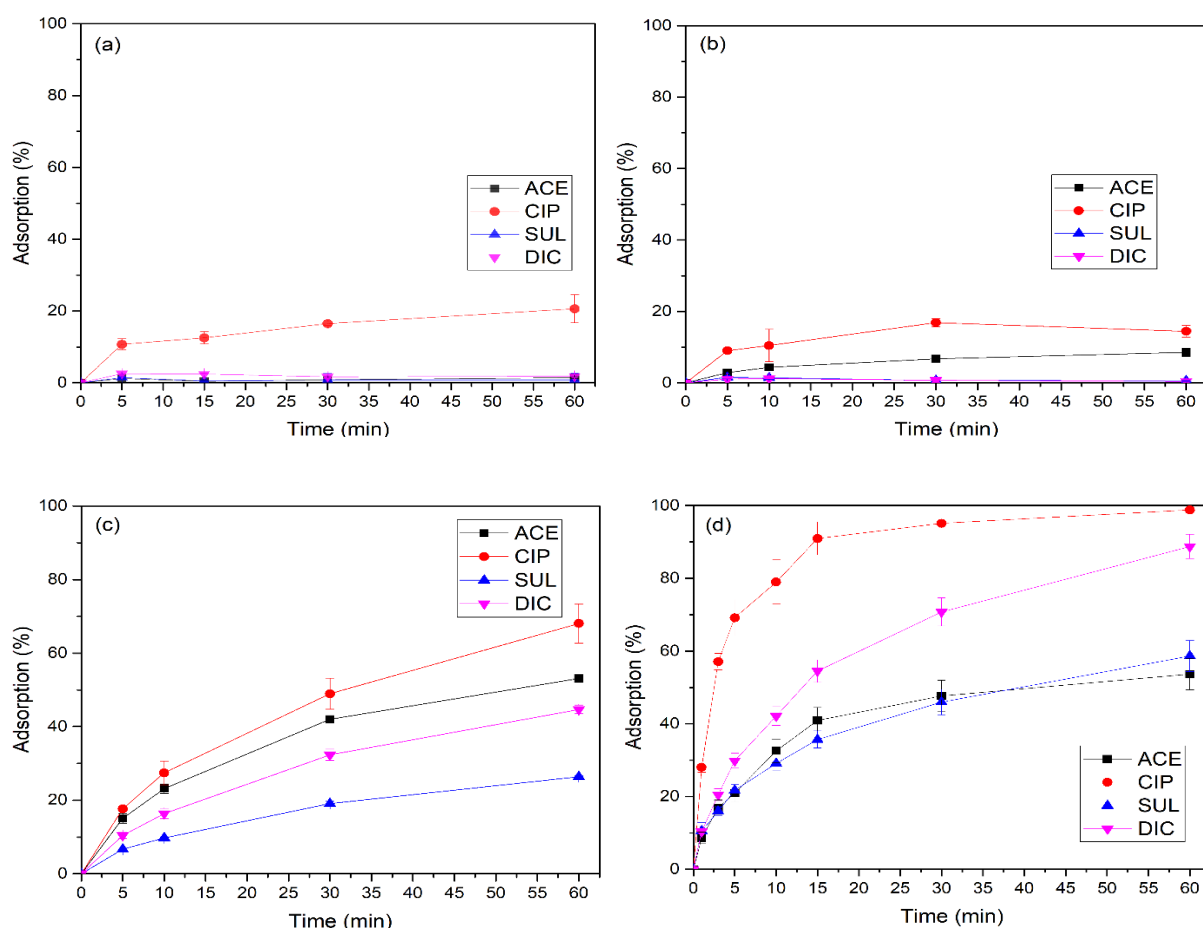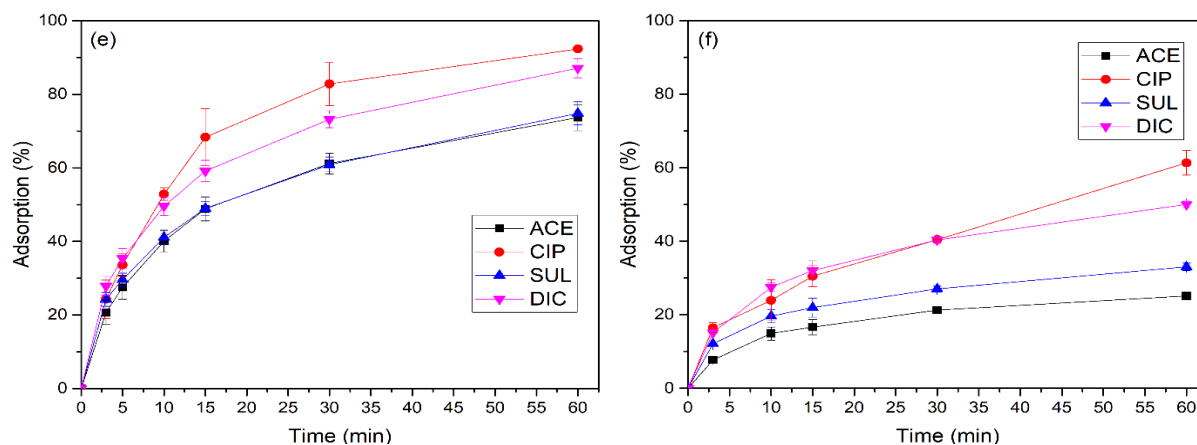
**Figure 8.** Adsorption of pharmaceuticals mixed in aqueous solution, using as activated carbon adsorbents prepared from RH and activated with NaOH, $ZnCl_2$ and $FeCl_3$ at temperature of 800°C. Conditions: Pharmaceuticals concentration 15 µM, adsorbent dose $0.2\ g\ L^{-1}$, pH 5.8 – 6.5 , particle size 75 – 150 µm, temperature 25°C, stirring rate 200 rpm. (a) RH; (b) RH-500°C; (c) RH-800°C; (d) RH-NaOH-800°C; (e) RH- $ZnCl_2$-800°C; (f) RH-$FeCl_3$-800°C.

These contaminants have a different molecular size. For example, for ACE it is 0.95 x 0.6 x 0.3 nm, CIP has 1.35 x 0.3 x 0.74 nm, SUL has 1.33 x 0.47 x 0.38 nm and DIC has 1.1 x 0.8 x 0.5 nm. Therefore, these can be adsorbed on the porosity of RH-500°C, RH-800°C, RH-NaOH-800°C, RH-$ZnCl_2$-800°C and RH-$FeCl_3$-800°C, which presented a $D_{AP}$ between 2.959 nm and 9.629 nm (Table 4). However, in addition to $D_{AP}$, the adsorption of pharmaceuticals can be influenced by other characteristics such as the $pH_{PZC}$ of the material (Fig. 9), and the pKa of the pollutant [136].
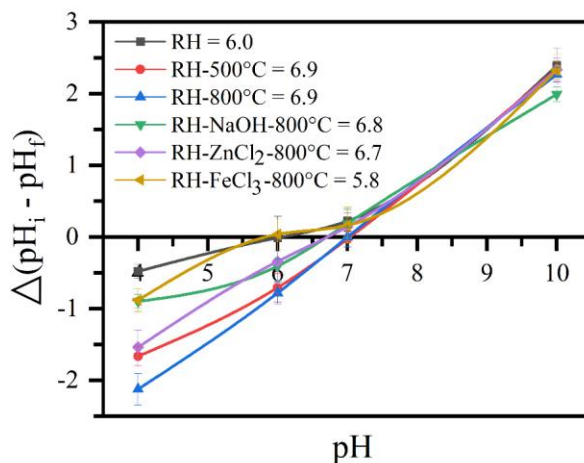
**Figure 9.** Determination of the $pH_{PZC}$ of natural adsorbent, RH carbonized at different temperatures without activating agents and activated carbons prepared from RH.

In this way, according to the value of their $pH_{PZC}$ (Fig. 9), at the pH of the solution (6.5) RH and RH-FeCl$_3$-800°C are negatively charged, while RH-500°C, RH-800°C, RH-ZnCl$_2$-800°C and RH-NaOH-800°C are predominantly positively charged. In it turn, at the pH of the experiment, ACE (pKa of 9.5) is in its neutral form [137]. Therefore, ACE adsorption should not be influenced by charges. Thus, the best ACE adsorption presented by RH-ZnCl$_2$-800°C (Fig. 8 (e)) can be associated with the proportional development of $S_{\mu P}$ and $S_{EXT}$ (Table 4), which allowed the transport of the pollutant through the macropores and mesopores to reach the micropores [138].

Acetaminophen is the smallest tested compound, which can go through the micropores of the materials. Interestingly, adsorption in RH-NaOH-800°C and RH-800°C was similar (see Fig. 8 and Table 5). This is probably because in spite of RH-NaOH-800°C has a higher surface area (BET), RH-800°C developed a higher microporosity (see Table 4). Additionally, RH-500°C and RH-FeCl$_3$-800°C (Fig. 8 (b) and (f), respectively), also presented a disproportionality between $S_{\mu P}$ and $S_{EXT}$; however, ACE adsorption was low due to its small $V_{TP}$ (Table 4). In this

way, it is possible to say that a high proportional development of $S_{\mu P}$ and $S_{EXT}$ and/or a development of microporosity in the material favors the adsorption of ACE.

In the case of CIP, removals are observed with all materials (Fig. 8-(CIP adsorption)). The pollutant is in its zwitterionic form ($pKa_1 = 6.1$, $pKa_2 = 8.7$) [139], where its negative charges are forming electrostatic attractions with the positive charges of RH-500°C, RH-800°C, RH-NaOH-800°C and RH-ZnCl$_2$-800°C. The opposite occurs for RH and RH-FeCl$_3$-800°C (Fig. 8 (a) and (f), respectively), which are negatively charged interacting with the positive charges of the pollutant. Despite the fact that CIP adsorption was possible due to the attraction of charges between the contaminant and the materials, the process was better using RH-NaOH-800°C (Fig. 8 (d)). This good result of RH-NaOH-800°C can be attributed to its highest $V_{TP}$ and $S_{EXT}$ associated with the its greater presence of mesopores (Table 4) [140], [141]. Therefore, it is possible to indicate that the adsorption of CIP with the different materials is through electrostatic attractions, but the process can be improved using activated carbons with high $S_{EXT}$ and $V_{TP}$.

On the other hand, SUL is negatively charged ($pKa_1 = 1.7$ and $pKa_2 = 5.6$) [139] presenting a repulsion with RH and RH-FeCl$_3$-800°C (Fig. 9). Despite the repulsive effect of the charges, it is observed that RH-FeCl$_3$-800°C removed around 30% of the contaminant in 60 min (Fig. 8 (f)), possibly due to the development of $S_{BET}$ (Table 4). Regarding RH-500°C, despite being favorable the electrostatic attraction with the contaminant, there is no appreciable adsorption (Fig. 8 (b)), possibly due to the low development of $S_{BET}$ of the material (Table 4). Furthermore, SUL removal was observed using RH-800°C, RH-NaOH-800°C and RH-ZnCl$_2$-800°C (Fig. 8 (c), (d) and (e), respectively), because these materials were positively charged, forming interactions with the negative charges of the pollutant. However, the best adsorption was achieved with RH-ZnCl$_2$-800°C (Fig. 8 (e)) because it presented a higher content of $S_{\mu P}$ compared to the other materials (Table 4). This indicates that the adsorption of SUL can be

governed by attraction of charges and it can be improved by using an activated carbon with high $S_{\mu P}$. Interestingly, in the materials RH-NaOH-800°C and RH-ZnCl2-800°C, the adsorption of SUL and ACE presented similar behavior, which can be explained by the high development of surface area and microporosity in these materials, which facilitated the retention of ACE in the pores and the electrostatic attraction of SUL on the surface of the adsorbents.

Additionally, the adsorption of DIC, which was negatively charged (pKa 4.15) [142] was evaluated. Therefore, it presented a repulsion with RH and RH-FeCl$_3$-800°C (Fig. 8 (a) and (f), respectively) and an attraction with RH-500°C, RH-800°C, RH-NaOH-800°C and RH-ZnCl$_2$-800°C (Fig. 8 (b), (c), (d) and (e), respectively). However, RH-FeCl$_3$-800°C (Fig. 8 (f)) showed 50% of DIC removal in 60 min, possibly because this material developed $S_{BET}$ (Table 4). However, the best adsorption was achieved with the material impregnated with NaOH (Fig. 8 (d)) associated with the greater development of $S_{EXT}$ and mesopores content greater of 9.0 nm (Table 4). In this way, it can be indicated that the removal of DIC is favored in materials having a high $S_{EXT}$, which can be improved by attraction of charges between the contaminant and the material.

Additionally, the efficiency of each material was analyzed for the removal of contaminants in the mixture. In this way, it was found that the adsorbent capacity of pharmaceuticals on RH has the following order: CIP > SUL > DIC > ACE (Fig. 8 (a)). These results can be explained considering the molecular size in length, height, and width of the pharmaceuticals. For example, the molecular size of SUL is 1.33 x 0.47 x 0.38 nm [143], CIP is 1.35 x 0.3 x 0.74 nm [144], ACE is 0.95 x 0.6 x 0.3 nm and DIC is 1.1 x 0.8 x 0.5 nm [145]. Therefore, the similar adsorption of SUL and CIP is because these two contaminants have a molecular length greater than DIC and ACE, which allowed them to reach the surface of RH faster.

Additionally, using RH-500°C and RH-800°C (Fig. 8 (b) and (c), respectively), the pollutant removal order was CIP > ACE > DIC > SUL. Furthermore, it was observed that the activated carbons (Fig. 8 (d), (e) and (f)) showed the following order of adsorption of the pollutants CIP > DIC > SUL > ACE. The efficiency of the materials to remove CIP is associated with the zwitterionic form of the molecule that allows it to be attracted with positive and negative charges at the same time [146]. Also, the good removal of CIP may be related with the molecular size of this contaminant [144]. Thus, the greater length and lower height molecular allowed it to reach the porous structure of carbonized and activated carbons faster than the other pharmaceuticals [147]. For the other pollutants (DIC, SUL and ACE), the adsorbent capacity decreased, possibly due to a mixture of characteristics related to the molecular size of the pollutants (decrease in length and increase in molecular height), affinity for fillers and porosity sizes [148]. To determine the best adsorbent, the total adsorption of pharmaceuticals was calculated for each material and the results are listed in Table 5.

**Table 5.** Total adsorption of pharmaceutically using materials prepared from RH. The total milligrams (mg g$^{-1}$) of the pharmaceutical compounds are taken after 60 minutes adding the adsorbed milligrams for each pharmaceutically. Condition: concentration of contaminants: 15 µM , adsorbent dose $0.2 \ g \ L^{-1}$.

| Adsorbent | ACE (mg g$^{-1}$) | CIP (mg g$^{-1}$) | SUL (mg g$^{-1}$) | DIC (mg g$^{-1}$) | Total adsorption (mg g$^{-1}$) |
|---|---|---|---|---|---|
| **RH** | $0.0 \pm 0.001$ | $5.20 \pm 0.019$ | $0.53 \pm 0.002$ | $0.43 \pm 0.141$ | $6.16 \pm 0.157$ |
| **RH-500°C** | $1.03 \pm 0.139$ | $4.63 \pm 0.178$ | $0.33 \pm 0.039$ | $0.46 \pm 0.004$ | $6.45 \pm 0.353$ |
| **RH-800°C** | $6.37 \pm 0.095$ | $18.03 \pm 1.416$ | $5.28 \pm 0.058$ | $10.49 \pm 0.27$ | $40.17 \pm 1.646$ |
| **RH-NaOH-800°C** | $6.44 \pm 0.017$ | $26.18 \pm 0.001$ | $11.72 \pm 0.04$ | $20.86 \pm 0.04$ | $65.21 \pm 0.100$ |
| **RH-ZnCl$_2$-800°C** | $8.18 \pm 0.003$ | $23.92 \pm 0.001$ | $13.51 \pm 0.08$ | $19.18 \pm 0.04$ | $64.79 \pm 0.039$ |
| **RH-FeCl$_3$-800°C** | $3.01 \pm 0.127$ | $16.26 \pm 0.884$ | $6.61 \pm 0.211$ | $11.76 \pm 0.24$ | $37.65 \pm 0.304$ |

Conventions: The first two letters refer to the starrting material; $ZnCl_2$, $FeCl_3$ and NaOH are the agents used to activate the carbons, and the number means the temperature at which the carbons were activated.

Among the best materials for the removal of the four contaminants are RH-$ZnCl_2$-800°C and RH-NaOH-800°C, with an accumulative adsorption of the pollutants of 64.79 mg g$^{-1}$ and 65.21 mg L$^{-1}$, respectively (Table 5). In addition, it has been reported that washing with NaOH could lead to eliminate the silica present in the raw material [149] or the ashes contained in the activated carbon [150]. Thus, this information increases the interest to continue studying the adsorbent and surface characteristics of RH-NaOH-800°C. Consequently, RH-NaOH-800°C will be washed with NaOH (RH-NaOH-800°C post-washed) and a new activated carbon will be also prepared under the same conditions using RH previously washed with NaOH (RH-NaOH-800°C pretreated). Possible changes in the materials will be the subject of investigation in the next section.

### 3.2.3. Effect of the removal of ash from RH-NaOH-800°C on the adsorption of pharmaceuticals

RH-NaOH-800°C post-washed and RH-NaOH-800°C pretreated, showed changes in the surface with respect to RH-NaOH-800°C, which are reported in Tables 6 and 7. Thus, in the new materials, a decrease in the yield was observed, which is consistent with the loss of material in the pre-wash and post-washed with the NaOH step. However, the activated carbons increased the carbon and oxygen content according to the elemental analysis; and according to the TGA increased their fixed carbon and decreased their ash content (Table 6). These changes suggest better adsorbent characteristics in the new activated carbons, indicating that it is possible to eliminate or reduce the silicon using NaOH to wash the activated carbon or to pretreat the raw material [92].

**Table 6.** Activation process yield, pH$_{PZC}$, proximate analysis in dry base, elemental and EDS analysis of activated carbons prepared from RH and activated with NaOH at 800°C, with normal, pretreated and post-washed processes.

| Characteristics | Material | | |
|---|---|---|---|
| | RH-NaOH-800°C | RH-NaOH-800°C post- washed | RH-NaOH-800°C pretreated |
| **Yield (wt. %)** | 18.70 | 5.43 | 3.45 |
| **pH$_{PZC}$** | 6.8 | 7.1 | 7.6 |
| **Proximate analysis – dry base (wt. %)** | | | |
| Volatile matter | 5.8 | 15.4 | 8.9 |
| Fixed carbon | 11.6 | 75.8 | 50.7 |
| Ash | 82.6 | 8.8 | 40.4 |
| **EDS analysis (wt. %)** | | | |
| Si | 72.6 | 7.3 | 36.4 |
| **Elemental analysis (wt. %)** | | | |
| C | 27.4 | 73.7 | 53.6 |
| H | - | - | - |
| O | - | 19.0 | 10.0 |
| N | - | - | - |

Conventions: The first two letters refer to the starting material, NaOH is the agent used to activate the carbon, and the number means the temperature at which the carbons were activated.

**Table 7.** Characteristic parameters of the porous structure of the activated carbons prepared from RH and activated with NaOH at 800°C, with normal, pretreated and post-washed processes.

| Adsorbent | N₂ Physisorption | | | | | | |
|---|---|---|---|---|---|---|---|
| | $S_{BET}$ $(m^2\,g^{-1})$ | $S_{UP}$ $(m^2\,g^{-1})$ | $S_{EXT}$ $(m^2\,g^{-1})$ | $V_{UP}$ $(cm^3\,g^{-1})$ | $V_{EXT}$ $(cm^3\,g^{-1})$ | $V_{TP}$ $(cm^3\,g^{-1})$ | $D_{AP}$ $(nm)$ |
| **RH-NaOH-800°C** | 579.12 ± 7.627 | 45.24 | 533.88 | 0.027 | 1.363 | 1.39 | 9.629 |
| **RH-NaOH-800°C post-washed** | 1671.55 ± 30.87 | 52.52 | 1619.03 | 0.044 | 1.106 | 1.15 | 2.763 |
| **RH-NaOH-800°C pretreated** | 1032.51 ± 24.53 | 199.81 | 832.70 | 0.12 | 0.580 | 0.70 | 2.728 |

Conventions: The first two letters refer to the starting material, NaOH, $ZnCl_2$ and $FeCl_3$ are the agents used to activate the carbons, and the number means the temperature at which the carbons were activated. Specific surface areas ($S_{BET}$), micropores surface area ($S_{UP}$), external surface area ($S_{EXT}$), volume of the micropores ($V_{UP}$), external volume ($V_{EXT}$), the total pore volume ($V_{TP}$), average pore diameter ($D_{AP}$).

The nitrogen adsorption/desorption isotherms of Fig. 10 showed that the amount of $N_2$ adsorbed with increasing relative pressure ($P/P_0$) presented the next order: RH-NaOH-800°C > RH-NaOH-800°C post-washed > RH-NaOH-800°C pretreated (Fig. 10). Thus, the $V_{TP}$ was bigger for RH-NaOH-800°C and lower for RH-NaOH-800°C post-washed and RH-NaOH-800°C pretreated (Table 7). However, the $S_{BET}$ was higher for RH-NaOH-800°C post-washed and decrease for the other materials (RH-NaOH-800°C pretreated > RH-NaOH-800°C) (Table 7). The best $S_{BET}$ presented by RH-NaOH-800°C post-washed, is due to the fact that the NaOH used in the wash reacts with the $SiO_2$ present in the material and forms sodium silicate ($Na_2SiO_3$). $Na_2SiO_3$ is soluble in water so it is removed in the wash [149]. Thus, the pores are unoccupied and therefore the $S_{BET}$ increases. On the other hand, RH-NaOH-800°C pretreated, showed a better $S_{BET}$ compared to RH-NaOH-800°C (Table 7), indicating the importance of pre-treating the raw material silicon. But at the same time, this shows that NaOH at room temperature is not capable of completely breaking the $SiO_2$ bonds present in RH [151]. Thus,

RH-NaOH-800°C pretreated developed a higher ash content (Table 6), which covered the porosity of the material causing the decrease in $S_{BET}$ compared to the activated carbon post-washed with NaOH (Table 7).
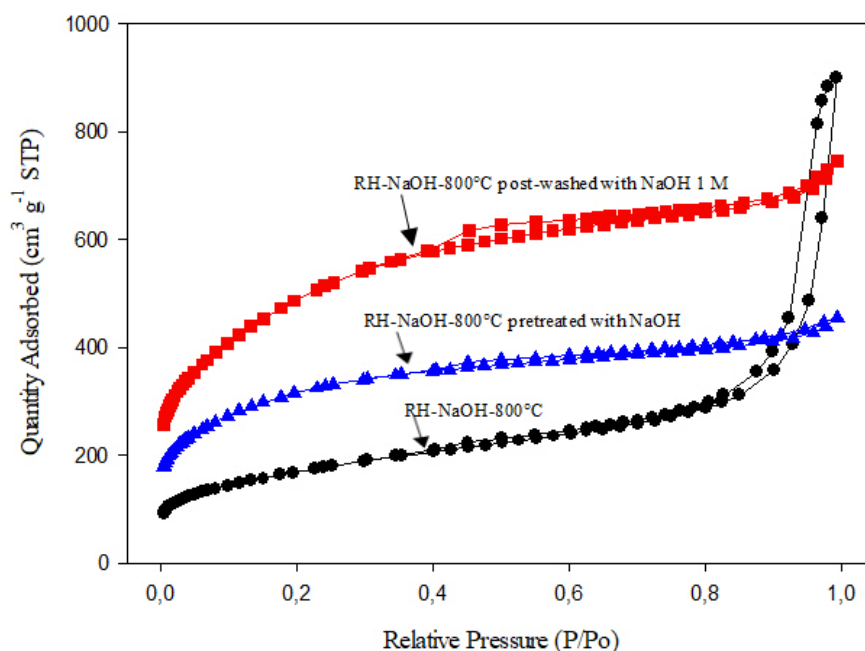


**Figure 10.** Nitrogen adsorption/desorption isotherms for RH-NaOH-800°C, RH-NaOH-800°C post-washed and RH-NaOH-800°C pretreatment.

In addition, according to IUPAC the isotherms of RH-NaOH-800°C post-washed and RH-NaOH-800°C pretreated showed in the Fig. 10, were classified as type IV of mesoporous adsorbents with a hysteresis loops H4 associated with narrow slit-like pore [134]. Therefore, the new activated carbons showed a higher development of $S_{EXT}$ and lower $S_{\mu P}$ (Table 7), indicating that the materials are mainly composed of mesopores and macropores rather than micropores. Consequently, a high $V_{EXT}$ and low $V_{\mu P}$ were observed (Table 7). However, the new activated carbons showed a decrease in $S_{EXT}$, $V_{EXT}$ and an increase in $S_{\mu P}$ and $V_{\mu P}$ with respect to RH-NaOH-800°C (Table 7). In this way, it is possible to indicate that the pre-treatment or post-washed with NaOH increases the microporosity of the activated carbons. In the case of pre-washing, the ash content present in RH decreased. The decrease can lead to an

increase in the activating agent/carbon ratio [149], which contributes to a better production of porosity. While in the post-washed, the NaOH solution diffuses through the macropores and mesopores, easily reaching the micropores of the material and eliminating ashes [150].

It is important to highlight that the three activated carbons have in common a higher $S_{EXT}$ development (Table 7), which is related to the presence of mesopores and macropores. However, Fig. 11 of $PSD_S$ shows for RH-NaOH-800°C pretreated and RH-NaOH-800°C post-washed a greater development of mesopores. In fact, a greater distribution of pores in the region between 1.5 nm and 4.0 nm, with a $D_{AP}$ around 2.7 nm is observed for the two new materials (Table 7) [134] . For RH-NaOH-800°C, the highest porosity distribution was observed in the region between 8.0 nm and 150 nm (Fig. 11), with a $D_{AP}$ of 9.629 (Table 7), which suggests a predominance of mesopores, but with a larger $V_{TP}$ than the other two materials. Again, it is confirmed that the post-washed or pre-treatment with NaOH in the materials reduces the presence of $SiO_2$ (Table 6), generating smaller porosity.
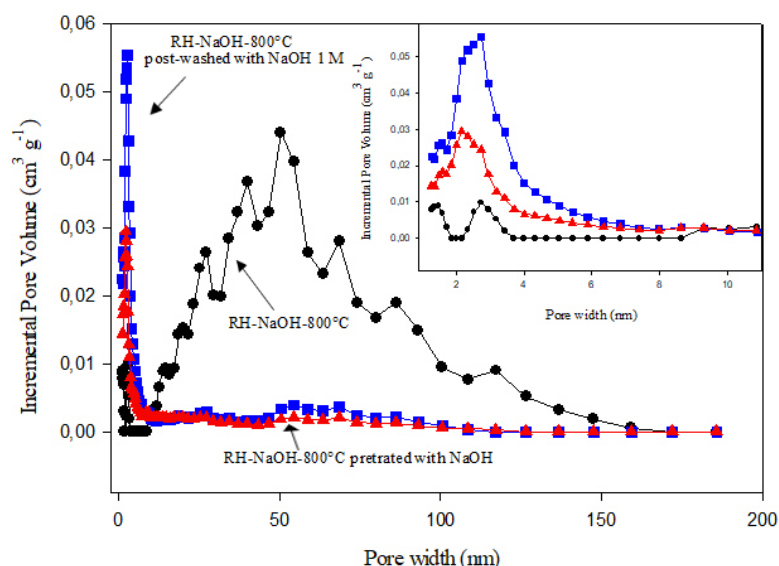


**Figure 11.** $PSD_S$ of activated carbon samples prepared RH-NaOH-800°C, RH-NaOH-800°C post-washed and RH-NaOH-800°C pretreatment. Insert: region of pore diameter between 0 and 11 nm.

The increases in porosity can be verified by SEM micrographs. Thus, the ashes removal increased the porosity (Fig. 12 (a)-(c)).
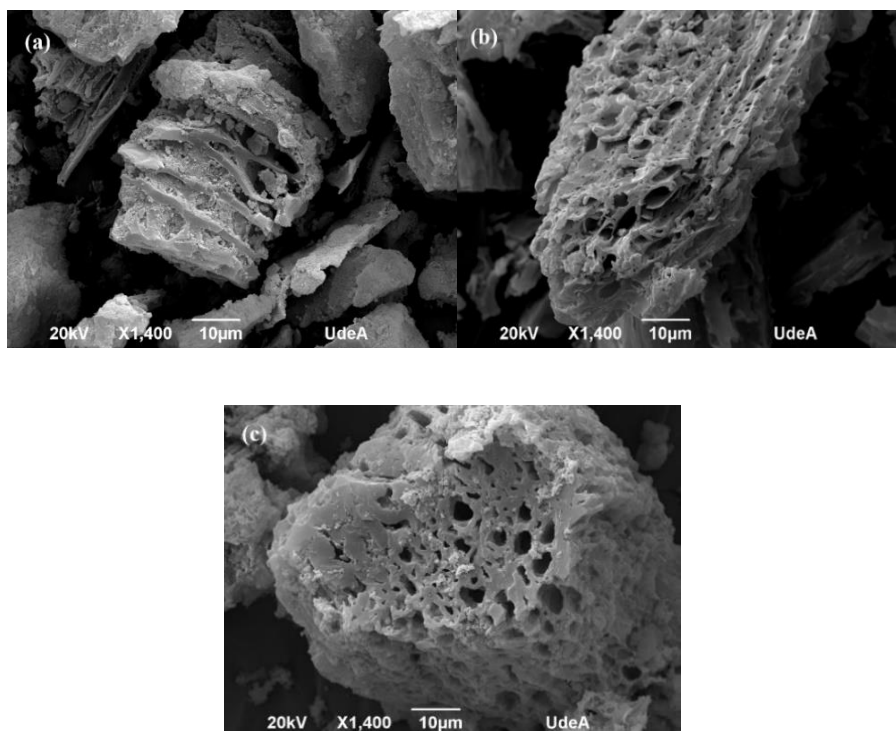


**Figure 12.** SEM micrographs activated carbon prepared from RH using NaOH as activating agent at 800°C, with normal, pretreated and post-washed processes. (a) RH-NaOH-800°C; (b) RH-NaOH-800°C post-washed; (c) RH-NaOH-800°C pretreated.

RH-NaOH-800°C pretreated and RH-NaOH-800°C post-washed improved their surface characteristics compared to RH-NaOH-800°C. However, their efficiency as adsorbents is unknown. Therefore, in Fig 13. the three materials were evaluated in the removal of a mix of the contaminants ACE, CIP, SUL and DIC, and were compared with a commercial activated carbon.
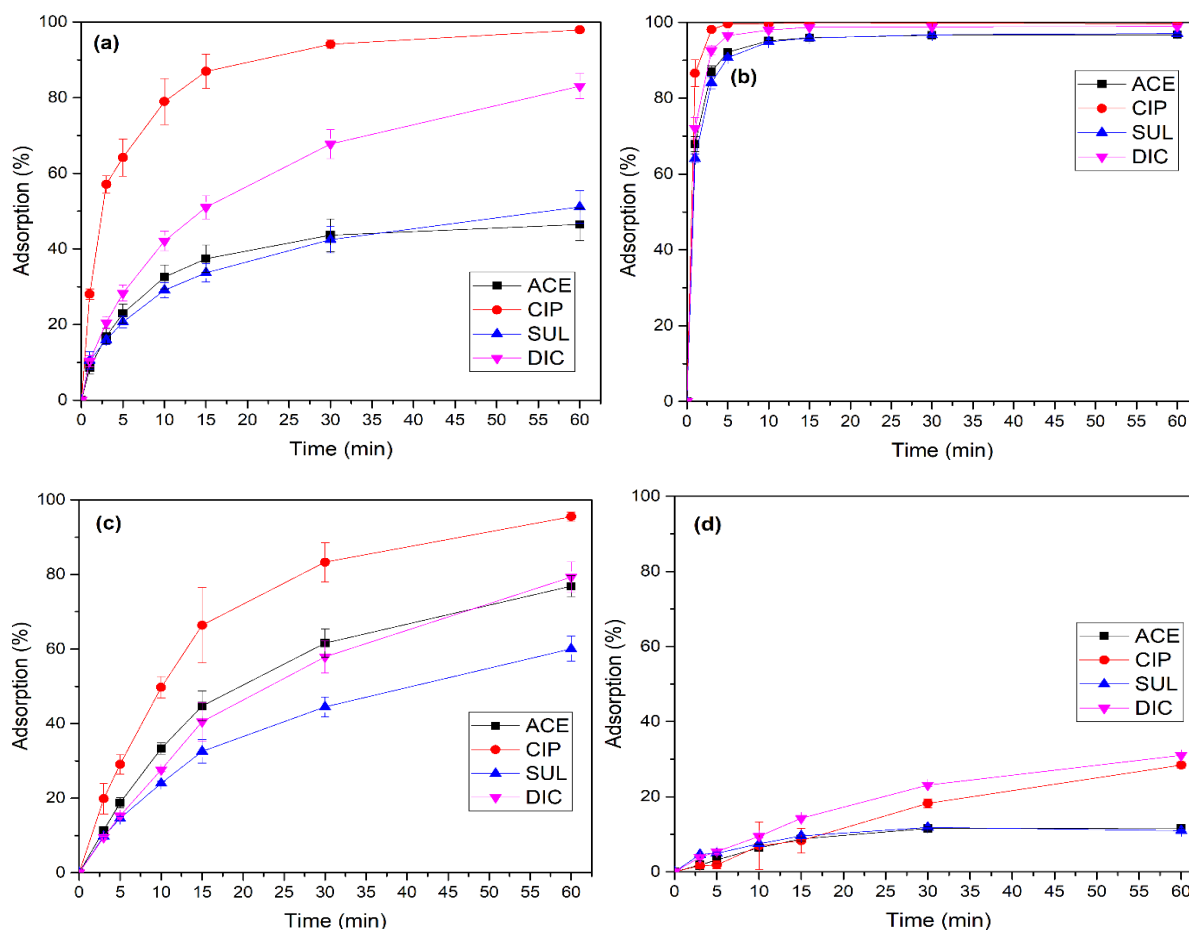
**Figure 13**. Adsorption of pharmaceuticals mixed in aqueous solution using RH-NaOH-800°C, enhanced by various techniques, and using a commercial activated carbon. Conditions: Pharmaceuticals concentration 15 µM, adsorbent dose 0,2 g L$^{-1}$, pH 5.8 – 6.5, particle size 75 – 150 µm, temperature 25°C, stirring rate 200 rpm. (a) RH-NaOH-800°C; (b) RH-NaOH-800°C post-washed; (c) RH-NaOH-800°C pretreated; (d) Commercial activated carbon.

The materials RH-NaOH-800°C post-washed, RH-NaOH-800°C pretreated and RH-NaOH-800°C, showed the best removals for CIP (compared to DIC, SUL and ACE), this fact is because at the pH of the experiment (pH 6.5), the CIP molecules are in their zwitterionic form (Fig. 1 (a)), and according to the pH$_{PZC}$ (Table 6), both negatives and positive charges are presents on the materials surface. Thus, the positive charges of the CIP interact by electrostatic attraction with the negative charges present on the surface of the materials, in the same way, the negative charges of the CIP interact with the positive charges on the surface of the materials.

Interestingly, among the three prepared carbons, the RH-NaOH-800°C pretreated presented the highest $pH_{PZC}$ values (Table 6). Therefore, a lower attraction of the negative part of CIP take place. This explain the lower CIP adsorption compared with the other two materials activated with NaOH.

DIC and SUL also present electrostatic attraction with the surface charges of the materials, but their lower adsorption (compared to CIP) can be explained because, at the pH of the experiment, these molecules are negatively charged (Fig. 1 (b) y (c)) and can only interact with the positive charges of the adsorbents. Although DIC has a smaller length size compared to SUL, it could be removed more easily due to its affinity with the mesopores present in the activated carbons [152]. Finally, electrostatic attraction is not favorable for ACE, since it is in its neutral form at the pH of the experiment (Fig. 1 (d)), but its adsorption similar to SUL, in RH-NaOH-800°C and RH-NaOH-800°C post-washed (Fig. 13 (a) and (b), respectively), and DIC, in RH-NaOH-800°C pretreated (Fig. 13 (c)), may be due to ACE efficient adsorbs on materials with a large microporous area [89], which explains its significant adsorption enhancement in RH-NaOH-800°C post-washed and RH-NaOH-800°C pretreated (Fig. 13 (b) and (c), respectively), which presented higher $S_{\mu P}$ and $V_{\mu P}$ (Table 7) than the RH-NaOH-800°C material.

Additionally, it was observed that the adsorption of the four contaminants was better using RH-NaOH-800°C post-washed (Fig. 13 (b)), this can be due, to the highest $S_{BET}$ and $S_{EXT}$ of the material. Therefore, RH-NaOH-800°C post-washed (Fig. 13 (b)) was used to compare it with a commercial activated carbon (Fig. 13 (d)). As seen, under work conditions, RH-NaOH-800°C resulted better than the commercial activated carbon. This result is interesting because commercial activated carbon presented $V_{TP}$ (1.31 cm$^3$ g$^{-1}$) higher than the reported for activated carbon with post-washed ($V_{TP}$ 1.15 cm$^3$ g$^{-1}$) (Table 7). However, commercial activated carbon has a smaller surface area (800 m$^2$ g$^{-1}$) and a $D_{AP}$ of 8.2 nm, indicating a large $S_{EXT}$ with

mesopores larger than those of RH-NaOH-800°C post-washed (2.76 nm) (Table 7). The above characteristics explain the lower adsorbent capacity of the commercial activated carbon.

It is known that the adsorption of pharmaceuticals can be affected by the presence of other pollutant in the same matrix. Therefore, this topic will be discussed in the next section, by evaluating the individual adsorption of each pharmaceutical on the RH-NaOH-800°C activated carbon with post-washed.

### 3.2.4. Evaluation of the adsorption of the pharmaceuticals mix in a complex matrix

Fig. 14 shows the adsorbent capacity of RH-NaOH-800°C post-washed for the removal of ACE, CIP, SUL and DIC, both individually and as a mix of them. It is observed, as expected, that when the compounds are alone in the matrix they are quickly eliminated (15 min). However, the system is also highly efficient for the mix. In fact, close of the 95% of all of them in the mix are eliminated in 15 min.
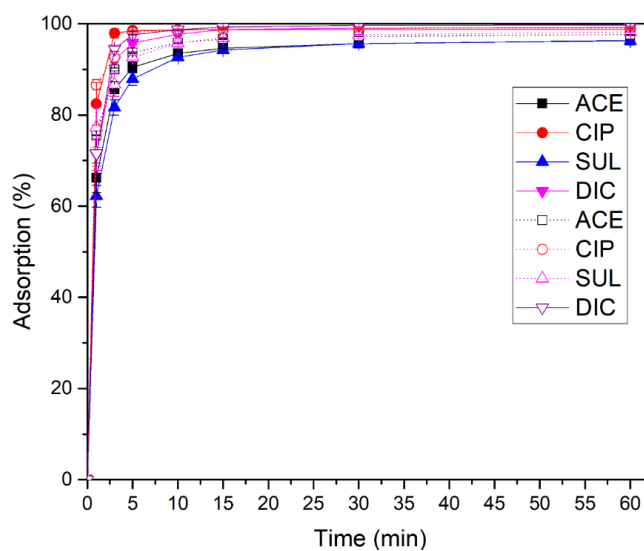


**Figure 14.** Adsorption of individual and mixed pharmaceuticals in aqueous solution using RH-NaOH-800°C post-washed. Conditions: Pharmaceutical concentration 15 µM, adsorbent dose 0.2 $g\ L^{-1}$ , pH 5.8 – 6.5 , particle size 75 – 150 µm, temperature 25°C, stirring rate 200 rpm. Solid symbol: Adsorption of pharmaceuticals mixed in distilled water; open symbol: Adsorption of pharmaceuticals singles in distilled water.

In spite of the excellent performances of the material in distilled water, the evaluation of its ability to remove the pollutants in a more complex matrix is a need. Therefore, the efficiency of the activated carbon with post-washed to remove of ACE, CIP, SUL and DIC in urine was tested (Fig. 15).
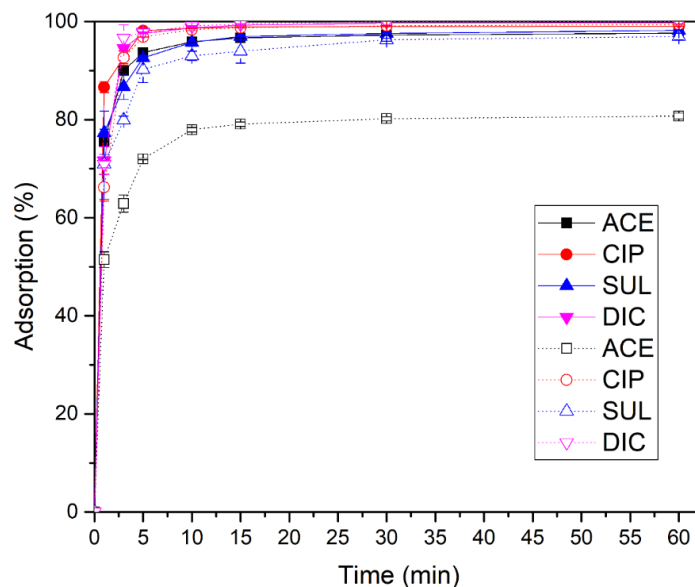


**Figure 15.** Adsorption of pharmaceuticals in distilled water and urine using RH-NaOH-800°C post-washed. Conditions: Pharmaceuticals concentration 15 µM, adsorbent dose 0,2 $g\,L^{-1}$, pH 5.8 – 6.5, particle size 75 – 150 µm, temperature 25°C, stirring rate 200 rpm. Solid symbol: distilled water; open symbol: urine.

Interestingly, a good adsorption is observed in a such complex matrix. In fact, about 80.74% of ACE in the urine is eliminated in 60 minutes, which is ~17% lower than that observed in distilled water (97.64%). Thus, the decrease in ACE adsorption could be by the presence of urea in urine, which is also a neutral molecule that competes with the pharmaceutical for the active sites of the material [89]. In the case of the other pharmaceuticals the inhibition by urine matrix was not significant (below 1.3%). This result indicates that despite the complexity of the urine matrix characterized by a high content of inorganic salts [73], the adsorbent RH-NaOH-800°C post-washed can efficiently remove the pharmaceutical contaminants.

RH-NaOH-800°C post-washed showed interesting results for the removal of contaminants in a urine matrix, being CIP and ACE the compounds having a higher and lower removal efficiency, respectively. Consequently, these two pollutants were chosen to study the mechanisms involved in the adsorption processes in urine.Thus, the study of the adsorption isotherms, as well as, kinetic and thermodynamic studies will be carried out in the next sections.

### 3.2.6. Study of adsorption isotherms

An isothermal equilibrium model represents the relationship of pharmaceuticals contaminant adsorbed on the activated carbon (adsorbent). The equation used for the adsorption isotherm indicates the diffusion of adsorbate from the liquid phase to the solid phase under equilibrium conditions [119]. Therefore, the correlation of the equilibrium data is necesssary for the interpretation of the process. For the adsorption of CIP and ACE in urine on RH-NaOH-800°C post-washed, three isotherm models were tested in the present study; i.e., Langmuir, Freundlich and Redlich-Peterson isotherm models, using an adsorbent dose of 0.2 g $L^{-1}$, pH 5.5, pharmaceutical concentrations of 5-120 mg $L^{-1}$ and an optimal adsorption time of 60 minutes. The Langmuir model assumes that the adsorption sites are uniformly distributed, the pollutant form a monolayer and there is no transmigration of the adsorbate on the adsorbent surface. On the other hand, the Freundlich model assumes a heterogeneous adsorbent surface, where the strongest binding sites are occupied first [153]. The Langmuir isotherm, was calculated using the Eq. 1. The experimental data fitted to the non—linear form of the Langmuir model are shown in Figure 16 (a) and (b), for ACE and CIP, respectively. The isothermal parameters obtained from the linear plots for ACE and CIP (Fig. 17 (a) and (b) respectively) are shown in Table 8.
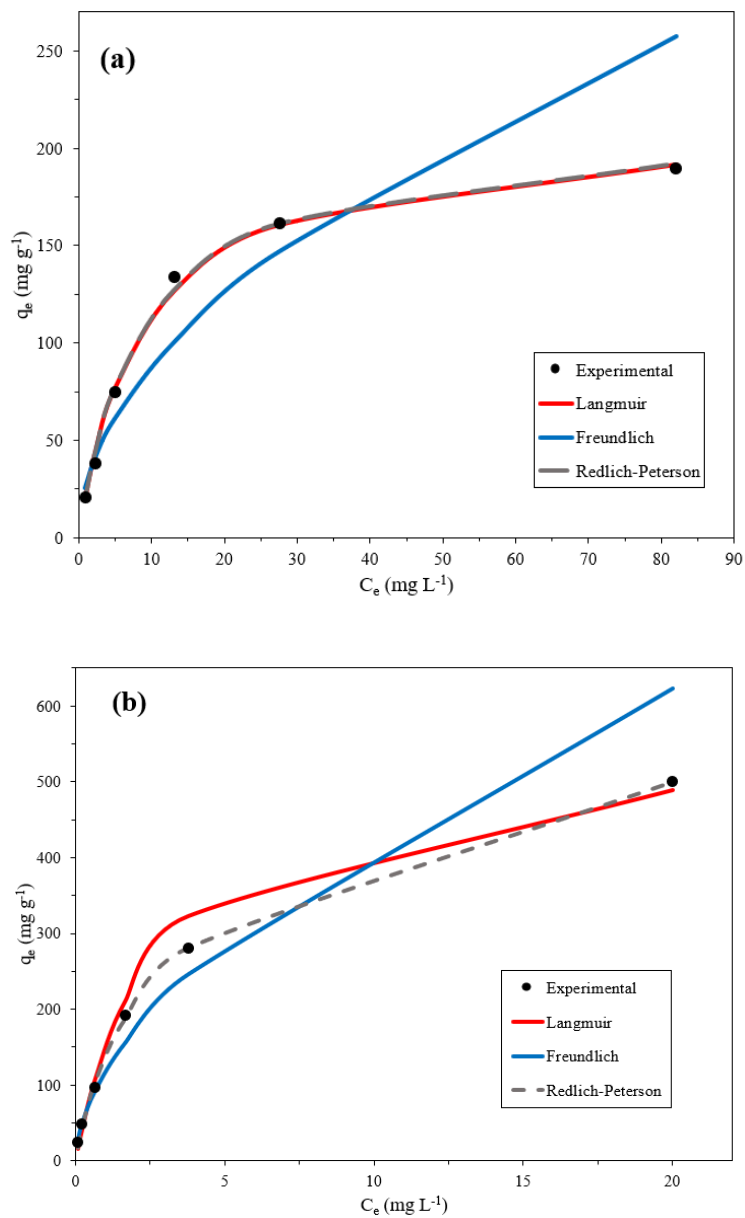
**Figure 16.** Comparison between the experimental and predicted isotherms (Langmuir, Freundlich and Redlich-Peterson) for the adsorption of pharmaceuticals in urine by RH-NaOH-800°C post-washed in an optimal time of 60 minutes. (a) ACE; (b) CIP. Conditions: Pharmaceuticals concentration 5-120 mg $L^{-1}$, adsorbent dose 0.2 g $L^{-1}$, pH 5.5, particle size 75 – 150 µm, temperature 25°C, stirring rate 200 rpm.
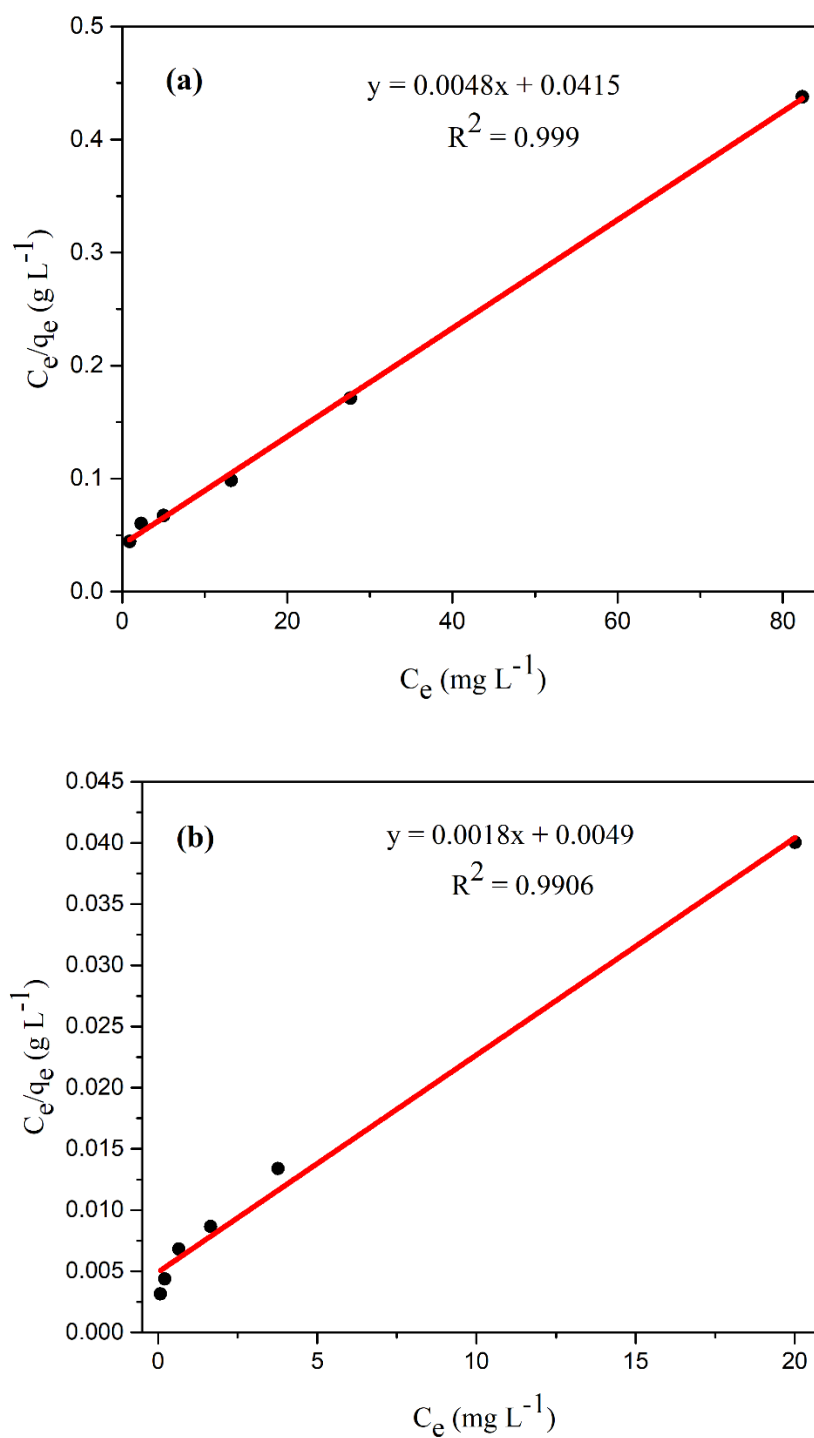
**Figure 17.** Langmuir isotherm for the removal of pharmaceuticals in urine using RH-NaOH-800°C post-washed. (a) ACE; (b) CIP. Conditions: pharmaceuticals concentration 5-120 mg L$^{-1}$, adsorbent dose 0.2 g L$^{-1}$, pH 5.5, particle size 75 – 150 µm, temperature 25°C, stirring rate 200 rpm.

**Table 8.** Adsorption parameters for the Langmuir, Freundlich, and Redlich-Peterson isotherms in the removal of ACE and CIP in urine using RH-NaOH-800°C post-washed. Conditions: Pharmaceuticals concentration 5-120 mg $L^{-1}$, adsorbent dose 0.2 g $L^{-1}$, pH 5.5, particle size 75 – 150 µm, temperature 25°C, stirring rate 200 rpm.

| Pharmaceuticals compounds | | CIP | ACE |
|---|---|---|---|
| Isotherm models | Parameters | Values | Values |
| Langmuir | $q_m$ (mg g$^{-1}$) | 555.56 | 210.55 |
| | $K_L$ (L mg$^{-1}$) | 0.37 | 0.11 |
| | $R_L$ | 0.35 – 0.02 | 0.63 – 0.07 |
| | $R^2$ | 0.991 | 0.999 |
| | APE (%) | 3.48 | 1.44 |
| | $\Delta q$ (%) | 5.86 | 3.32 |
| Freundlich | $K_F$ (mg g$^{-1}$)(L mg$^{-1}$)$^{1/n}$ | 117.59 | 26.70 |
| | n | 1.80 | 1.95 |
| | $R^2$ | 0.979 | 0.930 |
| | APE (%) | 5.03 | 4.38 |
| | $\Delta q$ (%) | 8.44 | 6.51 |
| Redlich-Peterson | $K_{RP}$ (L g$^{-1}$) | 256.70 | 24.30 |
| | aR (L mg$^{-1}$)$^{\beta}$ | 0.84 | 0.12 |
| | $\beta$ | 0.80 | 1 |
| | $R^2$ | 1 | 1 |
| | APE (%) | 1.02 | 1.04 |
| | $\Delta q$ (%) | 2.62 | 2.58 |

It can be observed that the activated carbon (RH-NaOH-800°C post-washed) in the adsorption of ACE presents a maximum capacity of adsorption, $q_m$, of 210.55 mg g$^{-1}$ and a constant of Langmuir, $K_L$, of 0.11 L mg$^{-1}$. As expected, these parameters were higher for adsorption of CIP, which showed a $q_m$ of 555.56 mg g$^{-1}$ and $K_L$ of 0.37 L mg$^{-1}$. For the adsorption of both pharmaceuticals a high $R^2$ value and low values of APE and $\Delta q$ were found. Additionally, the

$R_L$ value between 0 and 1 for ACE and CIP, suggested that the adsorption processes are favorable for the two pharmaceuticals. On the other hand, the Freundlich isotherm was studied using the Eq. 3. The experimental data fitted to the non linear form of the Freundlich model are presented in Fig. 16 (a) and (b) for ACE and CIP, respectively. Additionally, from *Eq. 4* the linear graph *Ln $q_e$* vs *Ln $C_e$*, where the slope represents $n$ and the intercept $K_F$, was obtained for ACE (Fig. 18 (a)) and CIP (Fig. 18 (b)). The results obtained for the Freundlich isotherm for ACE and CIP are shown in Table 8.



**Figure 18.** Freundlich isotherm for the removal of pharmaceuticals in urine using RH-NaOH-800°C post-washed. (a) ACE; (b) CIP. Conditions: pharmaceuticals concentration 5-120 mg L$^{-1}$, adsorbent dose 0.2 g L$^{-1}$, pH 5.5, particle size 75 – 150 μm, temperature 25°C, stirring rate 200 rpm.

The ACE and CIP presented an adsorption capacity, $K_F$, of 26.70 $mg^{1-\frac{1}{n}}L^{\frac{1}{n}}g^{-1}$ and 117.59 $mg^{1-\frac{1}{n}}L^{\frac{1}{n}}g^{-1}$, respectively; with a value of *n>1*, indicating a favorable adsorption process for both pharmaceuticals. However, low values of $R^2$ and high values of APE and Δq, suggest a bad fit of the data to the Freundlich isotherm. These results showed that the Langmuir isotherm better describes the experimental data than the Freundlich model.

In order to confirm the results obtained, the Redlich-Peterson isotherm, which is widely used as a compromise between the Langmuir and Freundlich systems [157], [158], was calculated. This model has three parameeters and incorporates the advantegeous significance of both models. The Redlich-Peterson model was represented using *Eq. 6*. A procedure was adopted to solve *Eq. 7* by minimization of *APE* between the predicted data for $q_e$ from *Eq. 6* and the experimental data, using the solver adding function of MS excel.

The experimental data fitted to the non-linear form of the Redlich-Peterson model are shown in Fig. 16 (a) for ACE and (b) for CIP. The isotherm constants obtained from the linear plots (Fig. 19 (a) for ACE and (b) for CIP) are listed in Table 8.
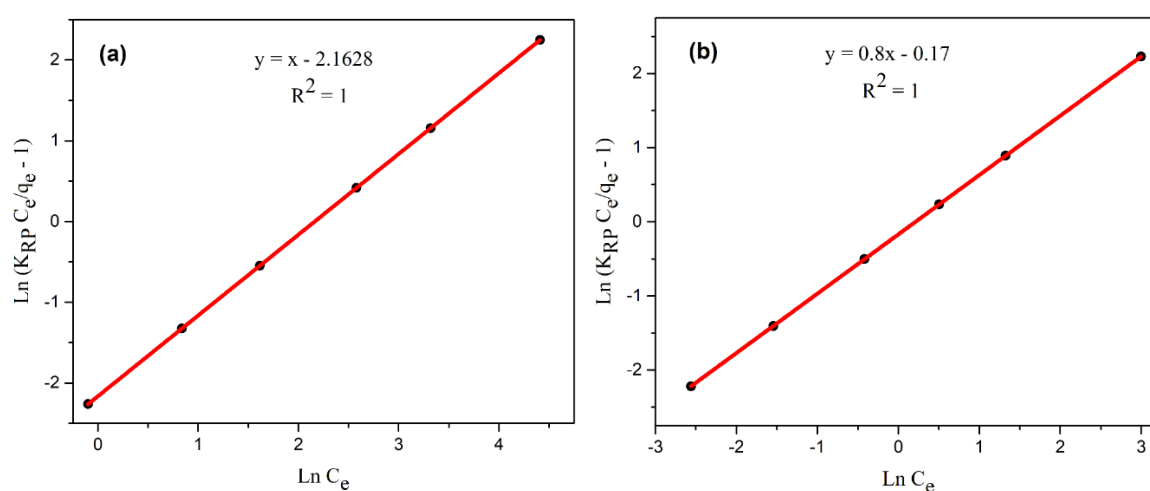


**Figure 19.** Redlich-Peterson isotherm for the removal of ACE and CIP in urine using RH-NaOH-800°C post-washed. (a) ACE; (b) CIP. Conditions: pharmaceuticals concentration 5-120 mg L$^{-1}$, adsorbent dose 0.2 g L$^{-1}$, pH 5.5, particle size 75 – 150 µm, temperature 25°C, stirring rate 200 rpm.

The results for ACE and CIP of $R^2$, *APE* and *Δq* were better than the reported values in Langmuir. Therefore, the sorption process of ACE and CIP on RH-NaOH-800°C post-washed, can be best represented by the Redlich-Peterson model. Additionally, the values of *β* for ACE and CIP were closer to 1 than 0 (Table 8), which means that the isotherm is more consistent

with the Langmuir than the Freundlich isotherm. Hence, the best fit of equilibrium data in both the Langmuir and Redlich-Peterson isotherm expressions confirm the monolayer coverage process of ACE and CIP on RH-NaOH-800°C post-washed.

The $q_m$ values found here for ACE (210.55 mg g$^{-1}$) and CIP (555.56 mg g$^{-1}$) in urine during the adsorption on RH-NaOH-800°C post-washed were compared with the adsorbent capacity of other materials used for removal of these two pharmaceuticals in distilled water (Table 9).

**Table 9.** A comparison of maximum adsorption capacities in urine matrix of ACE and CIP ($q_m$) onto different adsorbents in matrix of distilled water.

| Adsorbent | Pharmaceutical $q_m$ (mg g$^{-1}$) | Reference |
|---|---|---|
| **ACE** | | |
| RH-NaOH-800°C post-washed | 210.55 | This study |
| Activated carbons from urban residues | 159.0 | [159] |
| Magnetic activated carbon | 125.25 | [160] |
| AC Prepared from RH (urine matrix) | 48.31 | [89] |
| AC Prepared from RH | 20.96 | [161] |
| **CIP** | | |
| RH-NaOH-800°C post-washed | 555.56 | This study |
| Activated carbon desilicated RH | 461.9 | [162] |
| Activated carbon from *Enteromorpha prolifera* | 244 | [163] |
| Ordered mesoporous carbon from pitch resin and anthracene | 236 | [140] |
| Powdered activated commercial carbon | 64.93 | [164] |

Interestingly, the $q_m$ obtained in this study were higher than the reported for other adsorbents indicated in Table 9, which may be related to the greater surface area of the activaated carbon used in this study compared to the adsorbents reported in Table 9. Thus, RH-NaOH-800°C post-washed is richer in functional groups that promote the adsorption of pharmaceutical molecules [160]. Also, it was possible to make the comparison with a activated carbon from RH

impregnated with NaOH used for the ACE removal in urine [89], which presented a $q_m$ lower than that determined in this study, possibly due to the absense of post-washed and, therefore, the surface area is smaller, which can be related to a lower availability of functional groups that favor the adsorption of contaminanting molecules. These results indicate the importance of performing the post-washed with NaOH, which better eliminate ashes, and then the surface area and porosity increases, and consequently, the adsorbent capacity of the material is improved.

### 3.2.7. Study of Adsorption Kinetics

The adsorption kinetics can be adjusted to different mathematical models. Pseudo first order, pseudo second order and intraparticle diffusion methods were used. The kinetics of the process was determined using the same parameters with concentration of pharmaceuticals 5 - 120 mg $L^{-1}$, adsorbent dose 0.2 g $L^{-1}$, pH 5.5 and particle size 75 – 150 µm. The adsorption rate using the pseudo first order model was determined by *Eq. 8*. Thus, from *Eq. 8* it was plotted $ln\ (q_e - q_t)$ versus $t$, for ACE (Fig. 20 (a)-(f)) and CIP (Fig. 21 (a)-(f)), obtaining from the intercept, $q_e$, and from the slope, $k_1$. The values of the pseudo first order kinetic for ACE and CIP are reported in the Table 10 (a) and (b), respectively.

**Figure 20**. Pseudo-first order kinetics for the removal of ACE in urine using RH-NaOH-800°C post-washed as adsorbent and different concentrations of analgesic: (a) 5 mg L$^{-1}$; (b) 10 mg L$^{-1}$; (c) 20 mg L$^{-1}$; (d) 40 mg L$^{-1}$; (e) 60 mg L$^{-1}$ and (f) 120 mg L$^{-1}$. Conditions: Adsorbent dose 0.2 g L$^{-1}$, pH 5.5, particle size 75 – 150 µm, temperature 25°C, stirring rate 200 rpm.
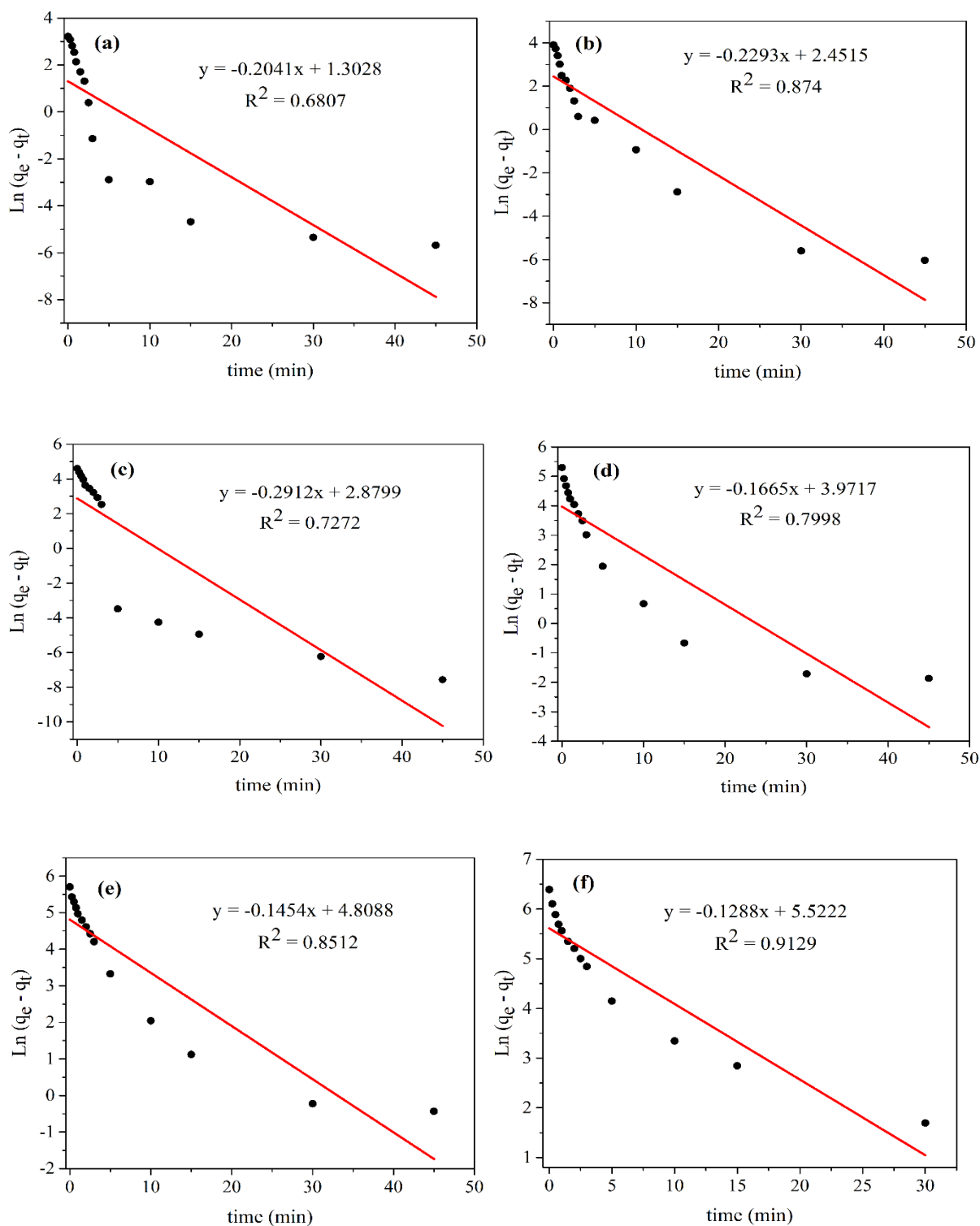
**Figure 21.** Pseudo-first order kinetics for the removal of CIP in urine using RH-NaOH-800°C post-washed as adsorbent and different concentrations of antibiotic: (a) 5 mg L$^{-1}$; (b) 10 mg L$^{-1}$; (c) 20 mg L$^{-1}$; (d) 40 mg L$^{-1}$; (e) 60 mg L$^{-1}$ and (f) 120 mg L$^{-1}$. Conditions: Adsorbent dose 0.2 g L$^{-1}$, pH 5.5, particle size 75 – 150 μm, temperature 25°C, stirring rate 200 rpm.
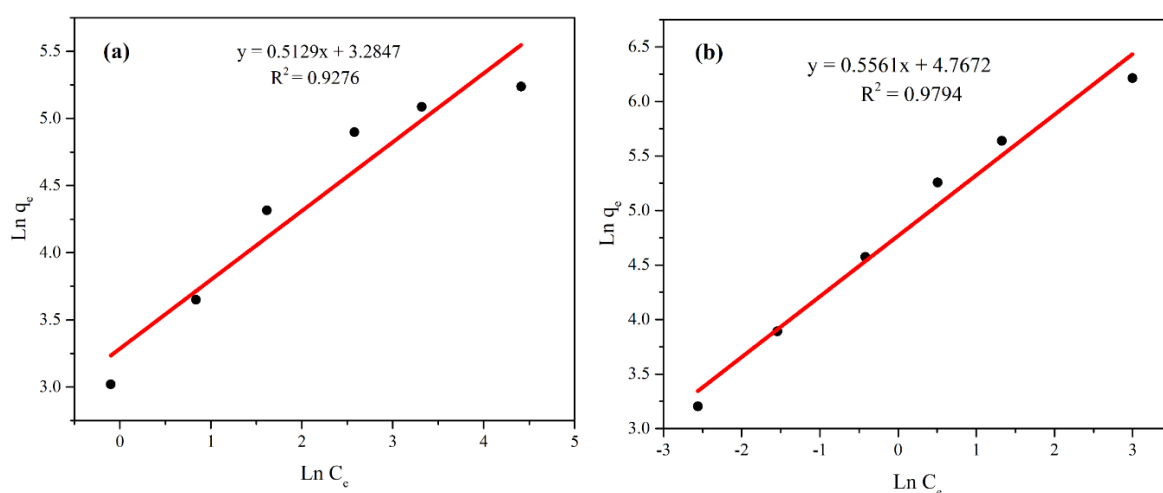
**Table 10.** Pseudo first order and pseudo second order kinetics of the removal of pharmaceutical in urine using RH-NaOH-800°C post-washed. (a) ACE; (b) CIP. Conditions: Pharmaceutical concentration 2.4-60 mg L$^{-1}$, adsorbent dose 0.2 g L$^{-1}$, pH 5.5, particle size 75-150 μm, temperature 25°C, stirring rate 200 rpm.

| | | Pseudo first order | | | | | Pseudo second order | | | | |
|---|---|---|---|---|---|---|---|---|---|---|---|
| $C_0$ | $q_{eq,exp}$ | $q_{eq,cal}$ | $K_1$ | $R^2$ | APE | $\Delta q$ | $q_{eq,cal}$ | $K_2$ | $R^2$ | APE | $\Delta q$ |
| (mg L$^{-1}$) | (mg g$^{-1}$) | (mg g$^{-1}$) | (min$^{-1}$) | | (%) | (%) | (mg g$^{-1}$) | (mg g$^{-1}$ min$^{-1}$) | | (%) | (%) |
| **(a) ACE** | | | | | | | | | | | |
| 5 | 20.473 | 4.085 | 0.138 | 0.816 | 80.08 | 113.25 | 20.576 | 0.187 | 1 | 0.502 | 0.711 |
| 10 | 38.442 | 15.984 | 0.242 | 0.944 | 58.49 | 82.71 | 38.911 | 0.048 | 1 | 1.218 | 1.723 |
| 20 | 74.854 | 19.599 | 0.241 | 0.849 | 73.42 | 103.84 | 75.758 | 0.033 | 0.999 | 1.207 | 1.707 |
| 40 | 134.308 | 36.350 | 0.144 | 0.793 | 73.02 | 103.28 | 135.135 | 0.015 | 0.999 | 0.616 | 0.903 |
| 60 | 162.399 | 25.450 | 0.226 | 0.832 | 84.70 | 119.79 | 163.934 | 0.023 | 0.999 | 0.945 | 1.337 |
| 120 | 188.137 | 19.596 | 0.244 | 0.872 | 90.71 | 128.28 | 188.679 | 0.056 | 1 | 0.295 | 1.245 |
| **(b) CIP** | | | | | | | | | | | |
| 5 | 24.918 | 3.680 | 0.204 | 0.681 | 85.02 | 120.24 | 25.253 | 0.076 | 0.999 | 1.215 | 1.727 |
| 10 | 49.954 | 11.606 | 0.229 | 0.874 | 77.72 | 109.93 | 50.505 | 0.047 | 0.999 | 1.103 | 1.559 |
| 20 | 99.938 | 17.812 | 0.291 | 0.727 | 82.63 | 116.86 | 101.010 | 0.017 | 0.999 | 1.073 | 1.517 |
| 40 | 199.753 | 53.075 | 0.167 | 0.799 | 73.46 | 103.89 | 200.000 | 0.011 | 0.999 | 0.124 | 0.175 |
| 60 | 299.264 | 122.584 | 0.145 | 0.851 | 59.37 | 83.96 | 303.030 | 0.004 | 0.999 | 1.259 | 1.780 |
| 120 | 595.264 | 250.185 | 0.129 | 0.913 | 56.71 | 80.22 | 588.235 | 0.002 | 1 | 1.181 | 1.670 |

A great difference between the capacity of adsoption experimental $\left(q_{eq,exp}\right)$ and the calculated $\left(q_{eq,cal}\right)$, for all concentrations of ACE and CIP, were observed. For example, for a concentration of 5 mg L$^{-1}$, for ACE, the $q_{eq,exp}$ was 20.473 mg g$^{-1}$ and the value for $q_{eq,cal}$ was 4.085 mg g$^{-1}$. A similar case occurred for CIP, which presented a $q_{eq,exp}$ of 24.918 mg g$^{-1}$ and a $q_{eq,cal}$ of 3.680 mg g$^{-1}$. Additionally, low $R^2$ and high *APE* and *Δq* values were reported for

both pharmaceuticals (Table 10), which indicates that the experimental data does not fit a pseudo first order kinetics. This result led to fit the data to another model.

Therefore, the pseudo-second order kinetic was calculated used *Eq. 9*. The plots of $t/q_t$ versus $t$, obtained for ACE (Fig. 22 (a)-(f)) and CIP (Fig. 23 (a)-(f)), allows from the slope and intercept determine $q_e$ and $k_2$, respectively.



(a) y = 0.0486x + 0.0126, $R^2 = 1$

(b) y = 0.0257x + 0.0138, $R^2 = 1$

(c) y = 0.0132x + 0.0053, $R^2 = 0.9999$

(d) y = 0.0074x + 0.0036, $R^2 = 0.9999$
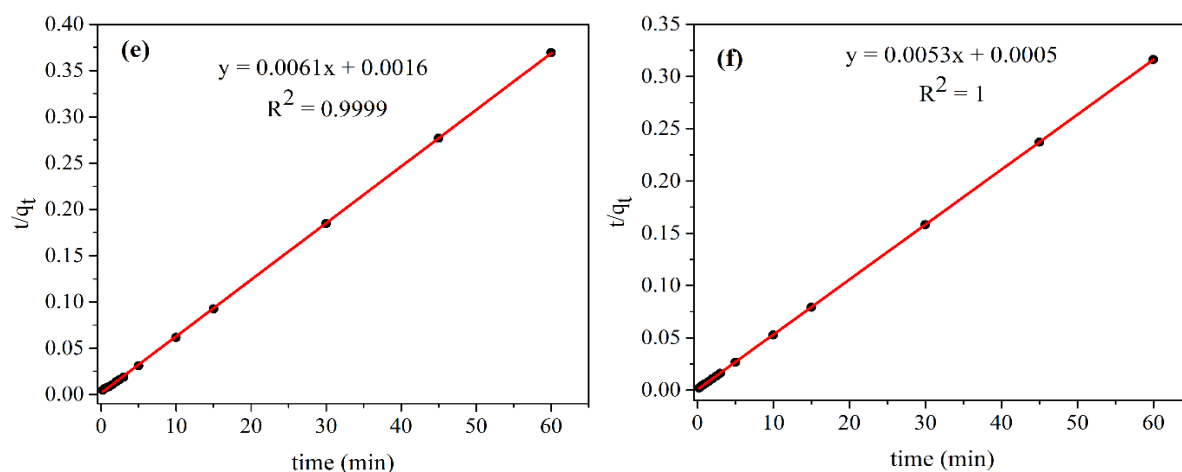
**Figure 22.** Pseudo-second order kinetics for the removal of ACE in urine using RH-NaOH-800°C post-washed as adsorbent and different concentrations of analgesic: (a) 5 mg L$^{-1}$; (b) 10 mg L$^{-1}$; (c) 20 mg L$^{-1}$; (d) 40 mg L$^{-1}$; (e) 60 mg L$^{-1}$ and (f) 120 mg L$^{-1}$. Conditions: Adsorbent dose 0.2 g L$^{-1}$, pH 5.5, particle size 75 – 150 µm, temperature 25°C, stirring rate 200 rpm.
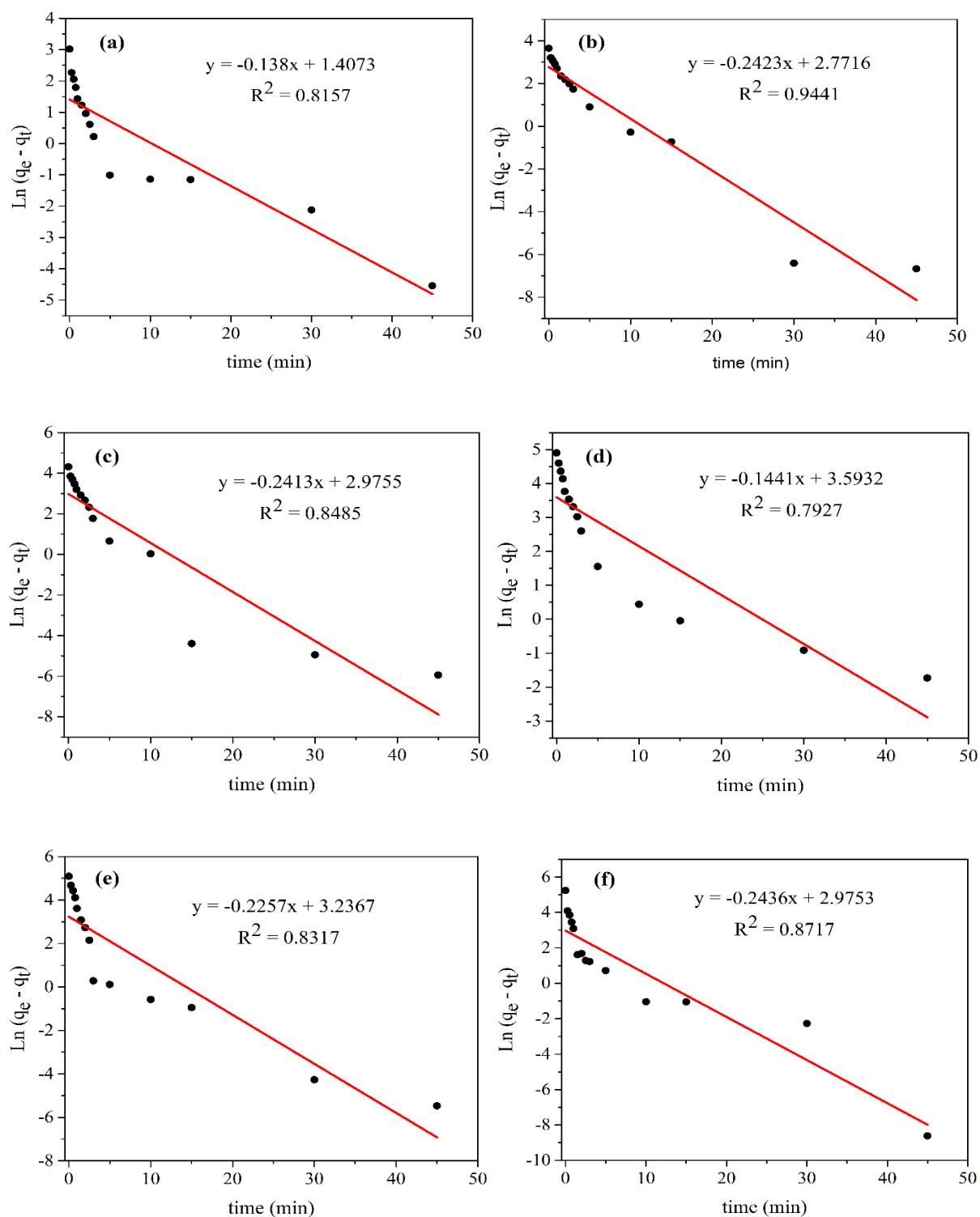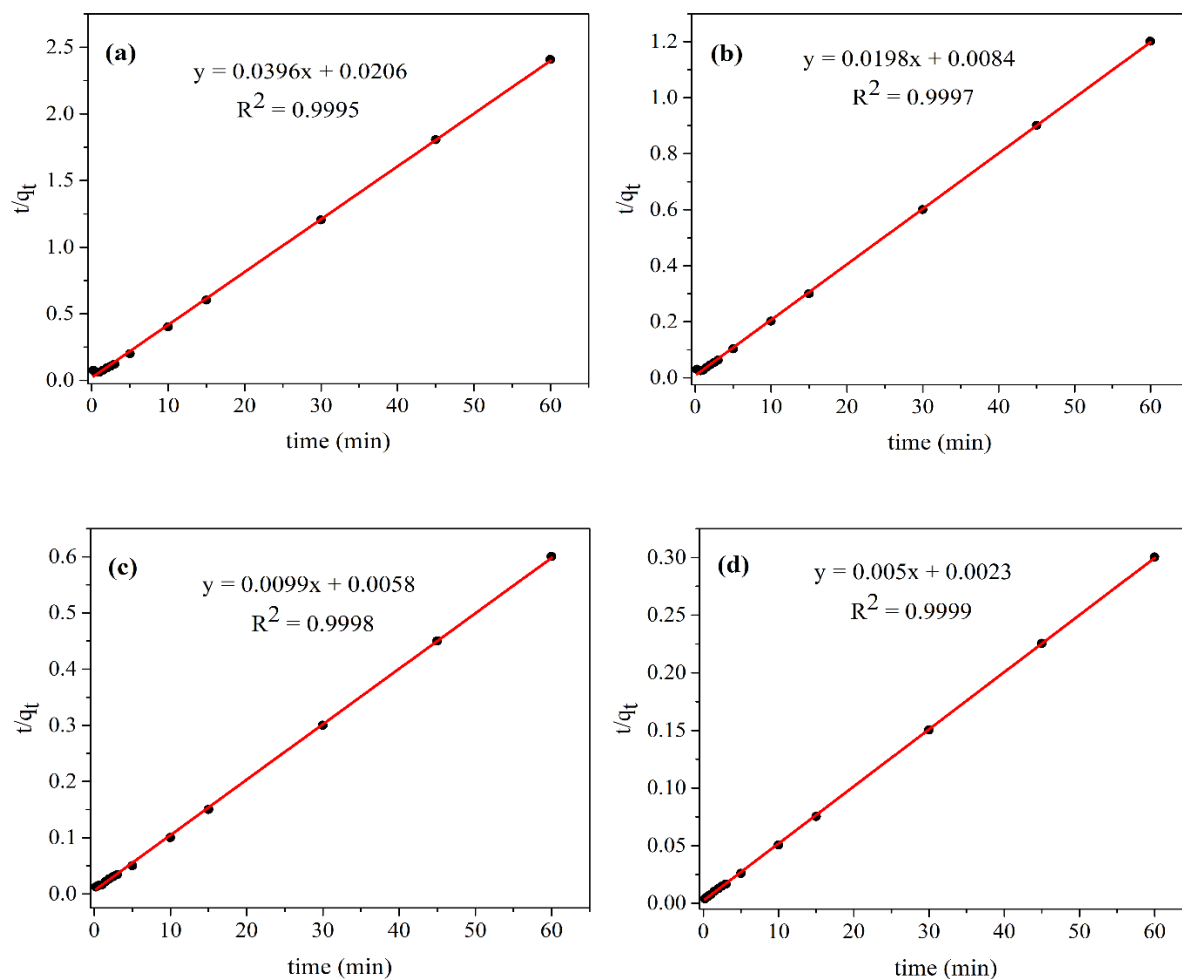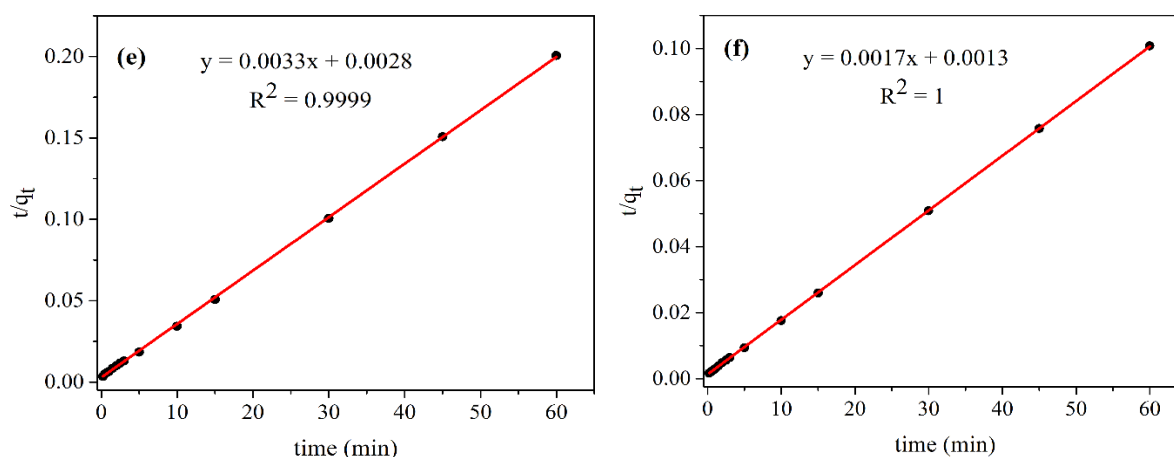
**Figure 23.** Pseudo-second order kinetics for the removal of CIP in urine using RH-NaOH-800°C post-washed as adsorbent and different concentrations of antibiotic: (a) 5 mg L$^{-1}$; (b) 10 mg L$^{-1}$; (c) 20 mg L$^{-1}$; (d) 40 mg L$^{-1}$; (e) 60 mg L$^{-1}$ and (f) 120 mg L$^{-1}$. Conditions: Adsorbent dose 0.2 g L$^{-1}$, pH 5.5, particle size 75 – 150 µm, temperature 25°C, stirring rate 200 rpm.

The data for the pseudo second order model for ACE and CIP are reported in the Table 10 (a) and (b), respectively. From the table, it can be observed that the calculated adsorption capacities were highly consistent with the experimental values. Again, for a concentration of 5 mg L$^{-1}$ for ACE, the $q_{eq,exp}$ was 20.473 mg g$^{-1}$ and the $q_{eq,cal}$ was 20.576 mg g$^{-1}$; while for CIP $q_{eq,exp}$ was 24.918 mg g$^{-1}$ and $q_{eq,cal}$ was 25.253 mg g$^{-1}$. Additionally, the high $R^2$ and low *APE* and *Δq* values indicated a goob fit of the model. These findings suggest that the adsorpetion of ACE and CIP on RH-NaOH-800°C post-washed follows the pseudo-second order kinetic.

The high correlation of the pseudo second order kinetic equation with the kinetic data presented here, is consistent with previous results, e.g., adsorption on ordered mesoporous carbon prepared from pitch resin and anthracene [140], sugarcane bagasse and activated commercial carbon [164], acid activated carbon prepared from *Prosopis juliflora* wood [170], activated carbon prepared from urban and industrial residues [159], activated carbon synthesized from spent tea leaves [171], as well as natural adsorbents prepared from rice and coffee husk [89].

Additionally, the kinetic rate constant, $k_2$, determines how fast the adsorption occurs [165]. From Table 10, it can be also noted that for ACE and CIP the value of the rate constant $k_2$ decreased with the increase of the initial concentration of pharmaceuticals ($C_0$). The reason for this behavior can be attributed to lower competition for the adsorption surface sites at lower concentrations of ACE and CIP. At higher concentrations of the pharmaceutals, the competition for the surface active sites will be high and consequently lower sorption rates are obtained [169].

However, the kinetic models of pseudo first order and pseudo second order do not allow to identify the mechanism of diffusion, which is important to predict the rate-limiting step in an adsorption process [156]. The intraparticle diffusion model had shown to be suitable to investigate this. This model was determined using the Eq. 10. The graphical representation of the intraparticle diffusion model is shown in Fig. 24 ((a)-(f)) and Fig. 25 ((a)-(f)) for ACE and CIP, respectively, adsorbed on RH-NaOH-800°C post-washed.
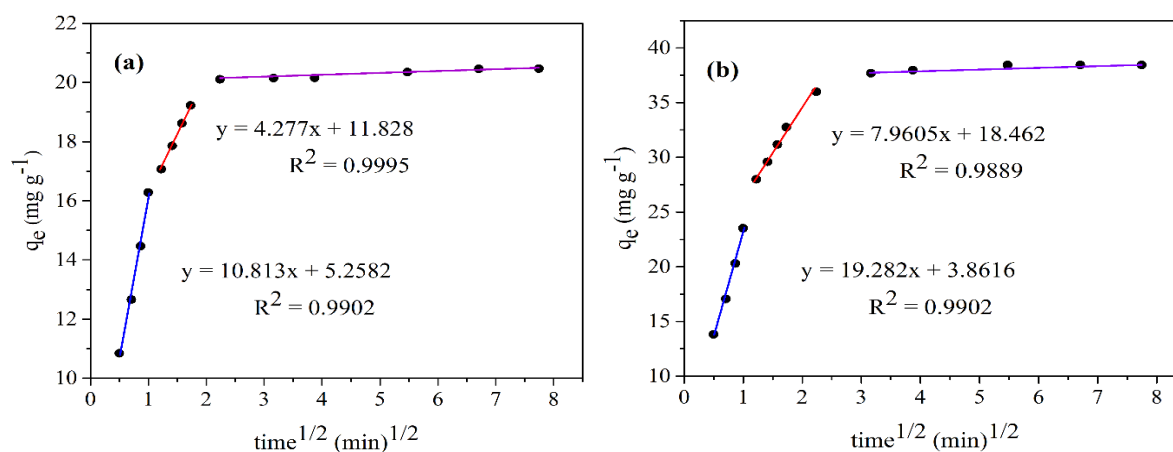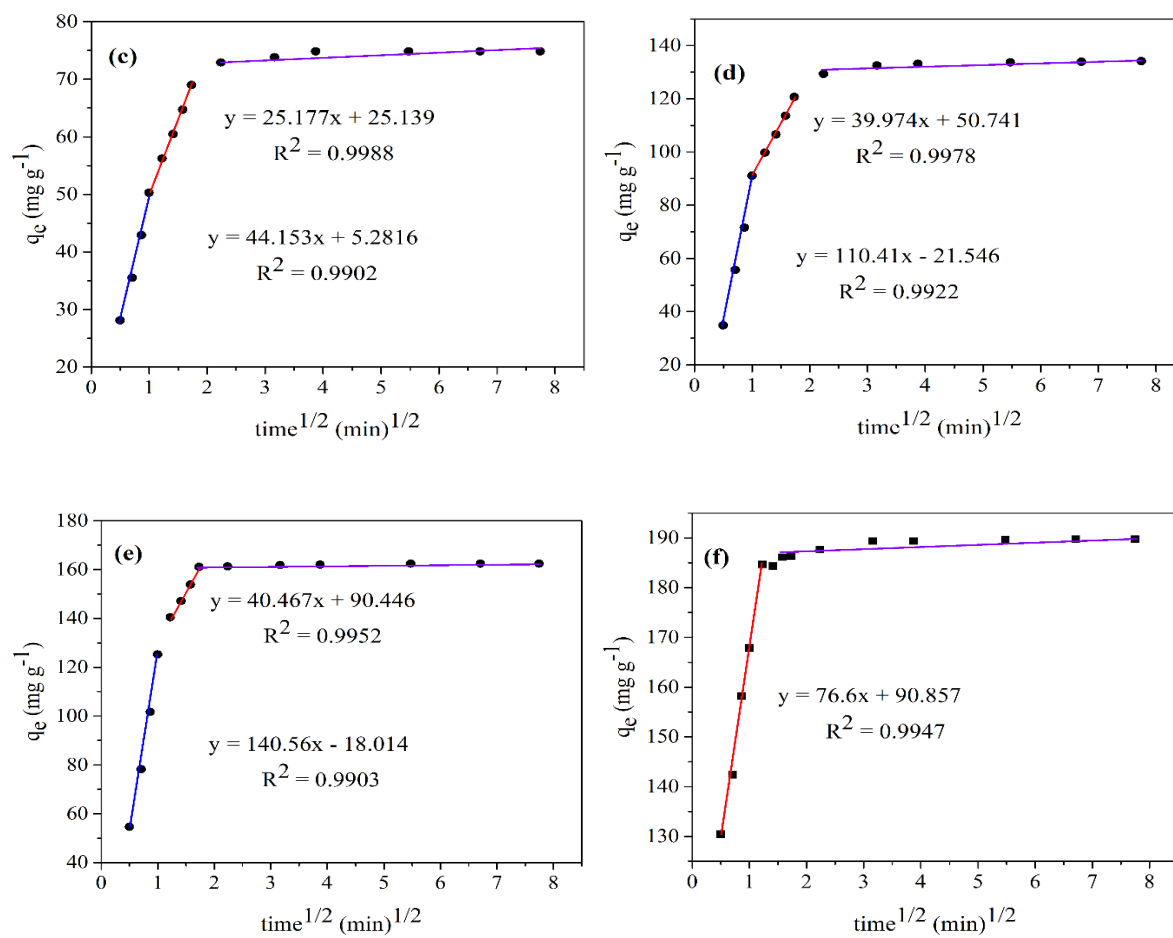
**Figure 24.** Intraparticle diffusion model for the removal of ACE in urine using RH-NaOH-800°C post-washed as adsorbent and different concentrations of analgesic: (a) 5 mg L$^{-1}$; (b) 10 mg L$^{-1}$; (c) 20 mg L$^{-1}$; (d) 40 mg L$^{-1}$; (e) 60 mg L$^{-1}$ and (f) 120 mg L$^{-1}$. Conditions: Adsorbent dose 0.2 g L$^{-1}$, pH 5.5, particl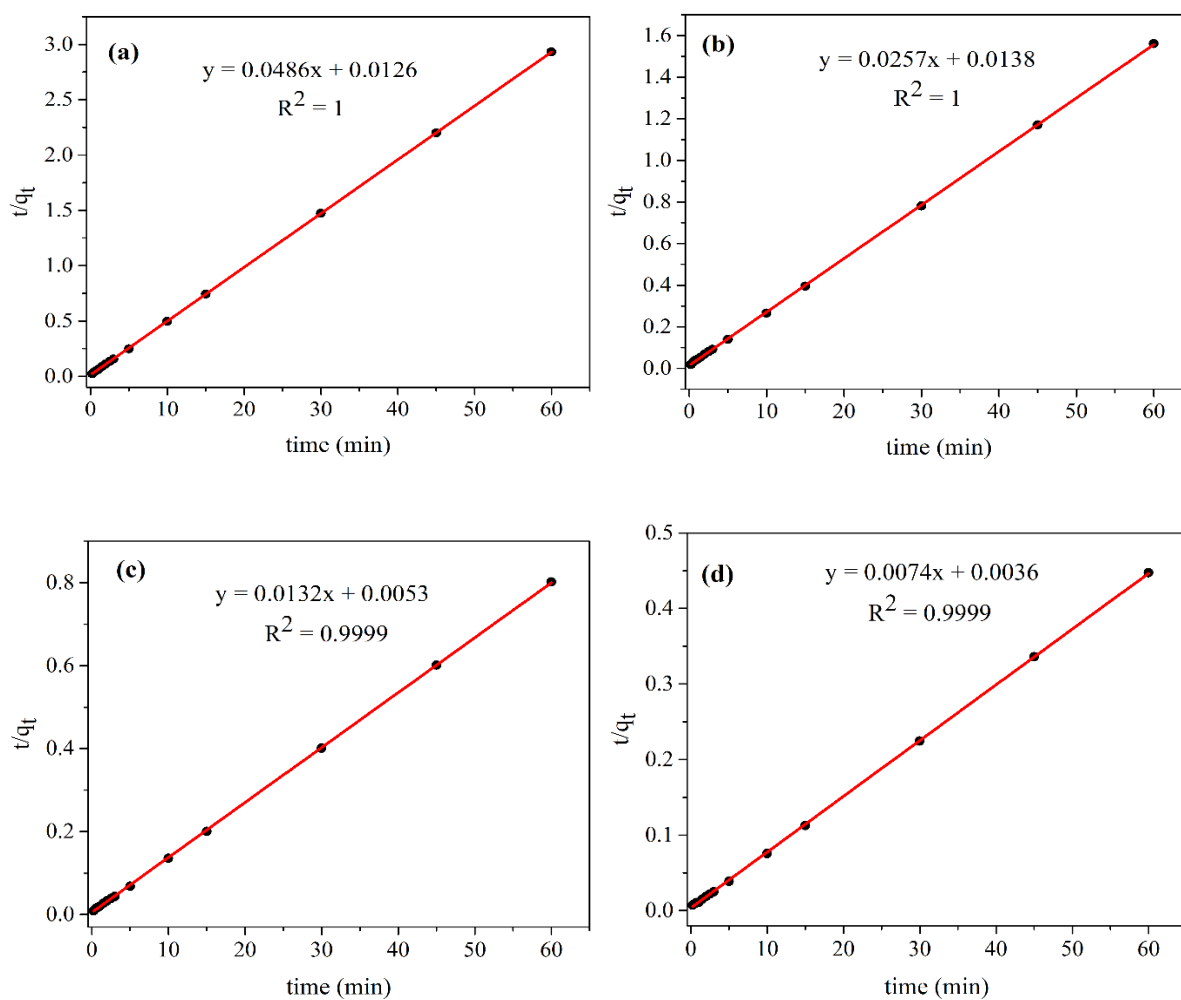e size 75 – 150 µm, temperature 25°C, stirring rate 200 rpm. Color conventions: first stage: blue; second stage: red and third stage: violet.
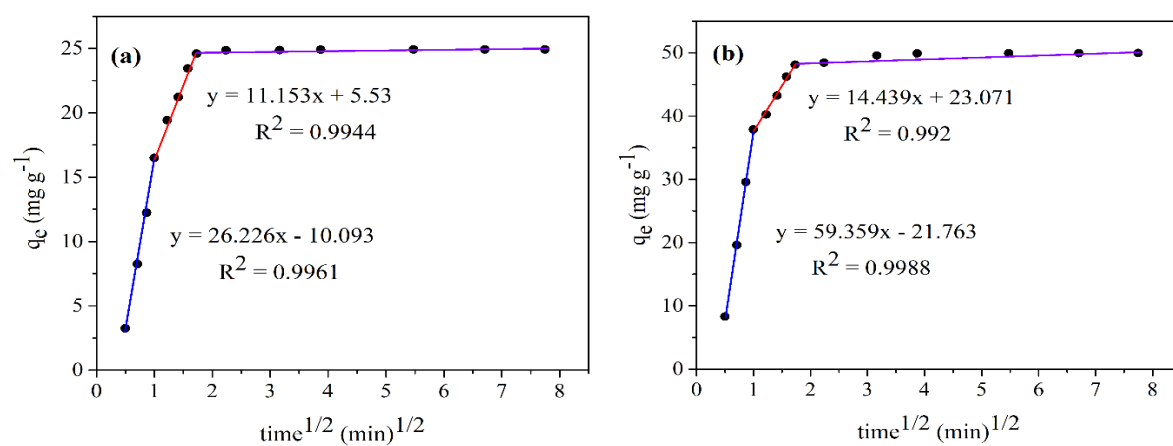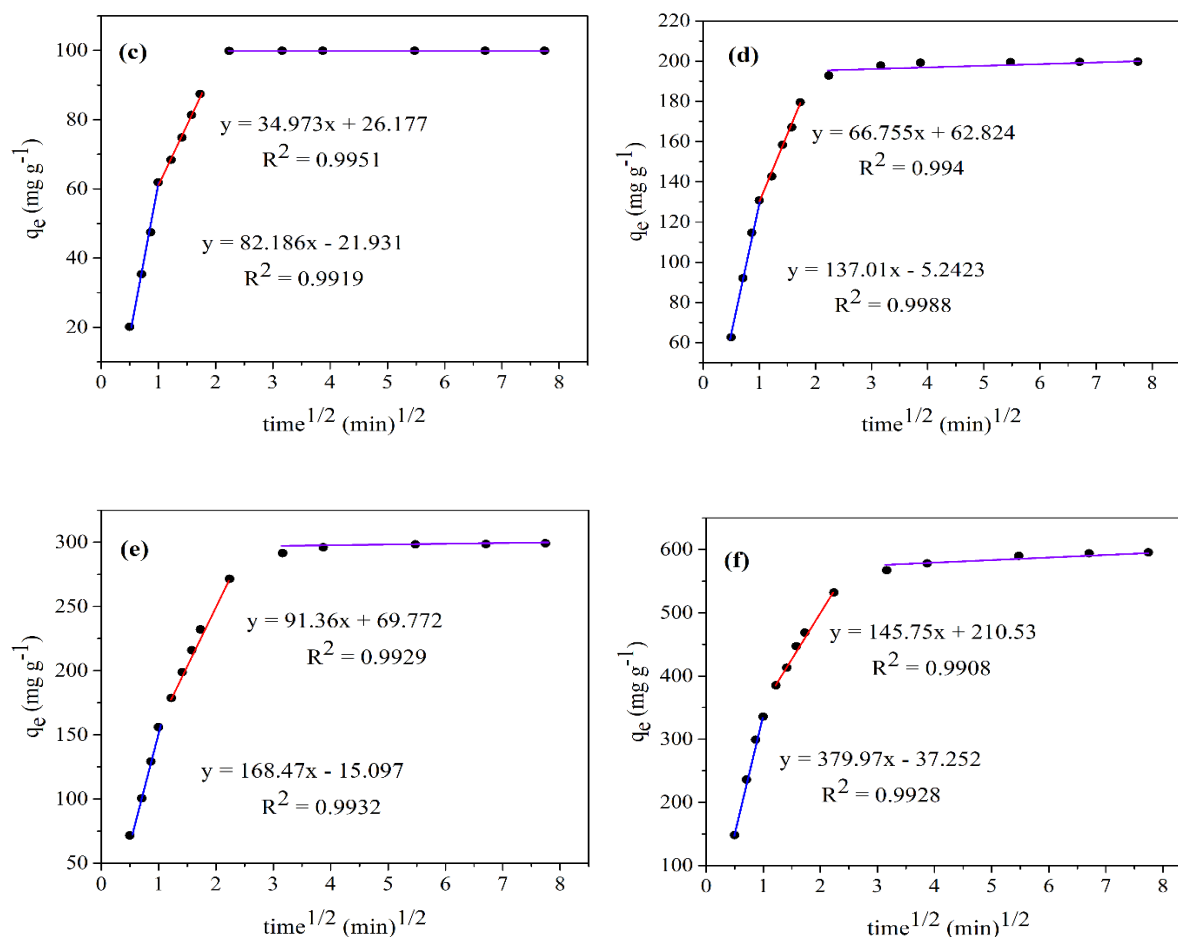
**Figure 25.** Intraparticle diffusion model for the removal of CIP in urine using RH-NaOH-800°C post-washed as adsorbent and different concentrations of antibiotic: (a) 5 mg L$^{-1}$; (b) 10 mg L$^{-1}$; (c) 20 mg L$^{-1}$; (d) 40 mg L$^{-1}$; (e) 60 mg L$^{-1}$ and (f) 120 mg L$^{-1}$. Conditions: Adsorbent dose 0.2 g L$^{-1}$, pH 5.5, particle size 75 – 150 µm, temperature 25°C, stirring rate 200 rpm. Color conventions: first stage: blue; second stage: red and third stage: violet.

The graphic representation of the intraparticle diffusion model showed a multilinearity during the adsorption of ACE (Fig. 24 (a)-(f)) and CIP (Fig. 25 (a)-(f)) on RH-NaOH-800°C post-washed. For the case of the two pharmaceuticals, three stages were observed (Fig. 24 (a)-(f) for ACE and Fig. 25 for CIP (a)-(f)). The first stage can be attributed to the diffusion of adsorbate through the solution to the external surface of adsorbent. The second portion describes the gradual adsorption stage, where intraparticle diffusion is the rate-limiting step. The third portion

is attributed to the final equilibrium stage, where intraparticle diffusion starts to slow down due to extremely low adsorbate concentration in the solution [156]. However, is important highlight that when the concentration of ACE is very high (120 mg L$^{-1}$), the adsorption on the outer surface of the adsorbent occurs so fast that the first stage is not observed (Fig. 24 (f)). The calculated values of $K_{id}$ and $C$, for the first stage ($K_{id\ I}$ and $C_I$) and second stage ($K_{id\ II}$ and $C_{II}$) for ACE and CIP are reported in the Table 11 (a) and (b), respectively.

**Table 11.** Intraparticle diffusion of the removal of pharmaceuticals in urine using RH-NaOH-800°C post-washed as adsorbent. (a) ACE; (b) CIP. Conditions: Pharmaceutical concentration 5-120 mg L$^{-1}$, adsorbent dose 0.2 g L$^{-1}$, pH 5.5, particle size 75 – 150 µm, temperature 25°C, stirring rate 200 rpm.

| $C_0$ (mg L$^{-1}$) | $q_{eq,\ exp}$ (mg g$^{-1}$) | $q_{eq,\ cal}$ (mg g$^{-1}$) | $Ki_{d,\ I}$ (mg g$^{-1}$ min$^{-1/2}$) | $C_I$ (mg g$^{-1}$) | $R^2_{\ I}$ | $Ki_{d,\ II}$ (mg g$^{-1}$ min$^{-1/2}$) | $C_{II}$ (mg g$^{-1}$) | $R^2_{\ II}$ | APE (%) | $\Delta q$ (%) |
|---|---|---|---|---|---|---|---|---|---|---|
| **(a) ACE** | | | | | | | | | | |
| 5 | 20.473 | 20.113 | 10.813 | 5.258 | 0.990 | 4.277 | 11.828 | 0.999 | 1.743 | 2.466 |
| 10 | 38.442 | 37.706 | 19.282 | 3.862 | 0.990 | 7.961 | 18.462 | 0.989 | 1.890 | 2.673 |
| 20 | 74.854 | 74.842 | 44.153 | 5.2816 | 0.990 | 25.177 | 25.139 | 0.999 | 0.009 | 0.029 |
| 40 | 134.308 | 133.161 | 110.410 | 21.546 | 0.992 | 39.974 | 50.741 | 0.998 | 0.842 | 1.216 |
| 60 | 162.399 | 161.979 | 140.56 | 18.014 | 0.990 | 40.467 | 90.446 | 0.995 | 0.280 | 0.403 |
| 120 | 188.137 | 187.939 | - | - | - | 76.600 | 90.857 | 0.995 | 0.474 | 1.843 |
| **(b) CIP** | | | | | | | | | | |
| 5 | 24.918 | 24.611 | 26.226 | 10.093 | 0.996 | 11.153 | 5.530 | 0.994 | 1.233 | 1.746 |
| 10 | 49.954 | 48.119 | 59.359 | 21.763 | 0.999 | 14.439 | 23.071 | 0.992 | 3.673 | 5.195 |
| 20 | 99.938 | 99.908 | 82.186 | 21.931 | 0.992 | 34.973 | 26.177 | 0.995 | 0.029 | 0.042 |
| 40 | 199.753 | 199.224 | 137.010 | 5.2423 | 0.999 | 66.755 | 62.824 | 0.994 | 0.264 | 0.374 |
| 60 | 299.264 | 298.504 | 168.470 | 15.097 | 0.993 | 91.360 | 69.772 | 0.993 | 0.254 | 0.359 |
| 120 | 595.264 | 594.397 | 379.970 | 37.252 | 0.993 | 145.750 | 210.530 | 0.991 | 0.146 | 0.228 |

It is observed in both cases, that the values of $K_{id\ I}$ are larger than $K_{id\ II}$. This phenomenon suggests that the pharmaceuticals molecules were initially adsorbed very quickly by the external surface of the adsorbent. When the adsorption of the external surface reaches the saturation, the pharmaceuticals molecules entered into the pores within the particle and were eventually adsorbed on the active sites of the adsorbent internal surface. When the pharmaceuticals molecules were transported into the pore of the particle, the diffusion resistance increases and consequently the diffusion rate was lowered. With the decrease of the pharmaceutical concentration in the solution, the diffusion rate became much smaller and the diffusion processes reaches the final equilibrium stage [173]. Moreover, for this diffusion model the $R^2$ values are close to 1 and $APE$ and $\Delta q$ values are low. This indicates that the adsorption of pharmaceuticals in RH-NaOH-800°C post-washed can be modeled by the intraparticle diffusion model. However, the $C$ values showed that the lines do not pass through the origin ($C \neq 0$), which indicates that the intraparticle diffusion is probably not the only rate-limiting step and that boundary layer control may be also involved in the processes [158].

The above experiments carried out at room temperature allows to explain some phenomena occurring during the adsorption of pharmaceuticals on the adsorbent. However, to further investigate the adsorption mechanism as well as the feasibility and the spontaneous nature of the processes it is necessary to evaluate the behavior of the adsorption processes when subjected to thermal changes. Therefore, thermodynamic studies, at different temperatures, will be discussed in the next section.

### 3.2.8. Thermodynamic studies

To perform thermodynamics studies a pharmaceutical concentration of 40 mg L$^{-1}$, an adsorbent dose of 0.2 g L$^{-1}$ and pH 5.5 were established. It is important to note that a concentration of 40

mg L$^{-1}$ of the pharmaceuticals was chosen based in the highest removal observed for CIP (Fig. 26 (b)). The experimental data obtained in the removal of ACE and CIP in urine using the RH-NaOH-800°C post-washed at different temperatures (25, 45, 65°C) are reported in Fig. 26 (c) and (d), respectively.
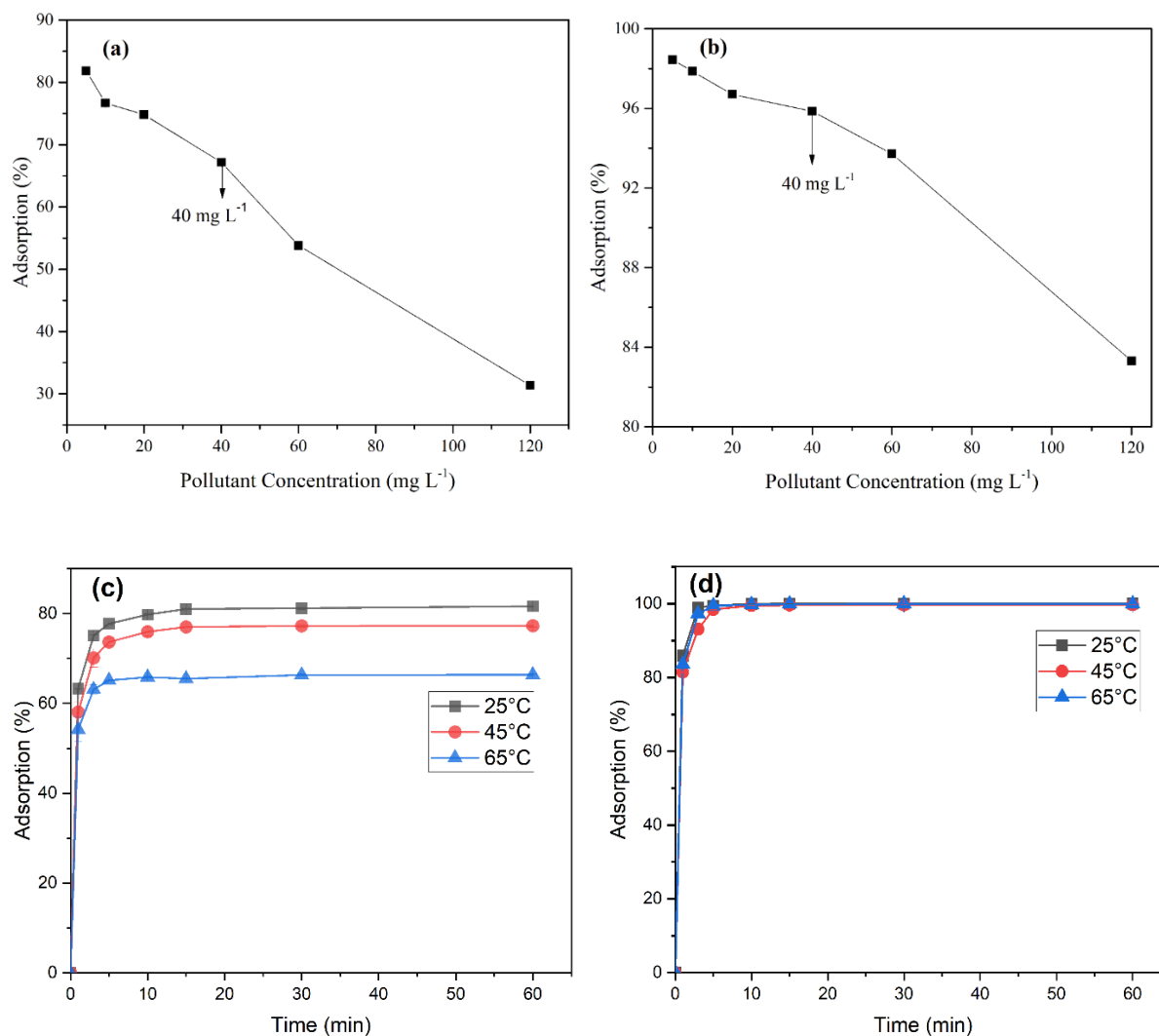


**Figure 26.** Effect of pharmaceuticals concentration, (a) ACE; (b) CIP using a pharmaceutical concentration 2.4, 5, 10, 20, 40, 60 and 120 mg L$^{-1}$, adsorbent dose 0.2 g L$^{-1}$, pH 5.5, particle size 75 – 150 µm, temperature 25°C, stirring rate 200 rpm and removal pharmaceuticals in urine at different temperatures, (c) ACE; (d) CIP using an pharmaceutical concentration 40 mg L$^{-1}$, adsorbent dose 0.2 g L$^{-1}$, pH 5.5, particle size 75 – 150, stirring rate 20 rpm.

Then thermodynamic parameters such as $E_a$, $\Delta G°$, $\Delta H°$, and $\Delta S°$ were calculated. Considering

that the kinetic data was adequately described by the pseudo second order reaction shown in

section 3.2.7, $k_2$ was used to calculate the $E_a$, which was estimated from Eq. 11. $E_a$ for ACE

and CIP was calculated from the slope of the plot $ln\ k_2$ vs $1/T$ (Fig. 27 (a) and (b), respectively)

and the thermodynamic parameters are reported in Table 12.
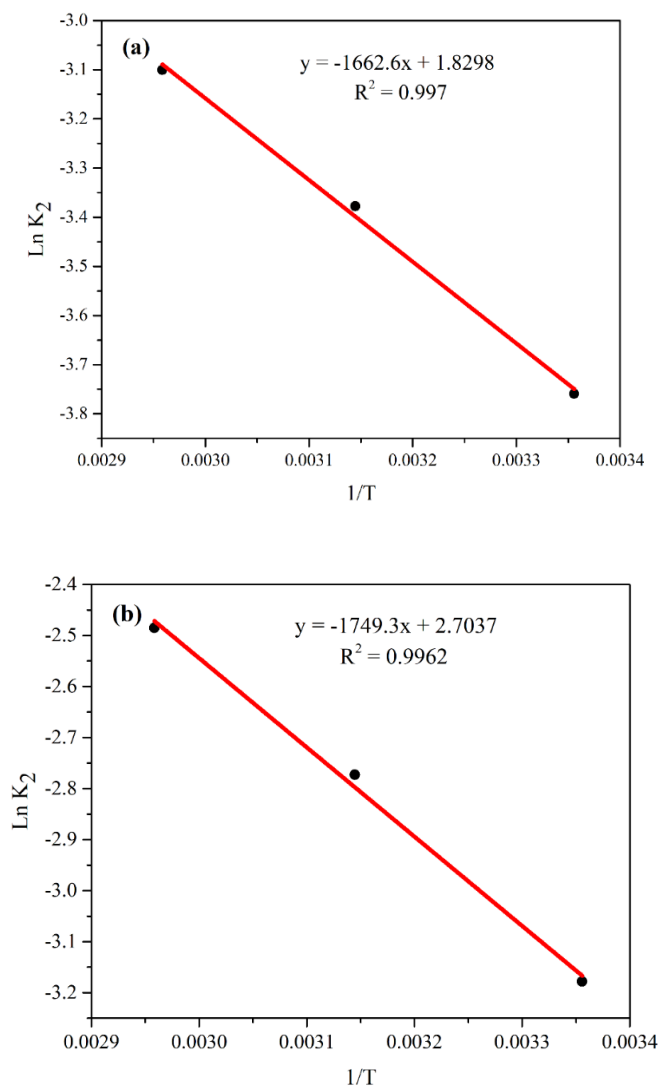


**Figure 27.** Ea of the adsorption process of pharmaceuticals using RH-NaOH-800°C post-washed as adsorbent. (a) ACE; (b) CIP. Conditions: pharmaceutical concentration 40 mg L$^{-1}$; temperature 25, 45 and 65°C, adsorbent dose 0.2 g L$^{-1}$, pH 5.5, particle size 75 – 150 µm, stirring rate 200 rpm.

**Table 12.** Thermodynamic parameters in the removal of pharmaceuticals using RH-NaOH-800°C post-washed as adsorbent. (a) ACE; (b) CIP. Conditions: Adsorbent dose 0.2 g L$^{-1}$, pH 5.5, particle size 75 – 150 µm, pharmaceutical concentration 40 mg L$^{-1}$, temperature 25, 45 and 65°C, stirring rate 200 rpm.

| Thermodynamic parameters | | | | | |
| --- | --- | --- | --- | --- | --- |
| Pharmaceutical | Temperature | $E_a$ | $\Delta G°$ | $\Delta H°$ | $\Delta S°$ |
| | (°C) | (kJ mol$^{-1}$) | (kJ mol$^{-1}$) | (kJ mol$^{-1}$) | (J mol$^{-1}$K$^{-1}$) |
| ACE | 25 | | -36.996 ± 0.03 | | |
| | 45 | 13.82 ± 1.79 | -38.375 ± 0.13 | -16.46 ± 1.40 | 68.90 ± 4.79 |
| | 65 | | -39.753 ± 0.22 | | |
| CIP | 25 | | -47.62 ± 0.07 | | |
| | 45 | 14.54 ± 0.15 | -53.26 ± 0.17 | 36.35 ± 5.16 | 281.79 ± 16.97 |
| | 64 | | -58.89 ± 0.41 | | |

The $E_a$ value found for the ACE adsorption on RH-NaOH-800°C post-washed was 13.82 kJ mol$^{-1}$, while the corresponding value for CIP was 14.54 kJ mol$^{-1}$ (Table 12). These results suggest that the mechanism is controlled by physisorption in both pharmaceuticals (activation energies values lower than 17.57 kJ mol-1) [167], similar results were reported in other studies [89], where they reported that the adsorption mechanism for these pharmaceutical molecules was controlled by physisorption .

Likewise, to determine the energy changes associated with the adsorption processes, the thermodynamic parameters: ΔS°, ΔH° and ΔG° were determined by using the *Eq. 12.* and *Eq. 13.* The plots *Ln $K_c$* versus 1/*T*, of ACE (Fig. 28 (a)) and CIP (Fig. 28 (b)), were used to calculated the slope and the intercept, which determined the parameters *ΔH°* and *ΔS°*, respectively.
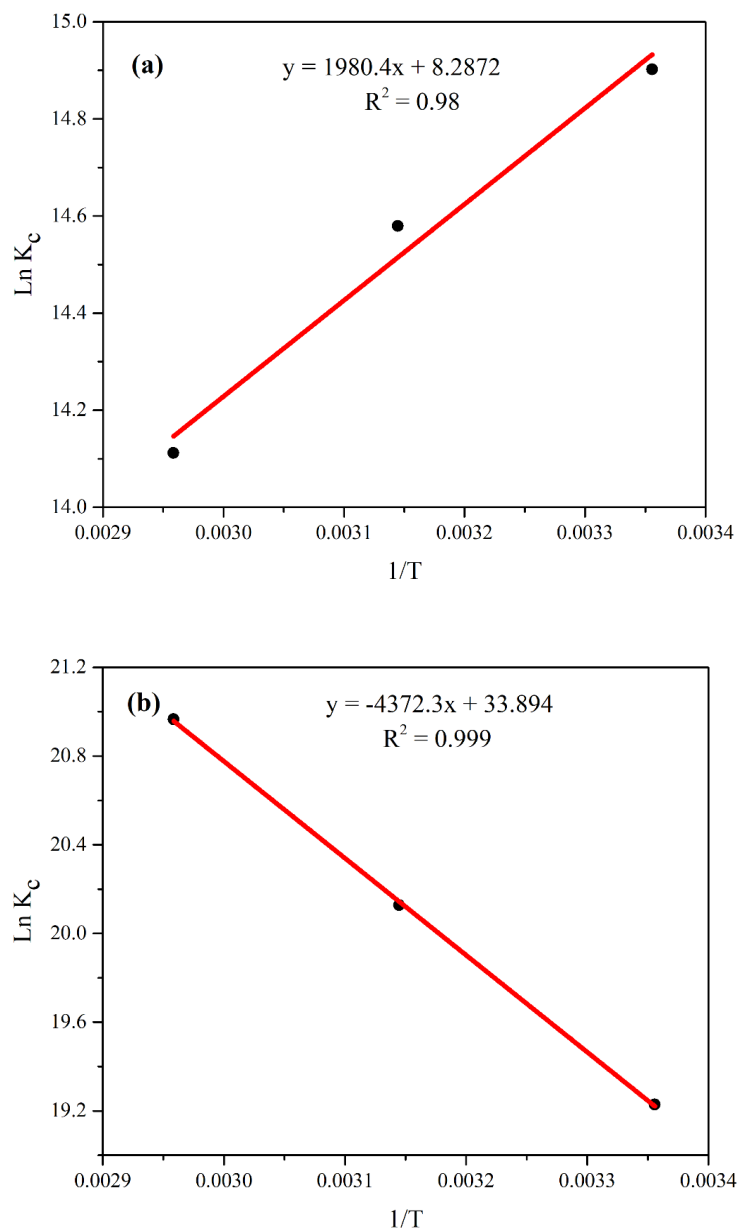
**Figure 28.** Calculation of thermodynamic parameters ($\Delta H°$ and $\Delta S°$) in the adsorption of pharmaceuticals using RH-NaOH-800°C post-washed as adsorbent. (a) ACE; (b) CIP. Conditions: pharmaceutical concentration 40 mg $L^{-1}$; temperature 25, 45 and 65°C, adsorbent dose 0.2 g $L^{-1}$, pH 5.5, particle size 75 – 150 µm, stirring rate 200 rpm.

The results in Table 12 shows that, for both pharmaceuticallys, the values $\Delta G°$ are negative, denoting that the adsorption of ACE and CIP in RH-NaOH-800°C post-washed are thermodynamically favorable and occurs spontaneously without any additional requirement

(i.e., energy or heating) [175]. $\Delta G°$ decreases with an increases in temperature, higlighting the spontaneity of ACE and CIP adsorption. The $\Delta H°$ values are lower than 80 kJ mol$^{-1}$, which is also consistent with physisorption mechanisms [176]. In addition, for CIP, $\Delta H°$ has a positive value, indicating that the adsorption is an endothermic process; while that $\Delta H°$ for ACE it was negative, consistent with a exothermic process. The fact that the process for ACE is exothermic and for CIP is endothermic, could be because thermal decomposition promotes removal of water and other volatile components from the matrices of biomasses [177] and subsequent activation results in the formation of temperature-dependent active sites [170]. If the energy involved for temperature dependent active sites is higher than the energy expelled while sorbate-sorbent interaction, the interaction would likely to be endothermic [170].Thus, the adsorption efficiency of the sorbate will increase with the increase in temperature as was reported for the adsorption of CIP (Table 12). Alternatively, if the energy involved for the active sites is less than the energy expelled durind sorbate-sorbent interaction; the adsorption phenomenon is likely to be exothermic [170]. So, the adsorption efficiency decreases with the increasing in temperature as indicated $\Delta H°$ for ACE, suggesting that the physical bond between the solute molecules and the active sites of the adsorbent weakens at higher temperatures. Additionally, positive $\Delta S°$ values denote that, at the solid/liquid interface, an increase in randomness occurs during adsorption and indicates an affinity of the adsorbent toward ACE and CIP. Finally, $\Delta H°$ values $\leq 40$ KJ mol$^{-1}$ and $E_a \leq 17.57$ KJ mol$^{-1}$, for both pharmaceuticals, means that the interaction between pharmaceuticals and RH-NaOH-800°C post-washed is mainly governed by physisorption [167], [178].

## 3.2.9 Adsorption mechanism

RH-NaOH-800°C post-washed proved to be a material with a high adsorption capacity for CIP and interesting removals for ACE, even in urine. However, the functional groups of activated carbon and of the contaminants involved in the adsorption process are unknown. Thus, to

identify the reaction mechanism of the study, a FT-IR analysis was performed, in distilled water

and urine, before and after the adsorption of ACE and CIP (Fig. 29 (a) and (b), respectively),

and an adsorption mechanism was proposed (Fig. 30 (a)-(e)).
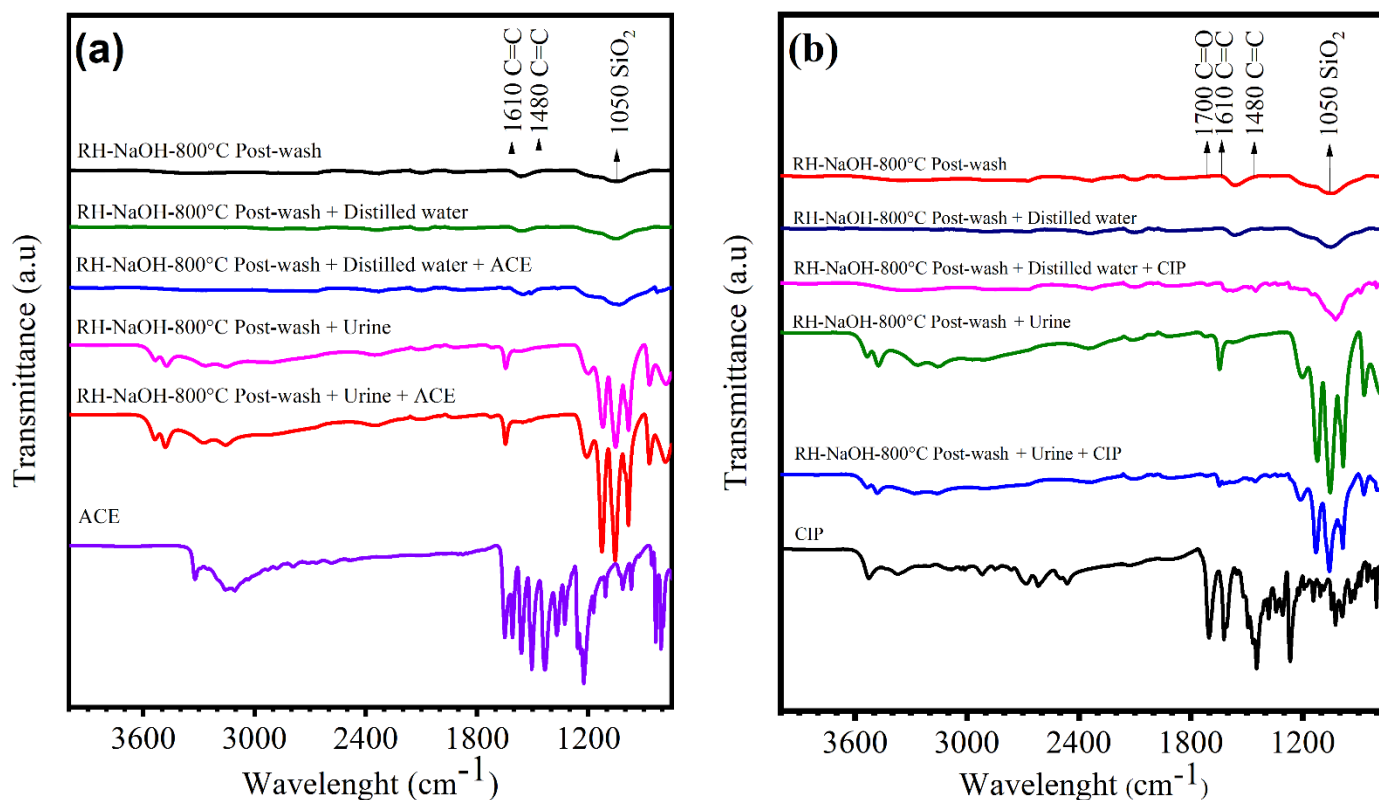


**Figure 29**. FT-IR of RH-NaOH-800°C post-washed before and after the adsorption of pharmaceuticals. (a) ACE; (b) CIP. Conditions: Pharmaceuticals concentration 15 µM , adsorbent dose 0,2 $g\ L^{-1}$ , pH 6.5 , particle size 75 – 150 µm, temperature 25°C, stirring rate 200 rpm.

**Figure 30.** ACE and CIP adsorption mechanism using RH-NaOH-800°C post-washed. Mechanism of adsorption ACE with (a) aromatic ring, (b) $SiO_2$. Mechanism of adsorption CIP with (c) aromatic ring, (d) carboxylic acid, (e) aldehydes, (f) ketones, (g) esters (h) $SiO_2$. Conditions: Pharmaceuticals concentration $15\,\mu M$, adsorbent dose $0{,}2\,g\,L^{-1}$, pH 6.5, particle size $75 - 150\,\mu m$, temperature 25°C, stirring rate 200 rpm.

In Fig. 29 (a) the FT-IR of the adsorption of ACE in distilled water and in urine using RH-NaOH-800°C post-washed is observed, both spectra show a widening of the band around 1480 cm$^{-1}$ - 1610 cm$^{-1}$ of the C=C stretch, possibly due to the π-π interaction between the aromatic rings of activated carbon and the aromatic ring of ACE (Fig. 30 (a)). In addition, at 1050 cm$^{-1}$ the increase of the SiO$_2$ band of the activated carbon is observed, possibly due to additive effect of the band at 1000 cm$^{-1}$ of the C-N stretch of the amide present in the ACE (Fig. 29 (a)), indicating the adsorption of the contaminant on the surface of the material. Here it is possible to assume that the pollutant is being adsorbed on the activated carbon by hydrogen bonds between the pairs of free electrons of the oxygen present in the Si-O-Si bonds with the hydrogen of the amide of pollutant (Fig. 30 (b)).

For the adsorption of CIP in distilled water and in urine, the widening of the band between 1480 cm$^{-1}$ and 1610 cm$^{-1}$ of the C=C stretch (Fig. 29 (b)) is observed, due to the interactions π-π between the aromatic rings of the activated carbon and the aromatic ring of the pollutant (Fig. 30 (c)). Also, in the Fig. 29 (b) a new band appeared around 1700 cm$^{-1}$ of the C=O stretch of the carboxylic acid, aldehydes, ketones, and esters [179]. This change is associated with the electrostatic interactions between the different functional groups of the activated carbon with the positive and negative charges of the pollutant. For example, the carboxylic acids present in the activated carbon are deprotonated [180], showing attraction for the positive nitrogen of the amine of the CIP (Fig. 30 (d)). Meanwhile, functional groups such as aldehydes, ketones, and esters of RH-NaOH-800°C post-washed at solution pH are positively charged [180]–[182], showing attraction for the negative charge of CIP (Fig. 30 (e), (f) and (g), respectively). Another observation was the increase of the band at 1050 cm$^{-1}$ of the SiO$_2$ bonds possibly to a summation with the band at 980 cm$^{-1}$ of C-F stretch present in the CIP (Fig. 29 (b)). This series of changes in the FT-IR spectra suggests that the CIP is being adsorbed onto the material possibly by hydrogen bonds between the free electrons of the SiO$_2$ oxygen of the activated carbon, with the

hydrogen of the amine (Fig. 30 (h)). Furthermore, $\pi$-$\pi$ interactions between the aromatic ring substituted with F, with the aromatic rings of activated carbon are possible (Fig. 30 (c)).  In this way, the $\pi$-$\pi$ and electrostatic interactions and hydrogen bonds that occur between activated carbon and pollutants (ACE and CIP) indicate that the adsorption process is physical as suggested by thermodynamics in section 3.2.8.

# CHAPTER 4

## Concluding remarks and perspectives

The overall results indicated that RH and its activated carbons proved to be adsorbents with high efficiency for the adsorption of pharmaceuticals such as ACE, CIP, SUL and DIC, which contributes to the solution of two enviromental problems at the same time, water contamination and the abundance of these residues in the environment. On the other hand, it was evidenced that the molecules that have, at the pH of the experiment, a Zwitterionic chemical structure, such as CIP, are easily adsorbed on the surface of the adsorbent materials. Molecules with larger molecular size ( such as DIC) require materials with high $S_{EXT}$ (RH-NaOH-800°C and RH-ZnCl$_2$-800°C)for their adsorption; while molecules with low molecular size, such as ACE, require materials with high microporosity (i.e RH-ZnCl$_2$-800°C). Therefore, the chemical structure of pharmaceuticals has a great influence on the adsorption process.

The results also demonstrated that the materials obtained from RH can be improved with an additional treatment (post-washed and pretreatment with NaOH), which reduces the silica content and increases the development of porosity and surface area. Therefore, the best activated carbon, RH-NaOH-800°C post-washed, proved to be highly effective for adsorption, even in complex mixtures, of all the tested pharmaceutical compounds, which exhibited a variety of chemical structures. Interestingly, except for ACE, the elimination of CIP, SUL and DIC in urine occurred efficiently without competition from pharmaceutical compounds and inorganic salts of urine. The study of kinetics and adsorption isotherms showed that the ACE and CIP adsorption data in RH-NaOH-800°C post-washed had a better fit to the pseudo-second order kinetic model and to the Langmuir isothermal model. Thus, the adsorbed pharmaceutical compounds form a monolayer on the surface of the adsorbent. Thermodynamic analysis showed that adsorption processes are exothermic and endothermic in nature for ACE and CIP, respectively, and both spontaneous. The FTIR analysis showed that the adsorption process is

carried out mainly through $\pi$-$\pi$ interactions and hydrogen bonds between activated carbon and contaminants.

Despite the good performances of the prepared materials, towards a real application of the technology it is necessary to consider the evaluation of the life cycle, reuse, regeneration and economic viability of the materials in future research. In addition, its is also necessary to test RH activated carbons in conventional treatment plants or as a tertiary treatment to complement conventional plants. Finally, it is pertinent to look for alternatives that allow a degradation of pharmaceutical contaminants within the material, in this way the development and preparation of catalytic materials combining the adsorptive properties of these materials with catalytic substrates with high oxidative power could be of great interest.

**References**

[1]     K. Kümmerer, "The presence of pharmaceuticals in the environment due to human use - present knowledge and future challenges," *J. Environ. Manage.*, vol. 90, no. 8, pp. 2354–2366, 2009, doi: 10.1016/j.jenvman.2009.01.023.

[2]     T. aus der Beek *et al.*, "Pharmaceuticals in the environment-Global occurrences and perspectives," *Environ. Toxicol. Chem.*, vol. 35, no. 4, pp. 823–835, 2016, doi: 10.1002/etc.3339.

[3]     A. B. A. Boxall *et al.*, "Pharmaceuticals and Personal Care Products in the Environment: What Are the Big Questions?," *Environ. Health Perspect.*, vol. 120, no. 9, pp. 1221–1229, 2012.

[4]     E. Fabbri and S. Franzellitti, "Human pharmaceuticals in the marine environment: Focus on exposure and biological effects in animal species," *Environ. Toxicol. Chem.*, vol. 35, no. 4, pp. 799–812, 2016, doi: 10.1002/etc.3131.

[5]     L. Minguez, J. Pedelucq, E. Farcy, C. Ballandonne, H. Budzinski, and M. P. Halm-Lemeille, "Toxicities of 48 pharmaceuticals and their freshwater and marine environmental assessment in northwestern France," *Environ. Sci. Pollut. Res.*, vol. 23, no. 6, pp. 4992–5001, 2016, doi: 10.1007/s11356-014-3662-5.

[6]     C. Cruz-Morató *et al.*, "Hospital wastewater treatment by fungal bioreactor: Removal efficiency for pharmaceuticals and endocrine disruptor compounds," *Sci. Total Environ.*, vol. 493, pp. 365–376, 2014, doi: 10.1016/j.scitotenv.2014.05.117.

[7]     S. Masson *et al.*, "Single, binary, and mixture adsorption of nine organic contaminants onto a microporous and a microporous/mesoporous activated carbon cloth," *Microporous Mesoporous Mater.*, vol. 234, pp. 24–34, 2016, doi:

10.1016/j.micromeso.2016.07.001.

[8] M. H. To, P. Hadi, C. W. Hui, C. S. K. Lin, and G. McKay, "Mechanistic study of atenolol, acebutolol and carbamazepine adsorption on waste biomass derived activated carbon," *J. Mol. Liq.*, vol. 241, pp. 386–398, 2017, doi: 10.1016/j.molliq.2017.05.037.

[9] A. Della-Flora, M. L. Wilde, P. S. Thue, D. Lima, E. C. Lima, and C. Sirtori, "Combination of solar photo-Fenton and adsorption process for removal of the anticancer drug Flutamide and its transformation products from hospital wastewater," *J. Hazard. Mater.*, vol. 396, no. April, p. 122699, 2020, doi: 10.1016/j.jhazmat.2020.122699.

[10] A. Della-Flora, M. L. Wilde, I. D. F. Pinto, É. C. Lima, and C. Sirtori, "Degradation of the anticancer drug flutamide by solar photo-Fenton treatment at near-neutral pH: Identification of transformation products and in silico (Q)SAR risk assessment," *Environ. Res.*, vol. 183, no. February, p. 109223, 2020, doi: 10.1016/j.envres.2020.109223.

[11] W. M. M. Mahmoud and K. Kümmerer, "Captopril and its dimer captopril disulfide: Photodegradation, aerobic biodegradation and identification of transformation products by HPLC-UV and LC-ion trap-MSn," *Chemosphere*, vol. 88, no. 10, pp. 1170–1177, 2012, doi: 10.1016/j.chemosphere.2012.03.064.

[12] M. Kovacic, J. Papac, H. Kusic, P. Karamanis, and A. Loncaric Bozic, "Degradation of polar and non-polar pharmaceutical pollutants in water by solar assisted photocatalysis using hydrothermal TiO2-SnS2," *Chem. Eng. J.*, vol. 382, no. June 2019, p. 122826, 2020, doi: 10.1016/j.cej.2019.122826.

[13] A. J. dos Santos, P. L. Cabot, E. Brillas, and I. Sirés, "A comprehensive study on the electrochemical advanced oxidation of antihypertensive captopril in different cells and

aqueous matrices," *Appl. Catal. B Environ.*, vol. 277, no. April, p. 119240, 2020, doi: 10.1016/j.apcatb.2020.119240.

[14]   G. Wang, D. Wang, Y. Xu, Z. Li, and L. Huang, "Study on optimization and performance of biological enhanced activated sludge process for pharmaceutical wastewater treatment," *Sci. Total Environ.*, vol. 739, p. 140166, 2020, doi: 10.1016/j.scitotenv.2020.140166.

[15]   V. Naddeo, M. F. N. Secondes, L. Borea, S. W. Hasan, F. Ballesteros, and V. Belgiorno, "Removal of contaminants of emerging concern from real wastewater by an innovative hybrid membrane process – UltraSound, Adsorption, and Membrane ultrafiltration (USAMe®)," *Ultrason. Sonochem.*, vol. 68, no. June, p. 105237, 2020, doi: 10.1016/j.ultsonch.2020.105237.

[16]   D. R. Lima *et al.*, "Efficient acetaminophen removal from water and hospital effluents treatment by activated carbons derived from Brazil nutshells," *Colloids Surfaces A Physicochem. Eng. Asp.*, vol. 583, no. July, p. 123966, 2019, doi: 10.1016/j.colsurfa.2019.123966.

[17]   H. N. Tran *et al.*, "Innovative spherical biochar for pharmaceutical removal from water: Insight into adsorption mechanism," *J. Hazard. Mater.*, vol. 394, no. January, p. 122255, 2020, doi: 10.1016/j.jhazmat.2020.122255.

[18]   K. P. Gopinath, N. V. Madhav, A. Krishnan, R. Malolan, and G. Rangarajan, "Present applications of titanium dioxide for the photocatalytic removal of pollutants from water: A review," *J. Environ. Manage.*, vol. 270, no. April, p. 110906, 2020, doi: 10.1016/j.jenvman.2020.110906.

[19]   C. Sophia A. and E. C. Lima, "Removal of emerging contaminants from the environment by adsorption," *Ecotoxicol. Environ. Saf.*, vol. 150, no. December 2017, pp. 1–17, 2018,

doi: 10.1016/j.ecoenv.2017.12.026.

[20]  Y. Piñeros Castro, Á. M. Otálvaro A, A. M. Campos, W. Cortés, J. Proaños, and G. A. Velasco, *Aplicación de tecnologías para el aprovechamiento de la cascarilla de arroz*. 2011.

[21]  Z. Shamsollahi and A. Partovinia, "Recent advances on pollutants removal by rice husk as a bio-based adsorbent: A critical review," *J. Environ. Manage.*, vol. 246, no. June, pp. 314–323, 2019, doi: 10.1016/j.jenvman.2019.05.145.

[22]  J. Garcia-ivars, L. Martella, M. Massella, C. Carbonell-alcaina, M.-I. Alcaina-Miranda, and M.-I. Iborra-Clar, "Nanofiltration as tertiary treatment method for removing trace pharmaceutically active compounds in wastewater from wastewater treatment plants," *Water Res.*, vol. 125, pp. 360–373, 2017, doi: 10.1016/j.watres.2017.08.070.

[23]  E. Cho, B. C. Bai, J. S. Im, C. W. Lee, and S. Kim, "Pore size distribution control of pitch-based activated carbon for improvement of electrochemical property," *J. Ind. Eng. Chem.*, vol. 35, pp. 341–346, 2016, doi: 10.1016/j.jiec.2016.01.012.

[24]  M. Fürhacker, "The Water Framework Directive – can we reach the target?," *Water Sci. Technol.*, vol. 57, no. 1, pp. 9–17, 2008, doi: 10.2166/wst.2008.797.

[25]  M. Salgot, E. Huertas, S. Weber, W. Dott, and J. Hollender, "Wastewater reuse and risk: definition of key objectives," *Desalination*, vol. 187, no. 1–3, pp. 29–40, 2006, doi: 10.1016/j.desal.2005.04.065.

[26]  T. A. Ternes, M. Bonerz, N. Herrmann, B. Teiser, and H. R. Andersen, "Irrigation of treated wastewater in Braunschweig , Germany: An option to remove pharmaceuticals and musk fragrances," *Chemosphere*, vol. 66, pp. 894–904, 2007, doi: 10.1016/j.chemosphere.2006.06.035.

[27]  S. Kleywegt *et al.*, "The Contribution of Pharmaceutically Active Compounds from Healthcare Facilities to a Receiving Sewage Treatment Plant in Canada," *Environ. Toxicol. Chem.*, vol. 35, no. 4, pp. 850–862, 2016, doi: 10.1002/etc.3124.

[28]  B. Tiwari, B. Sellamuthu, Y. Ouarda, P. Drogui, R. D. Tyagi, and G. Buelna, "Review on Fate and Mechanism of removal of pharmaceutical pollutants from wastewater using biological approach," *Bioresour. Technol.*, 2016, doi: 10.1016/j.biortech.2016.11.042.

[29]  E. Brezina, C. Prasse, J. Meyer, H. Mückter, and T. A. Ternes, "Investigation and risk evaluation of the occurrence of carbamazepine, oxcarbazepine, their human metabolites and transformation products in the urban water cycle," *Environ. Pollut.*, vol. 225, pp. 261–269, 2017, doi: 10.1016/j.envpol.2016.10.106.

[30]  V. S. Bessa, I. S. Moreira, M. E. Tiritan, and P. M. L. Castro, "Enrichment of bacterial strains for the biodegradation of diclofenac and carbamazepine from activated sludge," *Int. Biodeterior. Biodegradation*, vol. 120, pp. 135–142, 2017, doi: 10.1016/j.ibiod.2017.02.008.

[31]  Y. Zhang, S. Geißen, and C. Gal, "Carbamazepine and diclofenac: Removal in wastewater treatment plants and occurrence in water bodies," *Chemosphere*, vol. 73, no. 8, pp. 1151–1161, 2008, doi: 10.1016/j.chemosphere.2008.07.086.

[32]  A. M. Botero-coy *et al.*, "'An investigation into the occurrence and removal of pharmaceuticals in Colombian wastewater,'" *Sci. Total Environ.*, vol. 642, pp. 842–853, 2018, doi: 10.1016/j.scitotenv.2018.06.088.

[33]  M. Skoumal *et al.*, "Mineralization of paracetamol by ozonation catalyzed with Fe2+, Cu2+ and UVA light," *Appl. Catal. B Environ.*, vol. 66, pp. 228–240, 2006, doi: 10.1016/j.apcatb.2006.03.016.

[34]  J. Diaz-angulo, J. Lara-ramos, M. Mueses, A. Hernández-ramírez, G. Li Puma, and F. Machuca-Martínez, "Enhancement of the oxidative removal of diclofenac and of the TiO 2 rate of photon absorption in dye-sensitized solar pilot scale CPC photocatalytic reactors," *Chem. Eng. J.*, vol. 381, no. August 2019, p. 122520, 2020, doi: 10.1016/j.cej.2019.122520.

[35]  J. J. Sadhwani Alonso, N. El Kori, N. Melián-Martel, and B. Del Río-gamero, "Removal of ciprofloxacin from seawater by reverse osmosis," *J. Environ. Manage.*, vol. 217, pp. 337–345, 2018, doi: 10.1016/j.jenvman.2018.03.108.

[36]  V. Homem and L. Santos, "Degradation and removal methods of antibiotics from aqueous matrices - A review," *J. Environ. Manage.*, vol. 92, no. 10, pp. 2304–2347, 2011, doi: 10.1016/j.jenvman.2011.05.023.

[37]  K. Kümmerer, "Significance of antibiotics in the environment," *J. Antimicrob. Chemother.*, vol. 52, pp. 5–7, 2003, doi: 10.1093/jac/dkg293.

[38]  Z. Aksu and Ö. Tunç, "Application of biosorption for penicillin G removal : comparison with activated carbon," *Process Biochem.*, vol. 40, pp. 831–847, 2005, doi: 10.1016/j.procbio.2004.02.014.

[39]  CONPES, "Política Farmacéutica Nacional," *Doc. Conpes Soc. 155*, 2012.

[40]  N. H. El Najjar, A. Touffet, M. Deborde, R. Journel, and N. K. Vel Leitner, "Kinetics of paracetamol oxidation by ozone and hydroxyl radicals , formation of transformation products and toxicity," *Sep. Purif. Technol.*, vol. 136, pp. 137–143, 2014, doi: 10.1016/j.seppur.2014.09.004.

[41]  D. G. Ellenhorn, Matthew J.; Barceloux, "Medical Toxicology: Diagnosis and Treatment of Human Poisoning," *Hum. Toxicol.*, vol. 7, no. 4, pp. 387–388, 1988.

[42]  E. Villaroel, J. Silva-agredo, C. Petrier, G. Taborda, and R. A. Torres-palma, "Ultrasonic degradation of acetaminophen in water : Effect of sonochemical parameters and water matrix," *Ultrason. Sonochem.*, pp. 4–10, 2014, doi: 10.1016/j.ultsonch.2014.04.002.

[43]  L. H. M. L. M. Santos, A. N. Araújo, A. Fachini, A. Pena, C. Delerue-matos, and M. C. B. S. M. Montenegro, "Ecotoxicological aspects related to the presence of pharmaceuticals in the aquatic environment," *J. Hazard. Mater.*, vol. 175, pp. 45–95, 2010, doi: 10.1016/j.jhazmat.2009.10.100.

[44]  J. Radjenovic, M. Petrovic, and D. Barceló, "Complementary mass spectrometry and bioassays for evaluating pharmaceutical-transformation products in treatment of drinking water and wastewater," *Trends Anal. Chem.*, vol. 28, no. 5, 2009, doi: 10.1016/j.trac.2009.02.006.

[45]  T. Deblonde and P. Hartemann, "Environmental impact of medical prescriptions: assessing the risks and hazards of persistence, bioaccumulation and toxicity of pharmaceuticals," *Public Health*, vol. 127, no. 4, pp. 312–317, 2013, doi: 10.1016/j.puhe.2013.01.026.

[46]  M. E. Valdés, M. V. Amé, M. de los A. Bistoni, and D. A. Wunderlin, "Occurrence and bioaccumulation of pharmaceuticals in a fish species inhabiting the Suquía River basin (Córdoba, Argentina)," *Sci. Total Environ.*, vol. 472, pp. 389–396, 2014, doi: 10.1016/j.scitotenv.2013.10.124.

[47]  A. Zenker, M. R. Cicero, F. Prestinaci, P. Bottoni, and M. Carere, "Bioaccumulation and biomagnification potential of pharmaceuticals with a focus to the aquatic environment," *J. Environ. Manage.*, vol. 133, pp. 378–387, 2014, doi: 10.1016/j.jenvman.2013.12.017.

[48]  R. Panesar, S. Kaur, and P. S. Panesar, "Production of microbial pigments utilizing agro-industrial waste: a review," *Curr. Opin. Food Sci.*, vol. 1, pp. 70–76, 2015, doi:

10.1016/j.cofs.2014.12.002.

[49]    E. Menya, P. W. Olupot, H. Storz, M. Lubwama, and Y. Kiros, "Production and performance of activated carbon from rice husks for removal of natural organic matter from water: A review," *Chem. Eng. Res. Des.*, vol. 129, pp. 271–296, 2018, doi: 10.1016/j.cherd.2017.11.008.

[50]    Food and Agriculture Organization of the United Nations, "Rice Market Monitor," 2015.

[51]    Ankur, "'Ankur' Biomass Gasification Systems using Rice Husk as a Fuel." Ankur Scientific Energy Technologies (Pvt.) Ltd., Sama, Vadodara, India., 2010.

[52]    K. Kolecka, M. Gajewska, P. Stepnowski, and M. Caban, "Spatial distribution of pharmaceuticals in conventional wastewater treatment plant with Sludge Treatment Reed Beds technology," *Sci. Total Environ.*, vol. 647, pp. 149–157, 2019, doi: 10.1016/j.scitotenv.2018.07.439.

[53]    M. Borecka *et al.*, "Contamination of the southern Baltic Sea waters by the residues of selected pharmaceuticals : Method development and field studies," *Mar. Pollut. Bull.*, vol. 94, pp. 62–71, 2015, doi: 10.1016/j.marpolbul.2015.03.008.

[54]    M. Caban, E. Lis, J. Kumirska, and P. Stepnowski, "Determination of pharmaceutical residues in drinking water in Poland using a new SPE-GC-MS (SIM) method based on Speedisk extraction disks and DIMETRIS derivatization," *Sci. Total Environ.*, vol. 538, pp. 402–411, 2015, doi: 10.1016/j.scitotenv.2015.08.076.

[55]    E. S. Elmolla and M. Chaudhuri, "Degradation of the antibiotics amoxicillin, ampicillin and cloxacillin in aqueous solution by the photo-Fenton process," *J. Hazard. Mater.*, vol. 172, pp. 1476–1481, 2009, doi: 10.1016/j.jhazmat.2009.08.015.

[56]    C. Oliveira, D. L. D. Lima, C. P. Silva, V. Calisto, M. Otero, and V. I. Esteves,

"Photodegradation of sulfamethoxazole in environmental samples: The role of pH, organic matter and salinity," *Sci. Total Environ.*, vol. 648, pp. 1403–1410, 2019, doi: 10.1016/j.scitotenv.2018.08.235.

[57]   M. Biel-maeso, R. M. Baena-nogueras, C. Corada-fernández, and P. A. Lara-martín, "Occurrence, distribution and environmental risk of pharmaceutically active compounds (PhACs) in coastal and ocean waters from the Gulf of Cadiz (SW Spain)," *Sci. Total Environ.*, vol. 612, pp. 649–659, 2018, doi: 10.1016/j.scitotenv.2017.08.279.

[58]   W.-J. Sim, J.-W. Lee, E.-S. Lee, S.-K. Shin, S.-R. Hwang, and J.-E. Oh, "Occurrence and distribution of pharmaceuticals in wastewater from households, livestock farms, hospitals and pharmaceutical manufactures," *Chemosphere*, vol. 82, no. 2, pp. 179–186, 2011, doi: 10.1016/j.chemosphere.2010.10.026.

[59]   P. Verlicchi, M. Al Aukidy, and E. Zambello, "Occurrence of pharmaceutical compounds in urban wastewater: Removal, mass load and environmental risk after a secondary treatment — A review," *Sci. Total Environ.*, vol. 429, pp. 123–155, 2012, doi: 10.1016/j.scitotenv.2012.04.028.

[60]   P. Verlicchi, E. Zambello, and M. All Aukidy, *Removal of Pharmaceuticals by Conventional Wastewater Treatment Plants*, 2nd ed., vol. 62. Copyright © 2013 Elsevier B.V. All rights reserved., 2013.

[61]   E. Topp *et al.*, "Runoff of pharmaceuticals and personal care products following application of biosolids to an agricultural field," *Sci. Total Environ.*, vol. 396, pp. 52–59, 2008, doi: 10.1016/j.scitotenv.2008.02.011.

[62]   A. Y. Lin and Y. Tsai, "Occurrence of pharmaceuticals in Taiwan's surface waters: Impact of waste streams from hospitals and pharmaceutical production facilities," *Sci. Total Environ.*, vol. 407, no. 12, pp. 3793–3802, 2009, doi:

10.1016/j.scitotenv.2009.03.009.

[63]   C. G. Daughton and T. A. Ternes, "Pharmaceuticals and Personal Care Products in the Environment: Agents of Subtle Change?," *Environ. Health Perspect.*, vol. 107, 1999.

[64]   T. aus der Beek, F. Weber, and A. Bergmann, *Pharmaceuticals in the environment: Global occurrence and potential cooperative action under the Strategic Approach to International Chemicals Management ( SAICM )*, no. February 2019. German Environment Agency, 2016.

[65]   B. He, J. Wang, J. Liu, and X. Hu, "Eco-pharmacovigilance of non-steroidal anti-inflammatory drugs: Necessity and opportunities," *Chemosphere*, vol. 181, pp. 178–189, 2017, doi: 10.1016/j.chemosphere.2017.04.084.

[66]   E. Gracia-Lor, J. V Sancho, R. Serrano, and F. Hernández, "Occurrence and removal of pharmaceuticals in wastewater treatment plants at the Spanish Mediterranean area of Valencia," *Chemosphere*, vol. 87, no. 5, pp. 453–462, 2012, doi: 10.1016/j.chemosphere.2011.12.025.

[67]   M. Gros, M. Petrovi, A. Ginebreda, and D. Barceló, "Removal of pharmaceuticals during wastewater treatment and environmental risk assessment using hazard indexes," *Environ. Int.*, vol. 36, pp. 15–26, 2010, doi: 10.1016/j.envint.2009.09.002.

[68]   A. Jelic *et al.*, "Occurrence, partition and removal of pharmaceuticals in sewage water and sludge during wastewater treatment," *Water Res.*, vol. 45, pp. 1165–1176, 2010, doi: 10.1016/j.watres.2010.11.010.

[69]   C. Lacey, G. McMahon, J. Bones, L. Barron, A. Morrissey, and J. M. Tobin, "An LC-MS method for the determination of pharmaceutical compounds in wastewater treatment plant influent and effluent samples," *Talanta*, vol. 75, no. 4, pp. 1089–1097, 2008, doi:

10.1016/j.talanta.2008.01.011.

[70]   G. Teijon, L. Candela, K. Tamoh, A. Molina-Díaz, and A. R. Fernández-Alba, "Occurrence of emerging contaminants, priority substances (2008/105/CE) and heavy metals in treated wastewater and groundwater at Depurbaix facility (Barcelona, Spain)," *Sci. Total Environ.*, vol. 408, no. 17, pp. 3584–3595, 2010, doi: 10.1016/j.scitotenv.2010.04.041.

[71]   F. Hernández *et al.*, "LC-QTOF MS screening of more than 1,000 licit and illicit drugs and their metabolites in wastewater and surface waters from the area of Bogotá, Colombia," *Anal. Bioanal. Chem.*, no. 45, 2015, doi: 10.1007/s00216-015-8796-x.

[72]   J. Alexander, G. Knopp, A. Dötsch, A. Wieland, and T. Schwartz, "Ozone treatment of conditioned wastewater selects antibiotic resistance genes, opportunistic bacteria, and induce strong population shifts," *Sci. Total Environ.*, vol. 559, pp. 103–112, Jul. 2016, doi: 10.1016/J.SCITOTENV.2016.03.154.

[73]   S. D. Jojoa-sierra, J. Silva-agredo, E. Herrera-calderon, and R. A. Torres-palma, "Elimination of the antibiotic norfloxacin in municipal wastewater, urine and seawater by electrochemical oxidation on IrO2 anodes," *Sci. Total Environ.*, vol. 575, pp. 1228–1238, 2017, doi: 10.1016/j.scitotenv.2016.09.201.

[74]   E. A. Serna-galvis, K. E. Berrio-perlaza, and R. A. Torres-palma, "Electrochemical treatment of penicillin, cephalosporin, and fluoroquinolone antibiotics via active chlorine: evaluation of antimicrobial activity, toxicity, matrix, and their correlation with the degradation pathways," *Environ. Sci. Pollut. Res.*, no. 52, 2017, doi: 10.1007/s11356-017-9985-2.

[75]   J. Porras, C. Bedoya, J. Silva-agredo, A. Santamaría, J. J. Fernández, and R. A. Torres-palma, "Role of humic substances in the degradation pathways and residual antibacterial

activity during the photodecomposition of the antibiotic ciprofloxacin in water," *Water Res.*, vol. 94, pp. 1–9, 2016, doi: 10.1016/j.watres.2016.02.024.

[76]    S. R. Batchu, V. R. Panditi, K. E. O. O´Shea, and P. R. Gardinali, "Photodegradation of antibiotics under simulated solar radiation: Implications for their environmental fate," *Sci. Total Environ.*, vol. 470–471, pp. 299–310, 2014, doi: 10.1016/j.scitotenv.2013.09.057.

[77]    T. Wang, X. Pan, W. Ben, J. Wang, P. Hou, and Z. Qiang, "Adsorptive removal of antibiotics from water using magnetic ion exchange resin," *J. Environ. Sci.*, pp. 1–7, 2016, doi: 10.1016/j.jes.2016.03.017.

[78]    X. Weng, Y. Ji, R. Ma, F. Zhao, Q. An, and C. Gao, "Superhydrophilic and antibacterial zwitterionic polyamide nanofiltration membranes for antibiotics separation," *J. Memb. Sci.*, vol. 510, pp. 122–130, 2016, doi: 10.1016/j.memsci.2016.02.070.

[79]    S. Pan, M. Zhu, J. P. Chen, Z. Yuan, L. Zhong, and Y. Zheng, "Separation of tetracycline from wastewater using forward osmosis process with thin film composite membrane – Implications for antibiotics recovery," *Sep. Purif. Technol.*, vol. 153, pp. 76–83, 2015, doi: 10.1016/j.seppur.2015.08.034.

[80]    M. Yoosefian, S. Ahmadzadeh, M. Aghasi, and M. Dolatabadi, "Optimization of electrocoagulation process for efficient removal of ciprofloxacin antibiotic using iron electrode; kinetic and isotherm studies of adsorption," *J. Mol. Liq.*, 2016, doi: 10.1016/j.molliq.2016.11.093.

[81]    Y. Li, Z. Wang, X. Xie, J. Zhu, R. Li, and T. Qin, "Removal of Norfloxacin from aqueous solution by clay-biochar composite prepared from potato stem and natural attapulgite," *Colloids Surfaces A Physicochem. Eng. Asp.*, 2016, doi: 10.1016/j.colsurfa.2016.11.064.

[82]  Z. Hu, M. P. Srinivasan, and Y. Ni, "Novel activation process for preparing highly microporous and mesoporous activated carbons," *Carbon N. Y.*, vol. 39, pp. 877–886, 2001.

[83]  G. Z. Kyzas, E. A. Deliyanni, and K. A. Matis, "Activated carbons produced by pyrolysis of waste potato peels: Cobalt ions removal by adsorption," *Colloids Surfaces A Physicochem. Eng. Asp.*, 2015, doi: 10.1016/j.colsurfa.2015.11.038.

[84]  E. Altintig, G. Arabaci, and H. Altundag, "Preparation and characterization of the antibacterial efficiency of silver loaded activated carbon from corncobs," *Surf. Coatings Technol.*, vol. 304, pp. 63–67, Oct. 2016, doi: 10.1016/J.SURFCOAT.2016.06.077.

[85]  M. Ghaedi, A. G. Nasab, S. Khodadoust, M. Rajabi, and S. Azizian, "Application of activated carbon as adsorbents for efficient removal of methylene blue: Kinetics and equilibrium study," *J. Ind. Eng. Chem.*, vol. 20, no. 4, pp. 2317–2324, 2014, doi: 10.1016/j.jiec.2013.10.007.

[86]  K. Li, Z. Zheng, and Y. Li, "Characterization and lead adsorption properties of activated carbons prepared from cotton stalk by one-step H3PO4 activation," *J. Hazard. Mater.*, vol. 181, pp. 440–447, 2010, doi: 10.1016/j.jhazmat.2010.05.030.

[87]  B. G. P. Kumar, K. Shivakamy, L. R. Miranda, and M. Velan, "Preparation of steam activated carbon from rubberwood sawdust (Hevea brasiliensis) and its adsorption kinetics," *J. Hazard. Mater.*, vol. 136, pp. 922–929, 2006, doi: 10.1016/j.jhazmat.2006.01.037.

[88]  M. A. Ahmad and N. K. Rahman, "Equilibrium, kinetics and thermodynamic of Remazol Brilliant Orange 3R dye adsorption on coffee husk-based activated carbon," *Chem. Eng. J.*, vol. 170, no. 1, pp. 154–161, May 2011, doi: 10.1016/J.CEJ.2011.03.045.

[89]    M. Paredes-Laverde, M. Salamanca, J. Silva-Agredo, L. Manrique-Losada, and R. A. Torres-Palma, "Selective removal of acetaminophen in urine with activated carbons from rice (Oryza sativa) and coffee (Coffea arabica) husk: Effect of activating agent, activation temperature and analysis of physical-chemical interactions," *J. Environ. Chem. Eng.*, vol. 7, no. 5, p. 103318, 2019, doi: 10.1016/j.jece.2019.103318.

[90]    P. González-García, "Activated carbon from lignocellulosics precursors: A review of the synthesis methods, characterization techniques and applications," *Renew. Sustain. Energy Rev.*, vol. 82, no. August 2017, pp. 1393–1414, 2018, doi: 10.1016/j.rser.2017.04.117.

[91]    P. Chingombe, B. Saha, and R. J. Wakeman, "Surface modification and characterisation of a coal-based activated carbon," *Carbon N. Y.*, vol. 43, pp. 3132–3143, 2005, doi: 10.1016/j.carbon.2005.06.021.

[92]    Y. Chen, S. Zhai, N. Liu, Y. Song, Q. An, and X. Song, "Dye removal of activated carbons prepared from NaOH-pretreated rice husks by low-temperature solution-processed carbonization and H3PO4 activation," *Bioresour. Technol.*, vol. 144, pp. 401–409, 2013, doi: 10.1016/j.biortech.2013.07.002.

[93]    S. Yao *et al.*, "Removal of Pb (II) from water by the activated carbon modified by nitric acid under microwave heating," *J. Colloid Interface Sci.*, no. Ii, 2015, doi: 10.1016/j.jcis.2015.10.047.

[94]    S. Sugashini, K. Mohamed, and M. Sheriffa, "Preparation of activated carbon from carbonized rice husk by ozone activation for Cr (VI) removal," *New Carbon Mater.*, vol. 30, no. 3, pp. 252–261, 2015, doi: 10.1016/S1872-5805(15)60190-1.

[95]    K.-L. Chang *et al.*, "Rice straw-derived activated carbons for the removal of carbofuran from an aqueous solution," *New Carbon Mater.*, vol. 29, no. 1, pp. 47–54, 2014, doi:

10.1016/S1872-5805(14)60125-6.

[96]    S. L. Ng, C. E. Seng, and P. E. Lim, "Bioregeneration of activated carbon and activated rice husk loaded with phenolic compounds: Kinetic modeling," *Chemosphere*, vol. 78, no. 5, pp. 510–516, 2010, doi: 10.1016/j.chemosphere.2009.11.041.

[97]    N. Yalc and V. Sevinc, "Studies of the surface area and porosity of activated carbons prepared from rice husks," *Carbon N. Y.*, vol. 38, pp. 1943–1945, 2000.

[98]    P. T. Williams and A. R. Reed, "Pre-formed activated carbon matting derived from the pyrolysis of biomass natural fibre textile waste," *J. Anal. Appl. Pyrolysis*, vol. 70, pp. 563–577, 2003, doi: 10.1016/S0165-2370(03)00026-3.

[99]    J. Yang and K. Qiu, "Preparation of activated carbons from walnut shells via vacuum chemical activation and their application for methylene blue removal," *Chem. Eng. J.*, vol. 165, no. 1, pp. 209–217, 2010, doi: 10.1016/j.cej.2010.09.019.

[100]   O. Pezoti *et al.*, "NaOH-activated carbon of high surface area produced from guava seeds as a high-efficiency adsorbent for amoxicillin removal: Kinetic, isotherm and thermodynamic studies," *Chem. Eng. J.*, 2015, doi: 10.1016/j.cej.2015.12.042.

[101]   O. Pezoti Jr. *et al.*, "Adsorption studies of methylene blue onto ZnCl2-activated carbon produced from buriti shells (Mauritia flexuosa L.)," *J. Ind. Eng. Chem.*, 2014, doi: 10.1016/j.jiec.2014.02.007.

[102]   F. Gimbert, N. Morin-Crini, F. Renault, P. M. Badot, and G. Crini, "Adsorption isotherm models for dye removal by cationized starch-based material in a single component system: Error analysis," *J. Hazard. Mater.*, vol. 157, no. 1, pp. 34–46, 2008, doi: 10.1016/j.jhazmat.2007.12.072.

[103]   Z. Liu *et al.*, "New strategy to prepare ultramicroporous carbon by ionic activation for

superior CO2 capture," *Chem. Eng. J.*, vol. 337, no. December 2017, pp. 290–299, 2018, doi: 10.1016/j.cej.2017.11.184.

[104] L. S. Balistrieri and J. W. Murray, "The surface chemistry of goethite (alpha -FeOOH) in major ion seawater.," *Am. J. Sci.*, vol. 281, no. 6, pp. 788–806, 1981, doi: 10.2475/ajs.281.6.788.

[105] M. Paredes-Laverde, J. Silva-Agredo, and R. A. Torres-Palma, "Removal of norfloxacin in deionized, municipal water and urine using rice (Oryza sativa) and coffee (Coffea arabica) husk wastes as natural adsorbents," *J. Environ. Manage.*, vol. 213, pp. 98–108, 2018, doi: 10.1016/j.jenvman.2018.02.047.

[106] I. Anastopoulos, M. Karamesouti, A. C. Mitropoulos, and G. Z. Kyzas, "A review for coffee adsorbents," *J. Mol. Liq.*, vol. 229, pp. 555–565, 2017, doi: 10.1016/j.molliq.2016.12.096.

[107] X. Song, Y. Zhang, and C. Chang, "Novel method for preparing activated carbons with high specific surface area from rice husk," *Ind. Eng. Chem. Res.*, vol. 51, no. 46, pp. 15075–15081, 2012, doi: 10.1021/ie3012853.

[108] V. Balasundram *et al.*, "Thermogravimetric catalytic pyrolysis and kinetic studies of coconut copra and rice husk for possible maximum production of pyrolysis oil," *J. Clean. Prod.*, vol. 167, pp. 218–228, 2017, doi: 10.1016/j.jclepro.2017.08.173.

[109] S. Lv, C. Li, J. Mi, and H. Meng, "A functional activated carbon for efficient adsorption of phenol derived from pyrolysis of rice husk, KOH-activation and EDTA-4Na-modification," *Appl. Surf. Sci.*, vol. 510, no. November 2019, p. 145425, 2020, doi: 10.1016/j.apsusc.2020.145425.

[110] A. Bazan, P. Nowicki, P. Półrolniczak, and R. Pietrzak, "Thermal analysis of activated

carbon obtained from residue after supercritical extraction of hops," *J. Therm. Anal. Calorim.*, vol. 125, no. 3, pp. 1199–1204, 2016, doi: 10.1007/s10973-016-5419-5.

[111] P. Nowicki, "Effect of heat treatment on the physicochemical properties of nitrogen-enriched activated carbons," *J. Therm. Anal. Calorim.*, vol. 125, no. 3, pp. 1017–1024, 2016, doi: 10.1007/s10973-016-5254-8.

[112] K. Mohanty, D. Das, and M. N. Biswas, "Adsorption of phenol from aqueous solutions using activated carbons prepared from Tectona grandis sawdust by ZnCl2 activation," *Chem. Eng. J.*, vol. 115, no. 1–2, pp. 121–131, 2005, doi: 10.1016/j.cej.2005.09.016.

[113] J. Yang, Y. Zhao, S. Ma, B. Zhu, J. Zhang, and C. Zheng, "Mercury Removal by Magnetic Biochar Derived from Simultaneous Activation and Magnetization of Sawdust," *Environ. Sci. Technol.*, vol. 50, no. 21, pp. 12040–12047, 2016, doi: 10.1021/acs.est.6b03743.

[114] M. A. Lillo-Ródenas, D. Cazorla-Amorós, and A. Linares-Solano, "Understanding chemical reactions between carbons and NaOH and KOH: An insight into the chemical activation mechanism," *Carbon N. Y.*, vol. 41, no. 2, pp. 267–275, 2003, doi: 10.1016/S0008-6223(02)00279-8.

[115] J. Ponce *et al.*, "Alkali pretreated sugarcane bagasse, rice husk and corn husk wastes as lignocellulosic biosorbents for dyes," *Carbohydr. Polym. Technol. Appl.*, vol. 2, no. May 2020, p. 100061, 2021, doi: 10.1016/j.carpta.2021.100061.

[116] E. Hu *et al.*, "Investigation into the Morphology, Composition, Structure and Dry Tribological Behavior of Rice Husk Ceramic Particles," *Appl. Surf. Sci.*, vol. 366, pp. 372–382, 2016, doi: 10.1016/j.apsusc.2016.01.116.

[117] D. Imessaoudene, S. Hanini, A. Bouzidi, and A. Ararem, "Kinetic and thermodynamic

study of cobalt adsorption by spent coffee," *Desalin. Water Treat.*, vol. 57, no. 13, pp. 6116–6123, 2015, doi: 10.1080/19443994.2015.1041049.

[118] L. Wang, Z. Wang, X. Cheng, M. Zhang, Y. Qin, and C. Ma, "In situ DRIFTS study of the NO + CO reaction on Fe-Co binary metal oxides over activated semi-coke supports," *RSC Adv.*, vol. 7, no. 13, pp. 7695–7710, 2017, doi: 10.1039/c6ra26395j.

[119] Mebrahtom Gebresemati, Nigus Gabbiye, and O. Sahu, "Sorption of cyanide from aqueous medium by coffee husk: Response surface methodology," *J. Appl. Res. Technol.*, vol. 15, no. 1, pp. 27–35, 2017, doi: 10.1016/j.jart.2016.11.002.

[120] L. J. Kennedy, J. J. Vijaya, and G. Sekaran, "Effect of Two-Stage Process on the Preparation and Characterization of Porous Carbon Composite from Rice Husk by Phosphoric Acid Activation," *Ind. Eng. Chem. Res.*, vol. 43, no. 8, pp. 1832–1838, 2004.

[121] M. Ebrahimi, A. R. Caparanga, E. E. Ordono, O. B. Villaflores, and M. Pouriman, "Effect of ammonium carbonate pretreatment on the enzymatic digestibility , structural characteristics of rice husk and bioethanol production via simultaneous saccharification and fermentation process with Saccharomyces cerevisiae Hansen 2055," *Ind. Crops Prod.*, vol. 101, pp. 84–91, 2017, doi: 10.1016/j.indcrop.2017.03.006.

[122] A. Masoumi, K. Hemmati, and M. Ghaemy, "Low-cost nanoparticles sorbent from modified rice husk and a copolymer for efficient removal of Pb (II) and crystal violet from water," *Chemosphere*, vol. 146, pp. 253–262, 2016, doi: 10.1016/j.chemosphere.2015.12.017.

[123] J. Xu, N. Gao, D. Zhao, N. An, L. Li, and J. Xiao, "Bromate reduction and reaction-enhanced perchlorate adsorption by FeCl3-impregnated granular activated carbon," *Water Res.*, vol. 149, pp. 149–158, 2019, doi: 10.1016/j.watres.2018.11.005.

[124] J. Bedia, M. Peñas-Garzón, A. Gómez-Avilés, J. J. Rodriguez, and C. Belver, "Review on Activated Carbons by Chemical Activation with FeCl3," *C — J. Carbon Res.*, vol. 6, no. 2, p. 21, 2020, doi: 10.3390/c6020021.

[125] L. Wang *et al.*, "Preparation of carbon black from rice husk by hydrolysis, carbonization and pyrolysis," *Bioresour. Technol.*, vol. 102, no. 17, pp. 8220–8224, 2011, doi: 10.1016/j.biortech.2011.05.079.

[126] D. Van Nguyen, H. N. Do, H. N. Do, and Q. N. Long, "One-step preparation of rice husk-based magnetic biochar and its catalytic activity for p-nitrophenol degradation," *Chem. Eng. Trans.*, vol. 78, pp. 379–384, 2020, doi: 10.3303/CET2078064.

[127] D. W. Cho, J. Lee, K. Yoon, Y. S. Ok, E. E. Kwon, and H. Song, "Pyrolysis of FeCl3-pretreated spent coffee grounds using CO2 as a reaction medium," *Energy Convers. Manag.*, vol. 127, pp. 437–442, 2016, doi: 10.1016/j.enconman.2016.09.036.

[128] M. J. Saad, C. C. Hua, S. Misran, S. Zakaria, M. S. Sajab, and M. H. Abdul Rahman, "Rice husk activated carbon with naoh activation: Physical and chemical properties," *Sains Malaysiana*, vol. 49, no. 9, pp. 2261–2267, 2020, doi: 10.17576/jsm-2020-4909-23.

[129] A. F. Hassan and A. M. Youssef, "Preparation and characterization of microporous NaOH-activated carbons from hydrofluoric acid leached rice husk and its application for lead(II) adsorption," *Carbon Lett.*, vol. 15, no. 1, pp. 57–66, 2014, doi: 10.5714/cl.2014.15.1.057.

[130] K. Le Van and T. L. Thi Thu, "Preparation of Pore-Size Controllable Activated Carbon from Rice Husk Using Dual Activating Agent and Its Application in Supercapacitor," *Hindawi J. Chem.*, vol. 2019, p. 11, 2019, doi: 10.1155/2019/4329609.

[131] P. E. Hock and M. A. A. Zaini, "Activated carbons by zinc chloride activation for dye removal – a commentary," *Acta Chim. Slovaca*, vol. 11, no. 2, pp. 99–106, 2018, doi: 10.2478/acs-2018-0015.

[132] Y. Gao, Q. Yue, B. Gao, and A. Li, "Insight into activated carbon from different kinds of chemical activating agents: A review," *Sci. Total Environ.*, vol. 746, p. 141094, 2020, doi: 10.1016/j.scitotenv.2020.141094.

[133] D. Prahas, Y. Kartika, N. Indraswati, and S. Ismadji, "Activated carbon from jackfruit peel waste by H3PO4 chemical activation: Pore structure and surface chemistry characterization," *Chem. Eng. J.*, vol. 140, no. 1–3, pp. 32–42, 2008, doi: 10.1016/j.cej.2007.08.032.

[134] K. Sing *et al.*, "REPORTING PHYSISORPTION DATA FOR GAS/SOLID SYSTEMS with Special Reference to the Determination of Surface Area and Porosity," *Pure Appl. Chem.*, vol. 57, no. 4, pp. 603–619, 1985, doi: 10.1351 / pac198557040603.

[135] L. Shrestha, M. Thapa, R. Shrestha, S. Maji, R. Pradhananga, and K. Ariga, "Rice Husk-Derived High Surface Area Nanoporous Carbon Materials with Excellent Iodine and Methylene Blue Adsorption Properties," *C — J. Carbon Res.*, vol. 5, no. 1, p. 10, 2019, doi: 10.3390/c5010010.

[136] P. Del Vecchio, N. K. Haro, F. S. Souza, N. R. Marcílio, and L. A. Féris, "Ampicillin removal by adsorption onto activated carbon: Kinetics, equilibrium and thermodynamics," *Water Sci. Technol.*, vol. 79, no. 10, pp. 2013–2021, 2019, doi: 10.2166/wst.2019.205.

[137] S. Dastmalchi, M. Rashidi, and M. Rassi, "Simultaneous determination of the pKa and octanol/water partition coefficient (Pm) of acetaminophen," *J Sch Pharm Med Sci Univ Tehran*, vol. 4, pp. 7–14, 1995.

[138] L. Li, F. Sun, J. Gao, L. Wang, X. Pi, and G. Zhao, "Broadening the pore size of coal-based activated carbon: Via a washing-free chem-physical activation method for high-capacity dye adsorption," *RSC Adv.*, vol. 8, no. 26, pp. 14488–14499, 2018, doi: 10.1039/c8ra02127a.

[139] Z. Qiang and C. Adams, "Potentiometric determination of acid dissociation constants (pK a) for human and veterinary antibiotics," *Water Res.*, vol. 38, no. 12, pp. 2874–2890, 2004, doi: 10.1016/j.watres.2004.03.017.

[140] X. Peng, F. Hu, H. Dai, Q. Xiong, and C. Xu, "Study of the adsorption mechanisms of ciprofloxacin antibiotics onto graphitic ordered mesoporous carbons," *J. Taiwan Inst. Chem. Eng.*, vol. 65, pp. 472–481, 2016, doi: 10.1016/j.jtice.2016.05.016.

[141] N. Ren, C. Wang, W. Wei, J. Li, X. Yue, and G. Qin, "Ciprofloxacin adsorption on a mesoporous carbon prepared by a dual-template route," *Desalin. Water Treat.*, vol. 192, pp. 241–247, 2020, doi: 10.5004/dwt.2020.25760.

[142] C. Ràfols, M. Rosés, and E. Bosch, "A comparison between different approaches to estimate the aqueous pK(a) values of several non-steroidal anti-inflammatory drugs," *Anal. Chim. Acta*, vol. 338, no. 1–2, pp. 127–134, 1997, doi: 10.1016/S0003-2670(96)00496-5.

[143] L. Ji, Y. Wan, S. Zheng, and D. Zhu, "Adsorption of tetracycline and sulfamethoxazole on crop residue-derived ashes: Implication for the relative importance of black carbon to soil sorption," *Environ. Sci. Technol.*, vol. 45, no. 13, pp. 5580–5586, 2011, doi: 10.1021/es200483b.

[144] Y. Sun, H. Li, G. Li, B. Gao, Q. Yue, and X. Li, "Characterization and ciprofloxacin adsorption properties of activated carbons prepared from biomass wastes by H3PO4 activation," *Bioresour. Technol.*, vol. 217, pp. 239–244, 2016, doi:

10.1016/j.biortech.2016.03.047.

[145] D. Bahamon and L. F. Vega, "Pharmaceutical Removal from Water Effluents by Adsorption on Activated Carbons: A Monte Carlo Simulation Study," *Langmuir*, vol. 33, no. 42, pp. 11146–11155, 2017, doi: 10.1021/acs.langmuir.7b01967.

[146] D. Veclani and A. Melchior, "Adsorption of ciprofloxacin on carbon nanotubes: Insights from molecular dynamics simulations," *J. Mol. Liq.*, vol. 298, p. 111977, 2020, doi: 10.1016/j.molliq.2019.111977.

[147] Y. Lu, M. Jiang, C. Wang, Y. Wang, and W. Yang, "Impact of molecular size on two antibiotics adsorption by porous resins," *J. Taiwan Inst. Chem. Eng.*, vol. 45, no. 3, pp. 955–961, 2014, doi: 10.1016/j.jtice.2013.09.009.

[148] E. E. Chang, J. C. Wan, H. Kim, C. H. Liang, Y. D. Dai, and P. C. Chiang, "Adsorption of selected pharmaceutical compounds onto activated carbon in dilute aqueous solutions exemplified by acetaminophen, diclofenac, and sulfamethoxazole," *Sci. World J.*, vol. 2015, 2015, doi: 10.1155/2015/186501.

[149] T. H. Liou and S. J. Wu, "Characteristics of microporous/mesoporous carbons prepared from rice husk under base- and acid-treated conditions," *J. Hazard. Mater.*, vol. 171, no. 1–3, pp. 693–703, 2009, doi: 10.1016/j.jhazmat.2009.06.056.

[150] E. Khoshnood Motlagh, N. Asasian-Kolur, S. Sharifian, and A. Ebrahimian Pirbazari, "Sustainable rice straw conversion into activated carbon and nano-silica using carbonization-extraction process," *Biomass and Bioenergy*, vol. 144, no. December 2020, p. 105917, 2021, doi: 10.1016/j.biombioe.2020.105917.

[151] E. L. Foletto, E. Gratieri, L. H. de Oliveira, and S. L. Jahn, "Conversion of rice hull ash into soluble sodium silicate," *Mater. Res.*, vol. 9, no. 3, pp. 335–338, 2006, doi:

10.1590/S1516-14392006000300014.

[152] N. Ninwiwek, P. Hongsawat, P. Punyapalakul, and P. Prarat, "Removal of the antibiotic sulfamethoxazole from environmental water by mesoporous silica-magnetic graphene oxide nanocomposite technology: Adsorption characteristics, coadsorption and uptake mechanism," *Colloids Surfaces A Physicochem. Eng. Asp.*, vol. 580, no. July, p. 123716, 2019, doi: 10.1016/j.colsurfa.2019.123716.

[153] H. Fu *et al.*, "Activated carbon adsorption of quinolone antibiotics in water: Performance, mechanism, and modeling," *J. Environ. Sci. (China)*, vol. 56, pp. 145–152, 2017, doi: 10.1016/j.jes.2016.09.010.

[154] V. Ponnusami, S. Vikram, and S. N. Srivastava, "Guava (Psidium guajava) leaf powder: Novel adsorbent for removal of methylene blue from aqueous solutions," *J. Hazard. Mater.*, vol. 152, no. 1, pp. 276–286, 2008, doi: 10.1016/j.jhazmat.2007.06.107.

[155] M. S. Monteiro, R. F. de Farias, J. A. P. Chaves, S. A. Santana, H. A. S. Silva, and C. W. B. Bezerra, "Wood (Bagassa guianensis Aubl) and green coconut mesocarp (cocos nucifera) residues as textile dye removers (Remazol Red and Remazol Brilliant Violet)," *J. Environ. Manage.*, vol. 204, pp. 23–30, 2017, doi: 10.1016/j.jenvman.2017.08.033.

[156] E. K. Guechi and O. Hamdaoui, "Evaluation of potato peel as a novel adsorbent for the removal of Cu(II) from aqueous solutions: equilibrium, kinetic, and thermodynamic studies," *Desalin. Water Treat.*, vol. 57, no. 23, pp. 10677–10688, 2016, doi: 10.1080/19443994.2015.1038739.

[157] E. K. Guechi and O. Hamdaoui, "Sorption of malachite green from aqueous solution by potato peel: Kinetics and equilibrium modeling using non-linear analysis method," *Arab. J. Chem.*, vol. 9, pp. S416–S424, 2016, doi: 10.1016/j.arabjc.2011.05.011.

[158] O. Redlich and D. Peterson, "A useful adsorption isotherm," *J. Chem. Phys.*, vol. 63, no. 1958, p. 1024, 1958.

[159] I. Cabrita, B. Ruiz, A. S. Mestre, I. M. Fonseca, A. P. Carvalho, and C. O. Ania, "Removal of an analgesic using activated carbons prepared from urban and industrial residues," *Chem. Eng. J.*, vol. 163, no. 3, pp. 249–255, 2010, doi: 10.1016/j.cej.2010.07.058.

[160] L. Sellaoui, E. C. Lima, G. L. Dotto, and A. Ben Lamine, "Adsorption of amoxicillin and paracetamol on modified activated carbons: Equilibrium and positional entropy studies," *J. Mol. Liq.*, vol. 234, pp. 375–381, 2017, doi: 10.1016/j.molliq.2017.03.111.

[161] N.-A. George Nche, A. Bopda, D. Raoul Tchuifon Tchuifon, C. Sadeu Ngakou, I.-H. Tiotsop Kuete, and A. Solomon Gabche, "Removal of Paracetamol from Aqueous Solution by Adsorption onto Activated Carbon Prepared from Rice Husk," *J. Chem. Pharm. Res.*, vol. 9, no. 3, pp. 56–68, 2017.

[162] B. Zhang, X. Han, P. Gu, S. Fang, and J. Bai, "Response surface methodology approach for optimization of ciprofloxacin adsorption using activated carbon derived from the residue of desilicated rice husk," *J. Mol. Liq.*, vol. 238, pp. 316–325, 2017, doi: 10.1016/j.molliq.2017.04.022.

[163] M. Wang *et al.*, "Study of ciprofloxacin adsorption and regeneration of activated carbon prepared from Enteromorpha prolifera impregnated with H3PO4 and sodium benzenesulfonate," *Ecotoxicol. Environ. Saf.*, vol. 139, no. October 2016, pp. 36–42, 2017, doi: 10.1016/j.ecoenv.2017.01.006.

[164] M. E. Peñafiel, J. M. Matesanz, E. Vanegas, D. Bermejo, R. Mosteo, and M. P. Ormad, "Comparative adsorption of ciprofloxacin on sugarcane bagasse from Ecuador and on commercial powdered activated carbon," *Sci. Total Environ.*, vol. 750, 2021, doi:

10.1016/j.scitotenv.2020.141498.

[165] S. C. Angelo Earvin, S. Roces, N. Dugos, and M. Wan, "Adsorption of benzothiophene sulfone over clay mineral adsorbents in the frame of oxidative desulfurization," *Fuel*, vol. 205, pp. 153–160, 2017, doi: 10.1016/j.fuel.2017.05.070.

[166] C. Mary Jane C, D. B. Senoro, K. Chi-Chuan, J. W. L. Salvacion, F. Cybelle Morales, and M. Wan, "Adsorption of indium ( III ) ions from aqueous solution using chitosan-coated bentonite beads," *J. Hazard. Mater.*, vol. 277, pp. 120–126, 2014, doi: 10.1016/j.jhazmat.2014.04.043.

[167] S. Chakraborty, S. Chowdhury, and S. Papita Das, "Adsorption of Crystal Violet from aqueous solution onto NaOH-modified rice husk," *Carbohydr. Polym.*, vol. 86, no. 4, pp. 1533–1541, 2011, doi: 10.1016/j.carbpol.2011.06.058.

[168] C. C. V. Cruz, A. C. A. da Costa, C. A. Henriques, and A. S. Luna, "Kinetic modeling and equilibrium studies during cadmium biosorption by dead Sargassum sp. biomass," *Bioresour. Technol.*, vol. 91, pp. 249–257, 2004, doi: 10.1016/S0960-8524(03)00194-9.

[169] M. J. Ahmed and S. K. Theydan, "Fluoroquinolones antibiotics adsorption onto microporous activated carbon from lignocellulosic biomass by microwave pyrolysis," *J. Taiwan Inst. Chem. Eng.*, vol. 45, no. 1, pp. 219–226, 2014, doi: 10.1016/j.jtice.2013.05.014.

[170] A. Chandrasekaran, C. Patra, S. Narayanasamy, and S. Subbiah, "Adsorptive removal of Ciprofloxacin and Amoxicillin from single and binary aqueous systems using acid-activated carbon from Prosopis juliflora," *Environ. Res.*, vol. 188, no. April, p. 109825, 2020, doi: 10.1016/j.envres.2020.109825.

[171] S. Wong *et al.*, "Removal of acetaminophen by activated carbon synthesized from spent

tea leaves: equilibrium, kinetics and thermodynamics studies," *Powder Technol.*, vol. 338, pp. 878–886, 2018, doi: 10.1016/j.powtec.2018.07.075.

[172] K. Mohanty, J. T. Naidu, B. C. Meikap, and M. N. Biswas, "Removal of Crystal Violet from Wastewater by Activated Carbons Prepared from Rice Husk," *Ind. Eng. Chem. Res.*, vol. 45, pp. 5165–5171, 2006.

[173] W. H. Zou, L. Zhao, and L. Zhu, "Efficient uranium (VI) biosorption on grapefruit peel: kinetic study and thermodynamic parameters," *J. Radioanal. Nucl. Chem.*, vol. 292, no. 3, pp. 1303–1315, 2012, doi: 10.1007/s10967-011-1602-0.

[174] B. H. Hameed, A. A. Ahmad, and N. Aziz, "Isotherms, kinetics and thermodynamics of acid dye adsorption on activated palm ash," *Chem. Eng. J.*, vol. 133, no. 1–3, pp. 195–203, 2007, doi: 10.1016/j.cej.2007.01.032.

[175] É. C. Lima, F. J. Krug, J. A. Nóbrega, and A. R. A. Nogueira, "Determination of ytterbium in animal faeces by tungsten coil electrothermal atomic absorption spectrometry," *Talanta*, vol. 47, no. 3, pp. 613–623, 1998, doi: 10.1016/S0039-9140(98)00087-3.

[176] H. N. Tran, S. J. You, and H. P. Chao, "Thermodynamic parameters of cadmium adsorption onto orange peel calculated from various methods: A comparison study," *J. Environ. Chem. Eng.*, vol. 4, no. 3, pp. 2671–2682, 2016, doi: 10.1016/j.jece.2016.05.009.

[177] L. S. Rocha, D. Pereira, É. Sousa, M. Otero, V. I. Esteves, and V. Calisto, "Recent advances on the development and application of magnetic activated carbon and char for the removal of pharmaceutical compounds from waters: A review," *Sci. Total Environ. J.*, vol. 718, p. 137272, 2020, doi: 10.1016/j.scitotenv.2020.137272.

[178] R. Chang and J. W. Thoman Jr, "Intermolecular forces," in *Physical Chemistry for the Chemical Sciences*, University Science Books, 2014, pp. 779–808.

[179] A. B. . Nandiyanto, R. Oktiani, and R. Ragadhita, "How To Read and Interpret FTIR Sepectroscope of Organic Material," *Indones. J. Sci. Technol.*, vol. 4, no. 1, pp. 97–118, 2019, doi: http://dx.doi.org/10.17509/ijost.v4i1.15806.

[180] J. Barkauskas and M. Dervinyte, "An investigation of the functional groups on the surface of activated carbons," *Journal of the Serbian Chemical Society*, vol. 69, no. 5. pp. 363–375, 2004, doi: 10.2298/JSC0405363B.

[181] J. Peter Guthrie and J. Cossar, "The pKa values of simple aldehydes determined by kinetics of chlorination," *Can. J. Chem.*, vol. 64, pp. 2470–2474, 1986.

[182] U. Bhaumik, "1,4-Benzoquinone and 1,4-hydroquinone based determination of electron and superoxide radical formed in heterogeneous photocatalytic systems," *J. Photochem. Photobiol. A Chem.*, vol. 407, p. 151, 2021, doi: https://doi.org/10.1016/j.jphotochem.2020.113057.